Calhoun

Institutional Archive of the Naval Postgraduate School

Calhoun: The NPS Institutional Archive

DSpace Repository

Theses and Dissertations | 1. Thesis and Dissertation Collection, all items

2006-06

Objectively determined model derived parameters associated with forecasts of tropical cyclone formation

Cowan, Christy G.

Monterey, California. Naval Postgraduate School

http://hdl.handle.net/10945/2766

Downloaded from NPS Archive: Calhoun

DUDLEY KNOX LIBRARY

http://www.nps.edu/library

Calhoun is the Naval Postgraduate School's public access digital repository for research materials and institutional publications created by the NPS community. Calhoun is named for Professor of Mathematics Guy K. Calhoun, NPS's first appointed -- and published -- scholarly author.

Dudley Knox Library / Naval Postgraduate School
411 Dyer Road / 1 University Circle
Monterey, California USA 93943

NAVAL
POSTGRADUATE
SCHOOL

MONTEREY, CALIFORNIA

THESIS

OBJECTIVELY DETERMINED MODEL-DERIVED PARAMETERS ASSOCIATED WITH FORECASTS OF TROPICAL CYCLONE FORMATION

by

Christy G. Cowan

June 2006

Thesis Advisor: Patrick A. Harr
Second Reader: Russell L. Elsberry

Approved for public release; distribution is unlimited

THIS PAGE INTENTIONALLY LEFT BLANK

REPORT DOCUMENTATION PAGE

Form Approved OMB No. 0704-0188

Public reporting burden for this collection of information is estimated to average 1 hour per response, including the time for reviewing instruction, searching existing data sources, gathering and maintaining the data needed, and completing and reviewing the collection of information. Send comments regarding this burden estimate or any other aspect of this collection of information, including suggestions for reducing this burden, to Washington headquarters Services, Directorate for Information Operations and Reports, 1215 Jefferson Davis Highway, Suite 1204, Arlington, VA 22202-4302, and to the Office of Management and Budget, Paperwork Reduction Project (0704-0188) Washington DC 20503.

1. AGENCY USE ONLY *(Leave blank)*

2. REPORT DATE June 2006

3. REPORT TYPE AND DATES COVERED Master's Thesis

4. TITLE AND SUBTITLE: Objectively Determined Model-Derived Parameters Associated with Forecasts of Tropical Cyclone Formation

5. FUNDING NUMBERS

6. AUTHOR(S) Christy G. Cowan

7. PERFORMING ORGANIZATION NAME(S) AND ADDRESS(ES)
Naval Postgraduate School
Monterey, CA 93943-5000

8. PERFORMING ORGANIZATION REPORT NUMBER

9. SPONSORING /MONITORING AGENCY NAME(S) AND ADDRESS(ES)
N/A

10. SPONSORING/MONITORING AGENCY REPORT NUMBER

11. SUPPLEMENTARY NOTES The views expressed in this thesis are those of the author and do not reflect the official policy or position of the Department of Defense or the U.S. Government.

12a. DISTRIBUTION / AVAILABILITY STATEMENT
Approved for public release; distribution is unlimited

12b. DISTRIBUTION CODE

13. ABSTRACT (maximum 200 words)

During the 2005 North Atlantic hurricane season, an objective tropical cyclone vortex identification and tracking technique was applied to analyzed and forecast fields of three global operational numerical models- the National Centers for Environmental Prediction Global Forecast System (GFS), the Navy Operational Global Atmospheric Prediction System (NOGAPS), and the United Kingdom Meteorological Office model (UKMET). For the purpose of evaluating each model's performance with respect to forecasting tropical cyclone formation, 14 relevant parameters are cataloged for every tropical vortex.

In this study, nine of the fourteen parameters are subjected to a linear discriminant analysis applied to all forecast vortices that exceed vorticity and warm core thresholds. The goal is to determine the combination of parameters for each model, at each 12-h forecast period to 120h, that best discriminates between a vortex that is correctly forecast to intensify into a tropical cyclone (developer) and a vortex that is forecast to intensify into a tropical cyclone, but does not (false alarm). The performance of the resulting discriminant functions are then assessed using the Heidke Skill Score and Receiver Operating Characteristic curves. Overall, the methodology applied to forecasts from the UKMET model shows the most skill with regard to identifying correct forecasts of tropical cyclone formation.

14. SUBJECT TERMS Tropical Cyclone, Tropical Cyclone Formation, Hurricane, Linear Discriminant Analysis

15. NUMBER OF PAGES 121

16. PRICE CODE

17. SECURITY CLASSIFICATION OF REPORT Unclassified

18. SECURITY CLASSIFICATION OF THIS PAGE Unclassified

19. SECURITY CLASSIFICATION OF ABSTRACT Unclassified

20. LIMITATION OF ABSTRACT UL

NSN 7540-01-280-5500

Standard Form 298 (Rev. 2-89)
Prescribed by ANSI Std. 239-18

THIS PAGE INTENTIONALLY LEFT BLANK

Approved for public release; distribution is unlimited

OBJECTIVELY DETERMINED MODEL-DERIVED PARAMETERS ASSOCIATED WITH FORECASTS OF TROPICAL CYCLONE FORMATION

Christy G. Cowan
Lieutenant Commander, United States Navy
B.S., U.S. Naval Academy, 1995

Submitted in partial fulfillment of the
requirements for the degree of

MASTER OF SCIENCE IN METEOROLOGY AND PHYSICAL OCEANOGRAPHY

from the

NAVAL POSTGRADUATE SCHOOL
June 2006

Author: Christy G. Cowan

Approved by: Patrick A. Harr
Thesis Advisor

Russell L. Elsberry
Second Reader

Philip A. Durkee
Chairman, Department of Meteorology

THIS PAGE INTENTIONALLY LEFT BLANK

ABSTRACT

During the 2005 North Atlantic hurricane season, an objective tropical cyclone vortex identification and tracking technique was applied to analyzed and forecast fields of three global operational numerical models - the National Centers for Environmental Prediction Global Forecast System (GFS), the Navy Operational Global Atmospheric Prediction System (NOGAPS), and the United Kingdom Meteorological Office model (UKMET). For the purpose of evaluating each model's performance with respect to forecasting tropical cyclone formation, 14 relevant parameters are cataloged for every tropical vortex.

In this study, nine of the fourteen parameters are subjected to a linear discriminant analysis applied to all forecast vortices that exceed vorticity and warm core thresholds. The goal is to determine the combination of parameters for each model, at each 12-h forecast period to 120h, that best discriminates between a vortex that is correctly forecast to intensify into a tropical cyclone (developer) and a vortex that is forecast to intensify into a tropical cyclone, but does not (false alarm). The performance of the resulting discriminant functions are then assessed using the Heidke Skill Score and Receiver Operating Characteristic curves. Overall, the methodology applied to forecasts from the UKMET model shows the most skill with regard to identifying correct forecasts of tropical cyclone formation.

THIS PAGE INTENTIONALLY LEFT BLANK

TABLE OF CONTENTS

I. INTRODUCTION 1
   A. DEFINITION OF FORMATION 1
   B. FAVORABLE ENVIRONMENTAL CONDITIONS FOR TROPICAL CYCLONE FORMATION 2
   C. TROPICAL WAVES 3
   D. FORMATION MECHANISMS 4
   E. USE OF GLOBAL MODELS TO FORECAST FORMATION 5
   F. A GENESIS PARAMETER 6
   G. PLAN FOR THE THESIS 6

II. METHODOLOGY 9
   A. VORTRACK 9
      1. Tropical Cyclone Vortex Tracking Program (TCVTP) 10
   B. SOME DEFINITIONS 12
   C. PRELIMINARY ANALYSIS 13
   D. PROBABILITY DISTRIBUTION FUNCTIONS (PDFS) 17
   E. LINEAR DISCRIMINANT ANALYSIS 18
   F. JACKKNIFE ROUTINE 22
   G. HEIDKE SKILL SCORE (HSS) 22
   H. RECEIVER OPERATING CHARACTERISTICS (ROC) CURVES ...24

III. RESULTS 27
   A. PRESENTATION OF DISCRIMINANT ANALYSIS STATISTICS ..27
   B. DISCUSSION OF RESULTS 29
      1. 12-h Forecasts 29
         a. Application of Methodology to UKMET Forecast 29
         b. Results for 12-h Forecasts 34
      2. 24-h Forecasts 35
      3. 36-h Forecasts 36
      4. 48-h Forecasts 38
      5. 60-h Forecasts 39
      6. 72-h Forecasts 41
      7. 84-h Forecasts 41
      8. 96-h Forecasts 43
      9. 108-h Forecasts 45
      10. 120-h Forecasts 46
   C. CLASSIFICATION EXAMPLES 47
      1. Correctly Classified False Alarm 47
      2. Incorrectly Classified False Alarm 53

IV. CONCLUSIONS AND RECOMMENDATIONS 61

  - A. CONCLUSIONS 62
  - B. RECOMMENDATIONS FOR FUTURE WORK 63

APPENDIX A. SCATTERPLOTS FOR GFS 12-H FORECAST 65

APPENDIX B. SCATTERPLOTS INCLUDING OMEGA 69

APPENDIX C. PROBABILITY DISTRIBUTION FUNCTIONS 85

LIST OF REFERENCES 101

INITIAL DISTRIBUTION LIST 103

LIST OF FIGURES

Figure 1 A schematic of a wave in the easterly trade winds (From: NASA Earth Observatory Library http://earthobservatory.nasa.gov/Library/Hurricanes; June 2006)....................................4
Figure 2 Schematic of the TCVTP component of VORTRACK (From: Harr 2006)...............................10
Figure 3 A scatterplot of 850-500 hPa average relative vorticity and 700-500 hPa warm core for all vortices in the TCVTP database for the GFS model at the 12-h forecast time. The dark solid lines represent the calculated threshold values (for this model and forecast period) for these two parameters....................................14
Figure 4 As in Figure 3 except with non-developers, developers and three kinds of false alarms annotated as indicated in the inset.............15
Figure 5 As in Figure 4, except with vortices exceeding the threshold for the 500 hPa vertical motion (omega) parameter annotated as indicated in the inset...16
Figure 6 Probability Distribution Functions of non-developers in green, developers in blue, and false alarms in red for the nine parameters derived from the UKMET 12-h forecast relative to tropical vortices in the TCVTP..................18
Figure 7 ROC curves for 12-h forecasts based on an independent dataset. The curve for the function applied to GFS is displayed in red, UKMET in green, and NOGAPS in blue........................35
Figure 8 ROC curves as in Figure 7, except for 24-h forecasts......................................37
Figure 9 ROC curves as in Figure 7, except for 36-h forecasts......................................38
Figure 10 ROC curves, as in Figure 7, except for 48-h forecasts......................................39
Figure 11 ROC curves, as in Figure 7, except for 60-h forecasts......................................40
Figure 12 ROC curves as in Figure 7, except for 72-h forecasts......................................42
Figure 13 ROC curves as in Figure 7, except for 84-h forecasts......................................43

Figure 14 ROC curves as in Figure 7, except for 96-h forecasts and the curve for the UKMET function is omitted..44
Figure 15 ROC curves as in Figure 7, except for 108-h forecasts and the curve for the NOGAPS function is omitted..45
Figure 16 ROC curves as in Figure 7, except for 120-h forecasts and the curve for the NOGAPS function is omitted..46
Figure 17 Scatterplot of 850-500 hPa relative vorticity and 700-500 hPa warm core for all vortices in the TCVTP database for the UKMET model at the 48-h forecast interval. The case UKM_2005070712_17_015 is highlighted with a blue arrow. The case UKM_2005091900_018_002 is highlighted with a green arrow..................48
Figure 18 The analyzed track (black) and all UKMET forecast tracks (colors) for the case UKM_2005070712_17_015............................49
Figure 19 As in Figure 18, except with the UKMET forecast track initiated at 1200 UTC 14 July 2005 (blue) and the 48-h analyzed and forecast positions circled in red.................................49
Figure 20 Average relative vorticity (10^{-5} s^{-1}) between 850 and 500 hPa for case UKM_2005070712_17_015. The UKMET 48-h forecast values from 1200 UTC 14 July 2005 are plotted with red circles, while analyzed values are plotted with blue squares....50
Figure 21 As in Figure 20, except for warm core (°C) at 700-500 hPa......................................50
Figure 22 As in Figure 20, except for vertical wind shear (m s^{-1}) between 200 and 850 hPa. 51
Figure 23 As in Figure 20, except for vertical motion (m s^{-1} * 10) at 500 hPa. 51
Figure 24 As in Figure 20, except for vapor pressure (mb) between 700 and 500 hPa.........................52
Figure 25 As in Figure 20, except for sea-level pressure (mb)...52
Figure 26 The analyzed track (black) and all UKMET forecast tracks (colors) for the case UKM_20050919_018_002............................54
Figure 27 The analyzed track (black) and UKMET forecast track initiated at 1200 UTC 23 September 2005 (blue) for case UKM_20050919_018_002. The 48-h analyzed and forecast positions are circled in red..54

Figure 28 As in Figure 20, except for case UKM_20050919_018_002. The UKMET 48-h forecast values from 1200 UTC 23 September 2005 are plotted with red circles while analyzed values are plotted with blue squares.....................................55
Figure 29 As in Figure 28, except for warm core (°C) at 700-500 hPa.......................................56
Figure 30 As in Figure 28, except for vertical wind shear (m s^{-1}) between 200 and 850 hPa. 56
Figure 31 As in Figure 28, except for vertical motion (m s^{-1} * 10) at 500 hPa. 57
Figure 32 As in Figure 28, except for vapor pressure(mb) between 700 and 500 hPa..........................57
Figure 33 As in Figure 28, except for sea-level pressure (mb)...58

THIS PAGE INTENTIONALLY LEFT BLANK

LIST OF TABLES

Table 1 Analyzed and forecast quantities used to identify physical characteristics associated with each tropical vortex. Warm core measurements are defined as a temperature difference between the vortex and the environment (From: Harr 2006)....................11

Table 2 A contingency table in which forecast status is compared with observed status. Hits are represented by a, false alarms by b, misses by c, and correct nulls by d........................23

Table 3 Results of the Linear Discriminant Analysis......28

Table 4 List of parameters corresponding to numbers in column 3 of Table 3..............................28

Table 5 Classification results for the relevant discriminant function as applied to dependent data from the UKMET 12-h model. Column one lists the actual group membership of each vortex; a '1' represents a developer and a '2' represents a false alarm. Column two lists the group to which each vortex was assigned by the discriminant function. The probabilities, according to the discriminant function, that the vortex belongs to group '1' and '2' are listed in columns three and four, respectively. Shaded rows represent vortices that were misclassified by the discriminant function. The three light grey rows represent vortices that did develop, but were classified as false alarms. The two dark grey rows represent vortices that did not develop, but were classified as developers.......30

Table 6 Classification results from Table 5 summarized as a forecast contingency table. In this case, the HSS is 0.79.................................31

Table 7 Forecast contingency table for the relevant discriminant function as applied to independent data from the UKMET 12-h model. In this case, the HSS is 0.55.................................32

Table 8 Forecast contingency tables for the relevant discriminant function as applied to independent data from the UKMET 12-h model. Each two-row block gives the results produced using the threshold listed in column 1. The last column

gives the resulting hit and false-alarm rates that were used to plot a ROC curve for the discriminant function............................33
Table 9 Six parameters for case UKM_2005070712_17_015 (third row) compared to the mean values for developers (first row) and false alarms (second row). The fourth and fifth rows contain the differences between the values for this case and the mean values for developers and false alarms, respectively. The smaller differences are highlighted.....................................53
Table 10 Six parameters for case UKM_20050919_018_002 (third row) compared to the mean values for developers (first row) and false alarms (second row). The fourth and fifth rows contain the differences between the values for this case and the mean values for developers and false alarms, respectively. The smaller differences is highlighted.....................................59

ACKNOWLEDGMENTS

I would like to thank my thesis advisor, Professor Pat Harr and second reader, Professor Russell Elsberry. Professor Harr provided a direction for the thesis as well as constant guidance. His VORTRACK system, tireless efforts to provide datasets, and MATLAB expertise were pivotal to the completion of the thesis. The VORTRAC system was sponsored by the National Oceanic and Atmospheric Administration, Joint Hurricane Testbed Project and the Office of Naval Research, Marine Meteorology Program.

I would also like to thank my husband Chris for his continuous support throughout the completion of this degree.

THIS PAGE INTENTIONALLY LEFT BLANK

I. INTRODUCTION

Improvements in operational global models have resulted in increased accuracy of 72-h tropical cyclone track forecasts. In an effort to extend preparation lead-time, the National Hurricane Center (NHC) and the Joint Typhoon Warning Center (JTWC) began issuing track forecasts through 120h in 2003. Since a tropical cyclone could easily form and intensify to a powerful storm within this 120-h window, an increased need exists for accurate prediction of tropical cyclone formation from operational global models. While it is important to establish the accuracy of forecasts of tropical cyclone formation in global models, it is also important to identify and understand factors that distinguish forecasts of vortices that are correctly forecast to intensify into tropical cyclones (developers) from forecasts of vortices that are forecast to intensify into tropical cyclones, but do not (false alarms).

A. DEFINITION OF FORMATION

The criteria for defining tropical cyclone formation are not universally accepted, although all definitions require that a tropical cyclone be convective and non-frontal, originate over tropical waters, have a cyclonic surface circulation, and have a warm core with winds that are strongest at the surface and decrease with height. Elsberry (2003) defines formation to have occurred when there exists "a non-frontal, cyclonic circulation in the tropics that is closed (ground-relative westerly winds on the equatorward side for a westward moving storm) with maximum 10-minute averaged surface sustained winds of at least 25 kt (12.5 m s^{-1}) that is accompanied by deep (throughout most of the troposphere) convection and a radius of maximum winds such that the Rossby number is at least one.” A Rossby number of at least one would require a radius of maximum wind less than 500 km for a maximum wind of 12.5 m s^{-1} at 10° latitude. This criterion is included to distinguish between a tropical cyclone, which has maximum winds near the center, and a monsoon depression that has maximum winds at a larger radius.

Davis and Bosart (2003) use the requirement that the vortex be capable of self-amplification through air-sea interaction. This occurs around the time that the cyclone reaches wind speeds of 34 kt (17 m s^{-1}) at which point the character of the air-sea interaction changes such that there are enhanced fluxes of heat and moisture between the ocean and atmosphere. This is the typical ‘storm’ threshold. Most operational centers, including the NHC and JTWC begin issuing advisories when the vortex meets the ‘depression’ threshold of 25 kt (12 m s^{-1}). For the purpose of this study, formation will be considered to have occurred at the time of the first advisory issued by the NHC or JTWC, which is also the time of its first entry in the ‘best-track’ database.

B. FAVORABLE ENVIRONMENTAL CONDITIONS FOR TROPICAL CYCLONE FORMATION

Gray (1975) cited six physical parameters that create a favorable, though not sufficient, environment for the formation of tropical cyclones. They are: (i) large values of low-level relative vorticity; (ii) a location of at least 500 km from the equator (to gain some contribution from Coriolis force); (iii) weak vertical shear of the horizontal winds; (iv) sea-surface temperatures exceeding

26°C through a deep oceanic layer; (v) conditional instability through a deep atmospheric layer; and (vi) a moist lower- and mid-troposphere. The first three describe dynamical aspects of the environment while the last three relate to its thermodynamic state.

DeMaria et al. (2001) concluded that tropical cyclone formation in the Atlantic is constrained by vertical instability and midlevel moisture during the early part of the hurricane season, and by vertical wind shear in the latter part of the season. Molinari et al. (2000) demonstrated that because environmental conditions in the eastern North Pacific are almost always favorable for formation, it is the amplitude of approaching tropical waves that is the most important factor determining whether or not tropical cyclones will form.

C. TROPICAL WAVES

The most common pre-existing disturbance, or formation seedling, in both the Atlantic and eastern North Pacific is the tropical, or easterly, wave (Figure 1). A westward-moving wave train develops in the trade winds and convergence on the eastern side of the trough leads to convection. The tropical wave that affects these regions is the African Easterly Wave, which develops from baroclinic-barotropic instability in the mid-level easterly jet over Africa. In the Atlantic, 40% of hurricanes and 65% of major hurricanes originate as tropical waves in the area between North Africa and the Caribbean (DeMaria et al. 2001). Avila and Pasch (1995) state that almost all tropical cyclones in the eastern North Pacific can be traced to an African Easterly Wave.

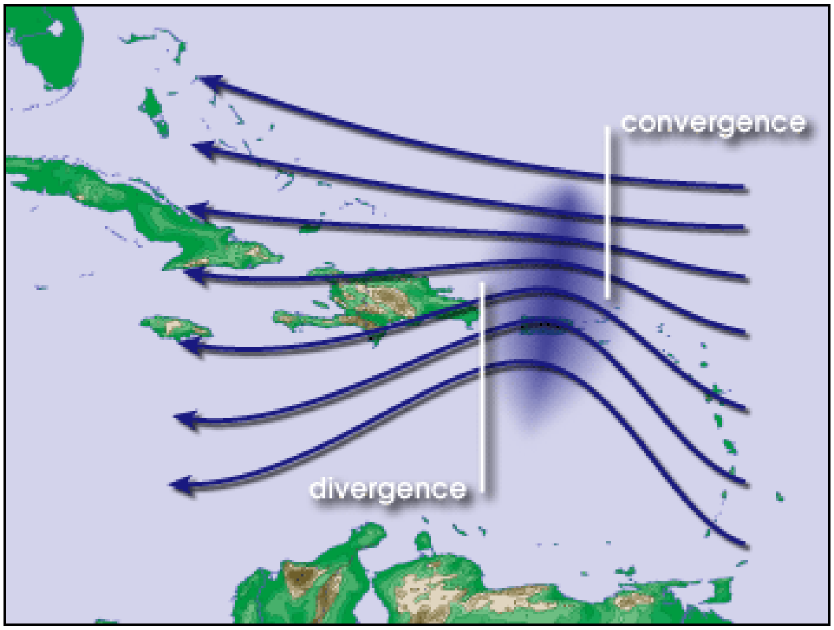

Figure 1 A schematic of a wave in the easterly trade winds (From: NASA Earth Observatory Library http://earthobservatory.nasa.gov/Library/Hurricanes; June 2006).

D. FORMATION MECHANISMS

While the environmental conditions required for formation are understood, and the importance of a pre-existing disturbance to organize convection and concentrate potential vorticity (Davis and Bosart 2001) is recognized, the processes that cause this disturbance to develop into a tropical cyclone are not well understood. Enhanced global models and higher resolution satellite imagery have improved the forecast process significantly, but insufficient "in-situ" observations have been available over the tropical oceans to verify hypotheses and confirm a single mechanism of formation.

In general, if the favorable environmental conditions are met, an area of convection experiences positive feedback in that warm air rises, condenses and releases latent heat. That heat further increases the buoyancy of the air. In response to warming in the rising air, the surface pressure falls and leads to a rapid inflow of air, which, in turn, leads to more thunderstorms. Coriolis force will eventually cause the low-level inflow to develop a cyclonic circulation. Warming of the rising air causes air pressure to rise at the top of the storm. An anti-cyclonic outflow develops that provides an exhaust for the storm and allows the above sequence of events to continue.

E. USE OF GLOBAL MODELS TO FORECAST FORMATION

As described by Gray (1975) both dynamical and thermodynamic conditions may create a favorable environment for tropical cyclone formation. The favorable thermodynamic conditions exist over broad geographic regions, change slowly, and are fairly well resolved by global models. However, the dynamical conditions vary on a much smaller temporal and spatial scales. Not surprisingly, it is therefore much more difficult for global models to resolve changes in these variables.

Due to these limitations, some studies (e.g., Beven 1999) concluded that the global operational forecast models had no significant skill in forecasting tropical cyclone formation. Improved horizontal and vertical resolution in the models as well as remotely sensed observations has helped global models better resolve the physical processes on smaller and smaller scales. However, Hennon and Hobgood (2003) suggest that global models could provide skillful formation forecasts even if complex mesoscale processes are neglected. They found several characteristics associated with the large-scale environment over the North Atlantic that may provide significant measures to discriminate between cloud clusters that develop into tropical cyclones and those that do not develop.

F. A GENESIS PARAMETER

Gray (1975) used the product of his dynamic criteria (low-level relative vorticity, distance from the equator, and vertical shear of the horizontal winds) and the product of the thermodynamic criteria (sea-surface temperature, conditional instability and lower- and mid-tropospheric moisture) to define a Seasonal Genesis Parameter. DeMaria et al. (2001) developed a similar tropical cyclone genesis parameter for the Atlantic that was the product of vertical shear, vertical instability, and midlevel moisture variables.

Using eight predictors from large-scale analyses, Hennon and Hobgood (2003) developed a probabilistic prediction system for tropical cyclone formation. They manually tracked cloud clusters in satellite imagery and then submitted the eight variables associated with each cluster to a discriminant analysis. The resulting linear combination of the variables best separates cloud clusters that will develop into tropical depressions from those that will not.

G. PLAN FOR THE THESIS

In this thesis, a discriminant analysis similar to that used by Hennon and Hobgood (2003) is applied to forecasts of tropical vortices produced by several operational global models. Vortices are identified and tracked based on their analyzed and forecast vorticity as opposed to the Hennon and Hobgood approach of identifying candidate cloud clusters in satellite imagery. A probability-based model is used to define the likelihood that a tropical vortex that is forecast by the operational model to become a tropical cyclone will actually develop into a tropical cyclone. Whereas Hennon and Hobgood (2003) used the discriminant analysis approach for the broader problem of distinguishing between developing and non-developing cloud clusters, this study is limited to cases in which a vortex is forecast to develop into a tropical cyclone, and the objective is to provide the probability that the model forecast is true or false.

The Vortex Tracking (VORTRACK) system of Harr (2006) is the key to this type of data analysis. Therefore, the first part of Chapter II (Methodology) will describe the VORTRACK system. The data analysis approach will then be summarized. For each operational global model and forecast interval considered, the approach included producing scatterplots, probability distribution functions (PDFs), a linear discriminant analysis (which included a jackknife routine for application to independent data), and performance assessment to include the Heidke Skill Score (HSS) and Receiver Operating Characteristics (ROC) curves.

In Chapter III, the results will be presented, which will include the parameters used in each discriminant function along with relevant PDFs, as well as the HSS and ROC curve for each discriminant function. Chapter IV will summarize the conclusions, highlight some of the challenges posed by this type of data analysis, and make recommendations for further study.

THIS PAGE INTENTIONALLY LEFT BLANK

II. METHODOLOGY

To discriminate between operational model forecasts of developing and non-developing vortices, it is necessary to extract parameters that are relevant to tropical cyclone formation relative to each tropical vortex. These parameters must be identified in forecasts of varying lengths for comparison with the parameters in the verifying analyses. Furthermore, it is important to capture these characteristics among several operational models. The database defined by the VORTRACK system, which is summarized in Figure 2, is used to identify forecast model parameters that have the most predictive value with regards to formation.

The principal objective of this research is to create such a tool that can discriminate between a developer and a false alarm in the global model forecasts. This tool will be based on a probabilistic assessment derived from a linear discriminant analysis.

A. VORTRACK

The VORTRACK application was developed at the Naval Postgraduate School (NPS) so that output from numerical models could more easily be included in the process of forecasting the intensification of a tropical low into a tropical storm. A prototype was run for the 2005 hurricane season at both NPS and the NHC. There are two primary components of VORTRACK. The first is the data processing segment which is the Tropical Cyclone Vortex Tracking Program (TCVTP). This program outputs the tracks of all eligible tropical vortices as well as the corresponding values of 14 environmental parameters. The resulting ASCII text file is stored in one location if the vortex can be matched in space and time with a vortex in the verifying analysis field, and in another location if the vortex appears only the forecast fields. The second component of VORTACK is a web-interface output segment (Harr 2006). Vortex locations and environmental parameter characterizations from the TCVTP-generated ASCII text files were used for this thesis.

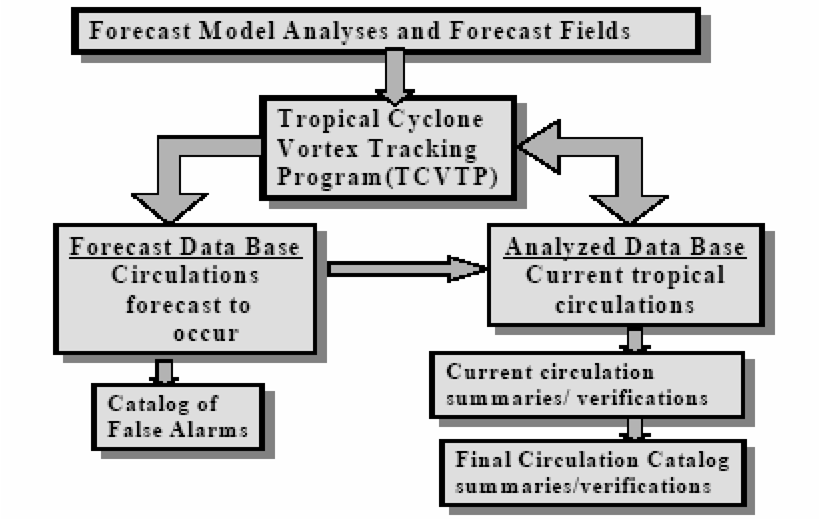
Forecast Model Analyses and Forecast Fields
Tropical Cyclone Vortex Tracking Program(TCVTP)
Forecast Data Base
Circulations forecast to occur
Analyzed Data Base
Current tropical circulations
Catalog of False Alarms
Current circulation summaries/ verifications
Final Circulation Catalog summaries/verifications

Figure 2 Schematic of the TCVTP component of VORTRACK (From: Harr 2006).

1. Tropical Cyclone Vortex Tracking Program (TCVTP)

The objective tropical vortex identification and tracking technique, TCVTP, was utilized to examine analyzed and forecast fields of three operational global numerical models during the 2005 hurricane season in the North Atlantic. The models that had been catalogued in the 2005 database include the Navy Operational Global Atmospheric Prediction System (NOGAPS), the National Centers for Environmental Prediction's Global Forecast System (GFS), and the United Kingdom Meteorological Office (UKMET) global model.

For each tropical vortex, which is defined by the 850 hPa relative vorticity above a threshold value of $1.0 \times 10^{-5}\ s^{-1}$, 14 environmental parameters in model analyses and forecasts that are relevant to tropical cyclone formation (Table 1) are catalogued in the TCVTP. In this study, only nine of the 14 parameters were used. Those parameters shaded on Table 1 were not used in this study. For example, the 850-500 hPa average relative vorticity was chosen over the 850 hPa relative vorticity. The 700-400 hPa, 700-300 hPa warm core, and precipitation parameters were not used because these values were not available for the UKMET model and therefore they could not be used for model inter-comparison.

Table 1 Analyzed and forecast quantities used to identify physical characteristics associated with each tropical vortex. Warm core measurements are defined as a temperature difference between the vortex and the environment (From: Harr 2006).

850 hPa Relative Vorticity	Sea-level pressure Minimum(mb)
Shallow Vertical Wind Shear (850-500 hPa)	Deep Vertical Wind Shear (850-200 hPa)
850-200 hPa Geopotential Height Thickness	700-500 hPa Warm Core
Vertical motion at 500 hPa	700-400 hPa Warm Core
700-500 hPa Vapor Pressure	700-300 hPa Warm Core
850-500 hPa Average Relative Vorticity	Sea-level Pressure Difference between the Vortex and the Environment
Total Precipitation	Convective Precipitation

B. SOME DEFINITIONS

The characterization of a vortex as developer or non-developer was based on the 850-500 hPA average relative vorticity and 700-500 hPa warm core values as compared to threshold values for these parameters. The threshold value (P_T) for each parameter is defined as the lowest tercile of that parameter averaged for all developers at the time of formation. Time of formation (T_0) is defined as the time that the tropical cyclone was first entered in the best-track database. A *developer* is any tropical vortex that was eventually entered in the best-track database. For the purpose of this study, this included all forecast *hits* (vortex was forecast to exceed the threshold values and the corresponding vortex in the verifying analysis was a developer) and *misses* (vortex was not forecast to exceed the threshold values but was in fact a developer).

A *non-developer* is defined as a vortex tracked in the TCVTP database that never entered the NHC best-track database, which may include three sub-categories. A *false alarm* is a tropical vortex that was forecast to exceed both threshold values, but is actually a non-developer because it did not verify above those threshold values. The majority of vortices in the TCVTP database was not forecast to exceed both threshold values and did not verify above the threshold values; these *correct nulls* were not considered in this study. The third category consists of vortices in the TCVTP that were forecast to be, and according to model analyses verified above, both threshold values but were never entered in the NHC best-track database. In these cases, there were other parameters not considered in this study (e.g., low-level wind shear) that must have prevented these vortices from becoming developers. Even though they meet the definition of non-developers, since the forecast verified in the correct category (i.e., upper-right quadrant of the scatterplots in Appendix A), they are not regarded as false alarms and were also not considered in this study.

C. PRELIMINARY ANALYSIS

Since by definition any tropical cyclone must have positive lower-tropospheric relative vorticity and a warm core, all tropical vortices in the TCVTP database for each model at each forecast interval were plotted on a graph with 850-500 hPa average relative vorticity on the x-axis and 700-500 hPa warm core on the y-axis. Figure 3 is an example of this scatterplot for the GFS 12-h model data. Two clusters were expected: developers with a centroid in the upper-right quadrant, and non-developers with a centroid in the lower-left quadrant. As evident on Figure 3, such a separation between developers and non-developers in the model forecasts was not observed.

This and scatterplots at longer forecast intervals demonstrated that the GFS model does not have skill in distinguishing between developers and non-developers when considering the two most basic prerequisites of tropical cyclones (positive relative vorticity and a warm core). Similar results were achieved with the NOGAPS and UKMET models at all forecast periods. As a result, the aim of this study was shifted to discrimination between developers and false alarms. Since a false alarm is a non-developing vortex with forecast values of 850-500 hPa average relative vorticity and 700-500 hPa warm core above threshold values, these false alarms also are in the upper-right quadrant on

Figure 3. That is, only developers entered in the best-track data and non-developers in the upper-right quadrant of the vorticity / warm core scatterplots are considered in the following sections.

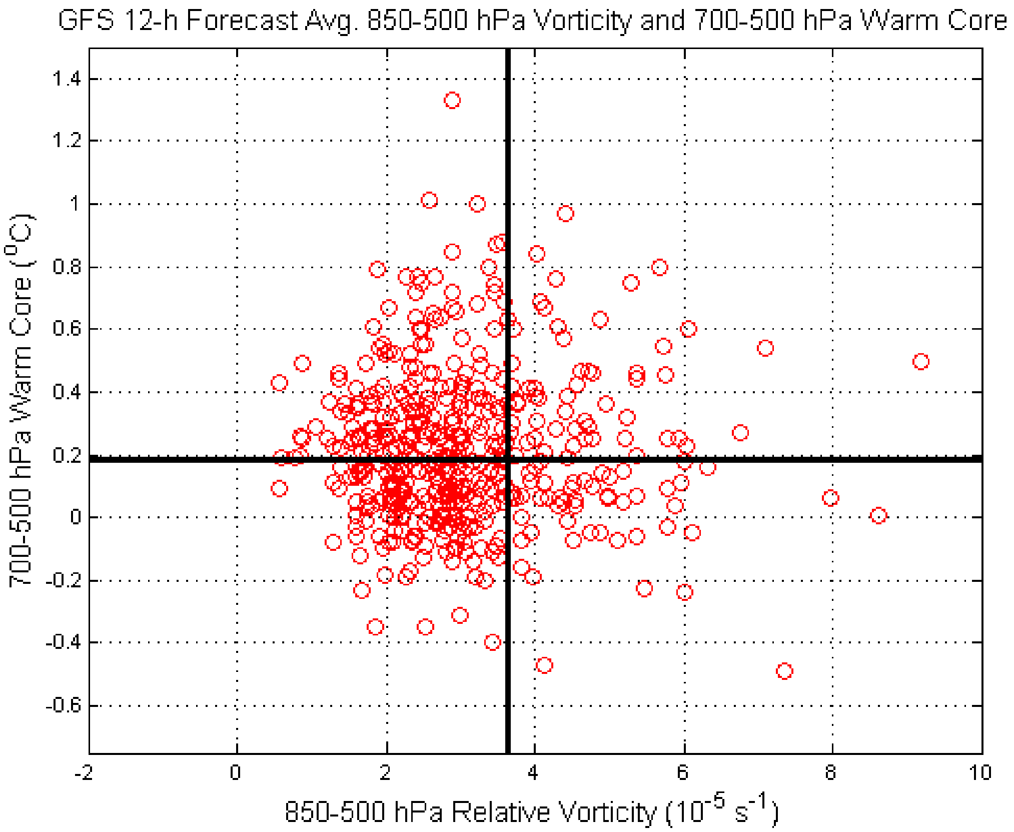

Figure 3 A scatterplot of 850-500 hPa average relative vorticity and 700-500 hPa warm core for all vortices in the TCVTP database for the GFS model at the 12-h forecast time. The dark solid lines represent the calculated threshold values (for this model and forecast period) for these two parameters.

For this GFS 12-h example, the vortices of interest are identified in Figure 4. On this figure, black squares represent developers. Solid circles represent false alarms. Cyan represents vortices that were false alarms in warm core only (i.e., verified above the vorticity threshold). Magenta represents vortices that were false alarms in vorticity only (i.e. verified above the warm core threshold). Green represents vortices that were false alarms in both warm core and vorticity. The objective of the linear discriminant analysis is then to distinguish between the developers (squares on Figure 4) and false alarms (solid colored circles on Figure 4).

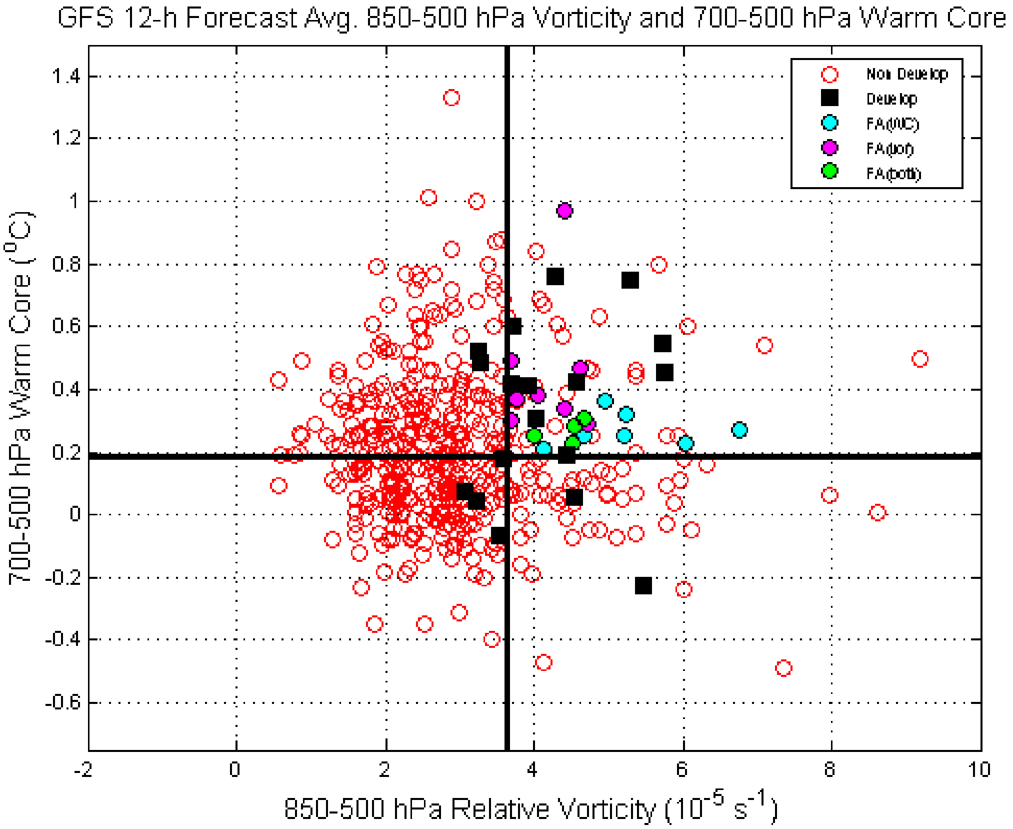

Figure 4 As in Figure 3 except with non-developers, developers and three kinds of false alarms annotated as indicated in the inset.

The next step in the data analysis was to include additional parameters on these scatterplots. In Figure 5, vortices are plotted as in Figure 4, except that vortices with 500 hPa omega values above the threshold value for that parameter are indicated (with a blue versus black square in the case of developers and with a triangle versus circle in the case of false alarms). The few open red circles in the upper right quadrant represent vortices that verified above the thresholds for both warm core and vorticity and were therefore not considered false alarms.

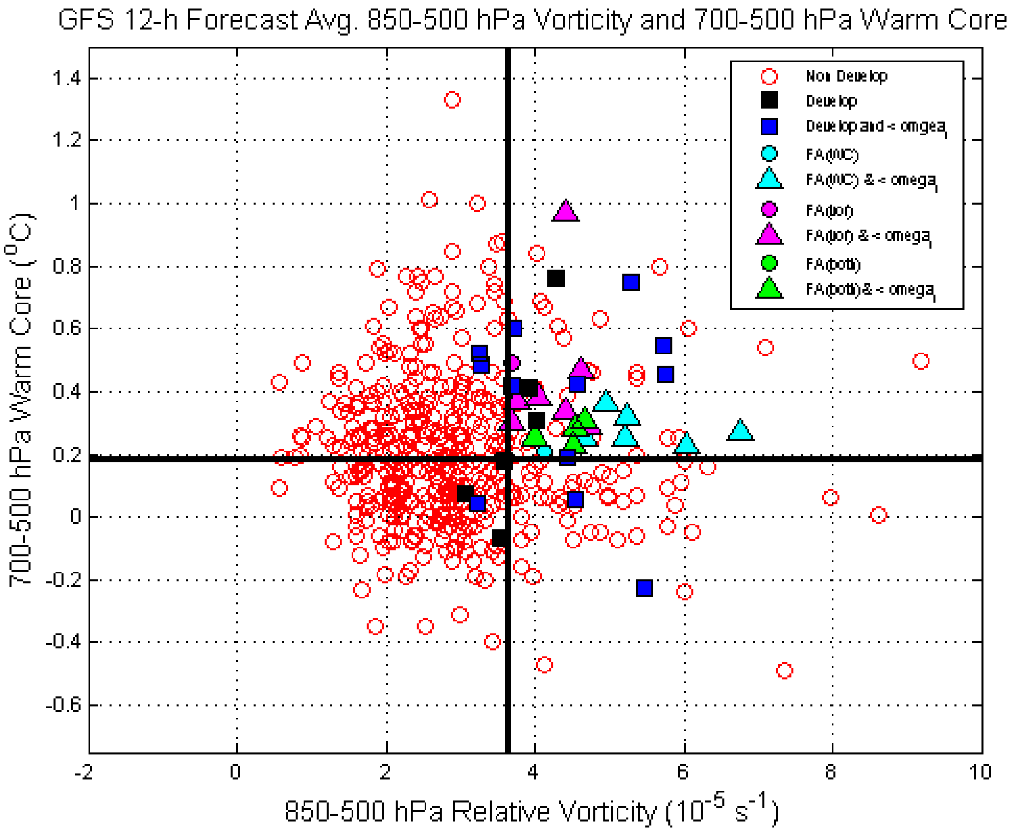

Figure 5 As in Figure 4, except with vortices exceeding the threshold for the 500 hPa vertical motion (omega) parameter annotated as indicated in the inset.

The goal in completing these scatterplots was to determine which parameters had the best potential for discriminating between developers and false alarms and thus to reduce the number of parameters considered in the discriminant analysis. However, inspection of the scatterplots revealed no systematic tendencies associated with various parameters that distinguished between developers and false alarms. Therefore PDFs of each parameter and vortex category were considered and are described in the next sub-section. For information purposes, the scatterplots including each of the seven parameters in the GFS model at 12h are displayed in Appendix A, and the scatterplots including omega in all three models at all ten forecast intervals are displayed in Appendix B. The scatterplots in Appendix B are useful for illustrating the number of cases considered in each test, which helps account for some of the problems encountered in the data analysis at the longer forecast intervals.

D. PROBABILITY DISTRIBUTION FUNCTIONS (PDFS)

Probability Density Functions (PDFs) were completed for the nine parameters in each model at each forecast interval and are contained in Appendix C. An example from the UKMET 12-h forecast data is provided in Figure 6. The goal in completing the PDFs was to reduce the number of parameters to be considered in the discriminant analysis. It was assumed that those parameters that had the smallest amount of overlap in the blue and red curves would be the best discriminators between developers and false alarms. Whereas this may be true when considering an individual parameter it became evident in preliminary linear discriminant analyses that the combinations of parameters behaved in ways that were not obvious from the individual plots (e.g., Figure 6). Thus, a more comprehensive analysis of all combinations of parameters needed to be conducted.

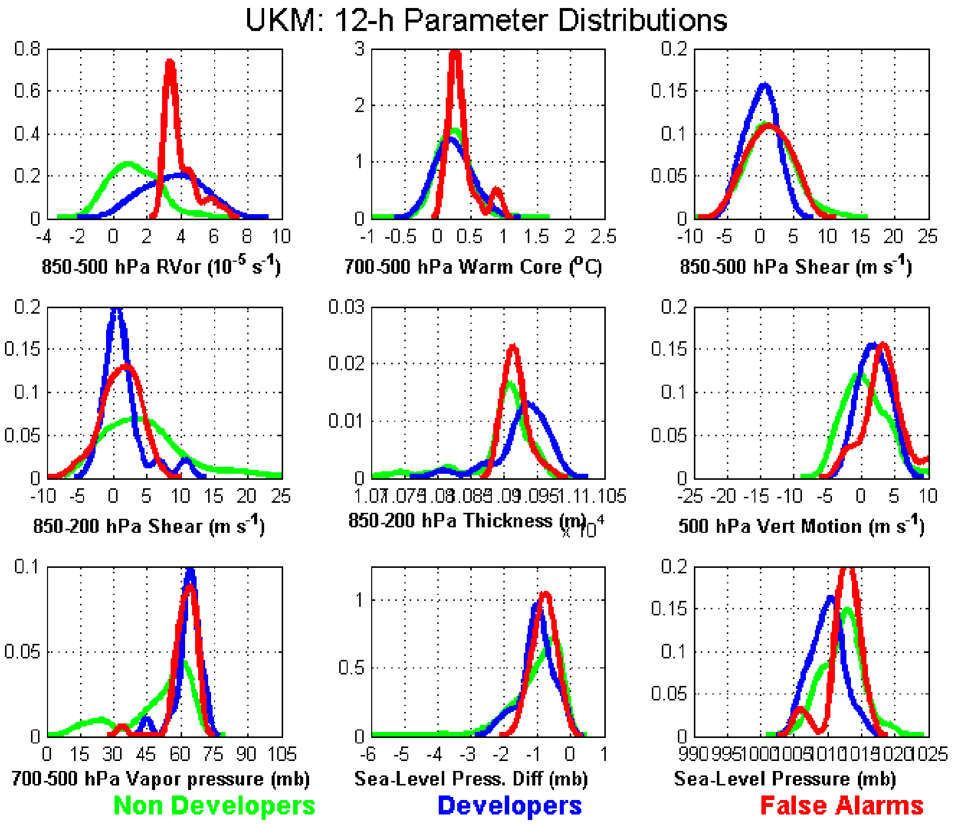

Figure 6 Probability Distribution Functions of non-developers in green, developers in blue, and false alarms in red for the nine parameters derived from the UKMET 12-h forecast relative to tropical vortices in the TCVTP.

E. LINEAR DISCRIMINANT ANALYSIS

The goal of a linear discriminant analysis is to discern group membership based on a vector (**x**) having k attributes that are observed for n cases (Wilks, 2005). A training sample that contains n cases is used to define the discriminant function. The number of groups (g) is specified a priori and each case must belong to one and only one group. Group membership must be specified for all cases in the training sample. In this study, g=2 since developers and false alarms are the two groups, and k=9 since nine parameters from the TCVTP database are considered. The training sample size (n) varies by model and forecast interval.

The discriminant analysis process consists of two segments. *Discrimination* is the process of using the training data to find a function of the attributes that best discriminates between the groups (the discriminant function). *Classification* is the process of assigning new cases to one of the groups using the discriminant function. Alternately, classification may involve estimating the probabilities of group membership. In this study, both methods of classification were also applied to independent data using a 'jackknife' technique to test the skill of the discriminant function. This process will be described in a later section.

A discriminant function is needed for each model and forecast interval (30 in total). For a given model and forecast interval, the data matrix (n x k) can be divided into the two groups that result in two matrices with dimensions (n_1 x k) and (n_2 x k) where $n = n_1 + n_2$. The number of developers (n_1) and false alarms (n_2) in the model data varies by model and forecast period. Hence, the first matrix has dimensions of (n_1 x 9) and the second matrix has dimensions (n_2 x 9). The goal is to find a linear function of the k parameters or the linear combination $\boldsymbol{a}^T\mathbf{x}$ that will best classify the group membership of future cases. This linear combination is defined as the discriminant function.

Assuming the two populations corresponding to the groups have the same covariance structure, Wilks (2005) summarizes the approach taken by statistician R.A. Fisher as finding "the vector $\boldsymbol{a}$ as that direction in the kdimensional space of the data that maximizes the separation of the two means, in standard deviation units, when the data are projected onto ***a***." This procedure requires that ***a*** maximizes

$$\frac{\left(\mathbf{a}^{\mathrm{T}}\overline{\mathbf{x}}_1 - \mathbf{a}^{\mathrm{T}}\overline{\mathbf{x}}_2\right)^2}{\mathbf{a}_{\mathrm{T}}\left[\mathrm{S}_{\mathrm{pool}}\right]\mathbf{a}}, \tag{1}$$

where $\overline{x}_1$ and $\overline{x}_2$ are the mean vectors for each group and S_{pool} is the estimated common covariance matrix of the two groups which is a weighted average of the two sample covariance matrices

$$\frac{n_1 - 1}{n_1 + n_2 - 2}\left[S_1\right] + \frac{n_2 - 1}{n_1 + n_2 - 2}\left[S_2\right]. \tag{2}$$

The advantage of finding the direction ***a*** is that the data vector, **x**, can be transformed into a scalar variable, $\delta_1 = \boldsymbol{a}^{\mathbf{T}}\mathbf{x}$, which is known as Fisher's linear discriminant function as defined above. The groups of multivariate data are hence transformed to groups of univariate data distributed along the ***a*** axis. The vector ***a***, which lies in the direction of maximum separation is given by

$$\mathbf{a} = \left[\mathrm{S}_{\mathrm{pool}}\right]^{-1}(\overline{\mathbf{x}}_1 - \overline{\mathbf{x}}_2), \tag{3}$$

and Fisher's linear discriminant function becomes

$$\delta_1 = \mathbf{a}^{\mathrm{T}}\mathbf{x} = (\overline{\mathbf{x}}_1 - \overline{\mathbf{x}}_2)^{\mathrm{T}}\left[\mathrm{S}_{\mathrm{pool}}\right]^{-1}\mathbf{x}. \tag{4}$$

This function maximizes the scaled distance (D) between the two sample means in the training data where it is defined by:

$$\mathbf{a}^{\mathrm{T}}(\overline{\mathbf{x}}_1 - \overline{\mathbf{x}}_2) = (\overline{\mathbf{x}}_1 - \overline{\mathbf{x}}_2)^{\mathrm{T}}[\mathrm{S}_{\mathrm{pool}}]^{-1}(\overline{\mathbf{x}}_1 - \overline{\mathbf{x}}_2) = \mathrm{D}^2. \tag{5}$$

Future cases will be classified as belonging to either Group 1 or Group 2 according to the value of δ_1. Because δ_1 is a dot product, it is a scalar, or one-dimensional projection of the vector **x** onto the direction of maximum separation, ***a***. The simplest method of classification is to assign an individual case in **x**, to Group 1 if the projection $\boldsymbol{a}^T\mathbf{x}$ is closer to the projection of the Group 1 mean and assign it to Group 2 if it is closer to the projection of the Group 2 mean.

The midpoint between the means of the two groups along the ***a*** axis is given by:

$$\hat{m} = \frac{1}{2}(\mathbf{a}^T\bar{\mathbf{x}}_1 + \mathbf{a}^T\bar{\mathbf{x}}_2) = \frac{1}{2}\mathbf{a}^T(\mathbf{x}_1 + \mathbf{x}_2) = \frac{1}{2}(\mathbf{x}_1 - \mathbf{x}_2)^T[S_{pool}]^{-1}(\mathbf{x}_1 + \mathbf{x}_2) \ . \qquad (6)$$

Therefore a case in **x** is classified according to the following rule:

$$\text{Assign to Group 1 if } a^T x \geq \hat{m}$$

$$\text{Assign to Group 2 if } a^T x < \hat{m} \ .$$

Alternately, a probabilistic classification can be done. Using this method, the probability that a case in **x** belongs to each of the two groups is determined according to Bayes' Theorem:

$$\Pr\{\text{Group 1}|x\} = \frac{p_1 f_1(x)}{p_1 f_1(x) + p_2 f_2(x)} , \qquad (7)$$

$$\Pr\{\text{Group 2}|x\} = \frac{p_2 f_2(x)}{p_1 f_1(x) + p_2 f_2(x)} \ . \qquad (8)$$

In Equations (7) and (8), the p_1 and p_2 values are the prior probabilities of group membership, which is simply the relative frequency with which group 1 and group 2, respectively, are represented in the training data. Thus f_1

and f_2 are the PDFs for groups 1 and 2, respectively. If it can be assumed that the PDFs are multivariate normal distributions, Equations (7) and (8) become:

$$\frac{p_1\left(\left|[S_1]\right|^{-\frac{1}{2}}\exp[-\frac{1}{2}(\mathbf{x}-\bar{\mathbf{x}}_1)^T[S_1]^{-1}(\mathbf{x}-\bar{\mathbf{x}}_1)]\right)}{p_1\left(\left|[S_1]\right|^{-\frac{1}{2}}\exp[-\frac{1}{2}(\mathbf{x}-\bar{\mathbf{x}}_1)^T[S_1]^{-1}(\mathbf{x}-\bar{\mathbf{x}}_1)]\right)+p_2\left(\left|[S_2]\right|^{-\frac{1}{2}}\exp[-\frac{1}{2}(\mathbf{x}-\bar{\mathbf{x}}_2)^T[S_2]^{-1}(\mathbf{x}-\bar{\mathbf{x}}_2)]\right)}, \quad (9)$$

$$\frac{p_2\left(\left|[S_2]\right|^{-\frac{1}{2}}\exp[-\frac{1}{2}(\mathbf{x}-\bar{\mathbf{x}}_2)^T[S_2]^{-1}(\mathbf{x}-\bar{\mathbf{x}}_2)]\right)}{p_1\left(\left|[S_1]\right|^{-\frac{1}{2}}\exp[-\frac{1}{2}(\mathbf{x}-\bar{\mathbf{x}}_1)^T[S_1]^{-1}(\mathbf{x}-\bar{\mathbf{x}}_1)]\right)+p_2\left(\left|[S_2]\right|^{-\frac{1}{2}}\exp[-\frac{1}{2}(\mathbf{x}-\bar{\mathbf{x}}_2)^T[S_2]^{-1}(\mathbf{x}-\bar{\mathbf{x}}_2)]\right)}. \quad (10)$$

In this study, the probability threshold at which a case was classified as belonging to one group or the other was incrementally adjusted between 0 and 1. This process is explained Chapter II, Section G which describes the ROC curves.

F. JACKKNIFE ROUTINE

A Jackknife routine eliminates one case at a time and recalculates the relevant statistics (Wilks 2005). For example, the first case can be removed from the data matrix which results in a matrix with dimensions ([n-1] x k). The linear discriminant analysis is performed on this matrix and the resulting discriminant function can then be used to classify the excluded case. The process is repeated by re-inserting the first case and removing the second case, and so on. This routine provides a method for testing the function with independent data in the absence of a new dataset.

G. HEIDKE SKILL SCORE (HSS)

Forecast verifications are often placed in contingency tables similar to Table 2.

Table 2 A contingency table in which forecast status is compared with observed status. Hits are represented by a, false alarms by b, misses by c, and correct nulls by d.

	Observed Yes	Observed No
Forecast Yes	A	b
Forecast No	C	d

According the Wilks (2006), the reference accuracy measure in the HSS is the proportion of random forecasts (statistically independent of the observations) that would be correct. Perfect forecasts receive a score of 1 and forecasts equivalent to random chance receive a score of 0. If the forecasts are worse than random forecasts, they receive a negative score. The probability of a correct "yes" forecast by chance is equal to the probability of a "yes" forecast times the probability of a "yes" observation, or

$$\frac{(a+b)}{n}\frac{(a+c)}{n}=\frac{(a+b)(a+c)}{n^2}, \qquad (11)$$

and the probability of a correct "no" forecast is

$$\frac{(b+d)}{n}\frac{(c+d)}{n}=\frac{(b+c)(c+d)}{n^2}. \qquad (12)$$

These definitions are equivalent to the assumption that the forecasts and observations are independent. The HSS is then equal to the ratio of the number correct to the number incorrect by chance, divided by one minus the number correct by chance, which simplifies to:

$$\mathrm{HSS}==\frac{2(ad-bc)}{(a+c)(c+d)+(a+b)(b+d)} \qquad (13)$$

The HSS is first calculated for discriminant functions containing all possible combinations of the nine parameters. The discriminant function that shows the most skill is then submitted to the jackknife procedure.

H. RECEIVER OPERATING CHARACTERISTICS (ROC) CURVES

The use of Receiver Operating Characteristic (ROC) curves originated in the signal processing community. In this sense, the threshold for which a signal is determined to be present is incrementally adjusted between the point at which a signal is always detected and the point at which a signal is never detected. The probability of detection, or hit rate (equivalent to d/(c+d) in Table 2), and the false-alarm rate (equivalent to b/(a+b) in Table 2) are calculated for each of these thresholds. These points are plotted on a graph with the false-alarm rate (0 to 1) along the x-axis and the hit rate (0 to 1) along the y-axis. The resulting points form the ROC curve.

A ROC curve that followed a diagonal from (0,0) to (1,1) would indicate that the 'receiver' produced as many false alarms as hits. The area under the curve in this case would be 0.5. The ideal ROC curve would follow along the left and top axes which would indicate that the receiver had a perfect hit rate and produced no false alarms. The area under this curve would be 1. In reality, most receivers fall somewhere between these two extremes. The closer a ROC curve is to the upper left corner, the closer the receiver is to ideal (all hits and no false alarms). Therefore, the area under the curve (AUC) is one measure of performance.

For purpose of this study, the threshold for which a candidate vortex was classified as being a developer was varied. By default, this number is 0.5. If, based on the jackknifed discriminant function, a vortex has classification scores of 0.51 for Group 1 (developers) and 0.49 for Group 2 (false alarms) it is automatically classified as a developer. By allowing the threshold to vary, some degree of fuzziness is introduced into the analysis and an additional measure of skill, the Area Under the Curve (AUC), becomes available. Furthermore, the classification threshold value that produces the point on the ROC curve that is farthest from the diagonal is chosen as the optimal threshold for the applicable model and forecast period.

THIS PAGE INTENTIONALLY LEFT BLANK

III. RESULTS

A. PRESENTATION OF DISCRIMINANT ANALYSIS STATISTICS

Table 3 is divided into ten blocks for the ten forecast intervals with a row for each of the three models. The first and second columns list the model and forecast period (tau), respectively. The third column lists the predictors that were used in the applicable discriminant function (Table 4 lists the parameters that corresponds to the numbers in this column). The fourth and fifth columns contain two HSS values. The first score is for the discriminant function using dependent data and the second score is for the discriminant function using the independent data. Both skill scores were calculated for a classification threshold of 0.5. The sixth column gives the Area Under the Curve (AUC) for the ROC curves displayed in the subsequent figures.

The next section includes a summary of the results for each forecast interval. One of the key results is the parameters that are common to the discriminant functions applied to each model. The relevant HSS and ROC curves are also summarized. In the summary of 12-h forecasts, a detailed example of the methodology as applied to the UKMET 12-h model data will be provided. The last section of this chapter will describe two classification case studies.

Table 3 Results of the Linear Discriminant Analysis.

Model	Tau	Predictors Used	Maximum HSS	Jackknife HSS	AUC
GFS	12h	1, 2, 4, 5	0.5924	0.2917	0.5382
NGP	12h	1, 2, 3, 5, 8, 9	0.6063	0.2475	0.5500
UKM	12h	1, 2, 3, 6, 7, 8, 9	0.7856	0.5470	0.7289
GFS	24h	1, 2, 3, 4, 5, 6, 7, 8	0.6071	0.3277	0.5778
NGP	24h	2,3,5,8,9	0.5259	0.2582	0.5974
UKM	24h	2,3,6,7,8,9	0.6528	0.4215	0.6447
GFS	36h	1, 2, 4, 6, 7, 8, 9	0.5086	0.1872	0.569
NGP	36h	1,2,4,5,6,9	0.5816	0.2763	0.5853
UKM	36h	2,3,5,6	0.6252	0.4250	0.6000
GFS	48h	1, 2, 3, 8	0.4811	0.3456	0.6033
NGP	48h	2, 5, 7, 8, 9	0.6476	0.3393	0.5500
UKM	48h	1,2,4,6,7,9	0.7952	0.5597	0.7500
GFS	60h	1, 7, 8	0.1261	0.1614	0.5500
NGP	60h	1,3,5,7,8,9	0.3902	0.0691	0.5136
UKM	60h	1,4,5,6,7,9	0.9344	0.4516	0.7250
GFS	72h	1, 2, 3, 4, 5, 7, 9	0.4167	0.1619	0.5611
NGP	72h	1,2,4,6,7,9	0.6704	0.3987	0.6000
UKM	72h	2, 3, 4	0.6102	0.3060	0.5800
GFS	84h	2, 4, 6, 7, 9	0.5098	0.2735	0.6375
NGP	84h	1,2,3,4,5,7	0.7492	0.3194	0.6409
UKM	84h	1,2,7,8	0.8095	0.4783	0.6643
GFS	96h	2, 3, 6, 8, 9	0.5000	0.3750	0.6167
NGP	96h	4,6,8	0.3241	0.2118	0.5500
UKM	96h	5	1.0000	0.0000	0.0000
GFS	108h	2, 3, 4	0.6038	0.3123	0.5800
NGP	108h	1	0.0000	-0.1030	0.4300
UKM	108h	1, 2, 9	1.0000	0.3077	0.6667
GFS	120h	1, 2, 3, 5, 6, 7	0.5503	0.0979	0.5500
NGP	120h	1	0.0000	-0.0593	0.3500
UKM	120h	2,3,6	0.7200	0.4235	0.6500

Table 4 List of parameters corresponding to numbers in column 3 of Table 3.

1	2	3	4	5	6	7	8	9
850-500 hPa Average Vorticity	700-500 hPa Warm Core	850-500 hPa Shear	850-200 hPa Shear	850-200 hPa Thickness	500 hPa Omega	700-500 hPa Vapor Pressure	SLP Difference	SLP Minimum

B. DISCUSSION OF RESULTS

1. 12-h Forecasts

a. Application of Methodology to UKMET Forecast

A total of 19 developers and 31 false alarms were identified in the scatterplot for the UKMET 12-h model data (see Appendix B). The pertinent matrices for developers (19 x 9) and false alarms (31 x 9) were submitted to a series of linear discriminant analyses that considered all possible combinations of the nine parameters. Using a contingency table (as in Table 2), the HSS was calculated for each of the discriminant functions and the function that resulted in the highest HSS was selected. In the UKMET 12-h case, a discriminant function using seven of the nine parameters (850-500 hPa Average Vorticity, 700-500 hPa Warm Core, 850-500 hPa Shear, 500 hPa Omega, 700-500 hPa Vapor Pressure, SLP Difference, and SLP Minimum) exhibited the most skill.

Table 5 indicates that only five cases were misclassified by the discriminant function applied to the UKMET 48-h forecast. Three cases did develop despite being classified as false alarms and two cases did not develop despite being classified as developers. These results, as applied to the calculation of the HSS, are more simply displayed in a contingency table (Table 6), which can also be used to compute hit and false-alarm rates for use in a ROC diagram.

The next step was to perform a jackknife routine on the UKMET 12-h forecast data and recalculate all relevant statistics. As expected, the contingency table for the discriminant function using the independent data (Table 7) has less skill (HSS=0.55) compared to that using dependent data (HSS=0.79).

Table 5 Classification results for the relevant discriminant function as applied to dependent data from the UKMET 12-h model. Column one lists the actual group membership of each vortex; a '1' represents a developer and a '2' represents a false alarm. Column two lists the group to which each vortex was assigned by the discriminant function. The probabilities, according to the discriminant function, that the vortex belongs to group '1' and '2' are listed in columns three and four, respectively. Shaded rows represent vortices that were misclassified by the discriminant function. The three light grey rows represent vortices that did develop, but were classified as false alarms. The two dark grey rows represent vortices that did not develop, but were classified as developers.

Observed	Forecast	Group 1 Probability	Group 2 Probability
1	1	0.9504	0.0496
1	1	0.6554	0.3446
1	1	0.6665	0.3335
1	1	0.9802	0.0198
1	1	0.6624	0.3376
1	1	0.5493	0.4507
1	2	0.2386	0.7614
1	1	0.9644	0.0356
1	1	0.9048	0.0952
1	2	0.1819	0.8181
1	2	0.2827	0.7173
1	1	0.6362	0.3638
1	1	0.9287	0.0713
1	1	0.5582	0.4418
1	1	0.8837	0.1163
1	1	0.9443	0.0557

Observed	Forecast	Group 1 Probability	Group 2 Probability
1	1	0.9136	0.0864
1	1	0.8541	0.1459
1	1	0.9724	0.0276
2	2	0.4337	0.5663
2	1	0.9111	0.0889
2	2	0.0458	0.9542
2	2	0.1063	0.8937
2	2	0.0131	0.9869
2	2	0.0027	0.9973
2	2	0.0257	0.9743
2	2	0.1172	0.8828
2	2	0.0228	0.9772
2	2	0.0104	0.9896
2	2	0.2150	0.7850
2	2	0.1772	0.8228
2	2	0.0466	0.9534
2	2	0.0409	0.9591
2	2	0.1677	0.8323
2	2	0.0039	0.9961
2	2	0.0083	0.9917
2	2	0.0016	0.9984
2	2	0.3498	0.6502
2	2	0.0792	0.9208
2	2	0.0900	0.9100
2	2	0.0285	0.9715
2	2	0.1034	0.8966
2	2	0.0851	0.9149
2	2	0.0998	0.9002
2	2	0.4097	0.5903
2	2	0.0946	0.9054
2	2	0.0285	0.9715
2	2	0.3352	0.6648
2	2	0.4662	0.5338
2	1	0.9547	0.0453

Table 6 Classification results from Table 5 summarized as a forecast contingency table. In this case, the HSS is 0.79.

	Observed Developer	Observed Non-developer
Forecast Developer	16	2
Forecast False alarm	3	29

Table 7 Forecast contingency table for the relevant discriminant function as applied to independent data from the UKMET 12-h model. In this case, the HSS is 0.55.

	Observed Developer	Observed Non-developer
Forecast Developer	15	7
Forecast False alarm	4	24

In both of the above scenarios the skill scores were calculated using a classification threshold of 0.5. For the purpose of calculating hit and false-alarm rates to generate ROC curves, contingency tables were produced for the independent data by adjusting the classification threshold from 0 to 1 by increments of 0.1 (Table 8). At a threshold of zero, every case is classified to be a developer, and at a threshold of 1.0, every case is classified as a false alarm. The hit and false-alarm rates resulting from the thresholds between these two extremes were plotted to form a ROC curve (Figure 7). In this UKMET 12-h case, the point plotted for the threshold of 0.4 is the farthest from the diagonal and is therefore regarded as the optimal threshold.

Table 8 Forecast contingency tables for the relevant discriminant function as applied to independent data from the UKMET 12-h model. Each two-row block gives the results produced using the threshold listed in column 1. The last column gives the resulting hit and false-alarm rates that were used to plot a ROC curve for the discriminant function.

Threshold		Observed Developer	Observed Non-Developer	
0.0	Forecast Developer	19	31	Hit Rate: 19/19
	Forecast False alarm	0	0	False-alarm Rate: 31/31
0.1	Forecast Developer	19	19	Hit Rate: 19/19
	Forecast False alarm	0	12	False-alarm Rate: 19/31
0.2	Forecast Developer	18	11	Hit Rate: 18/19
	Forecast False alarm	1	20	False-alarm Rate: 11/31
0.3	Forecast Developer	16	8	Hit Rate: 16/19
	Forecast False alarm	3	23	False-alarm Rate: 8/31
0.4	Forecast Developer	16	8	Hit Rate: 16/19
	Forecast False alarm	3	24	False-alarm Rate: 8/31
0.5	Forecast Developer	15	7	Hit Rate: 15/19
	Forecast False alarm	4	24	False-alarm Rate: 7/31
0.6	Forecast Developer	15	4	Hit Rate: 15/19
	Forecast False alarm	4	27	False-alarm Rate: 4/31
0.7	Forecast Developer	11	3	Hit Rate: 11/19
	Forecast False alarm	8	28	False-alarm Rate: 3/31
0.8	Forecast Developer	10	2	Hit Rate: 10/19
	Forecast	9	29	False-alarm

Threshold		Observed Developer	Observed Non-Developer	
	False alarm			Rate: 2/31
0.9	Forecast Developer	9	2	Hit Rate: 9/19
	Forecast False alarm	10	29	False-alarm Rate: 2/31
1.0	Forecast Developer	0	0	Hit Rate: 0/19
	Forecast False alarm	19	31	False-alarm Rate: 0/31

b. Results for 12-h Forecasts

At 12h, the discriminant functions applied to all models (Table 3) include vorticity and warm core parameters. The functions applied to GFS and NOGAPS also include the thickness parameter. Functions applied to the NOGAPS and UKMET models include the 850-500 hPa shear and both SLP parameters. The highest skill score is attained by the application of the discriminant function to the UKMET model. This score is 0.79 using dependent data (compared to 0.59 and 0.60 for GFS and NOGAPS, respectively) and 0.55 using independent data (compared to 0.29 and 0.25 for GFS and NOGAPS, respectively). The ROC curve for the UKMET function (Figure 7) also has the largest AUC (0.73 compared to 0.53 and 0.55 for GFS and NOGAPS, respectively) with an optimal classification threshold of 0.4. Therefore, the methodology applied to forecasts from the UKMET model, as described in the previous section, results in the most accurate discrimination between developing vortices and false alarms.

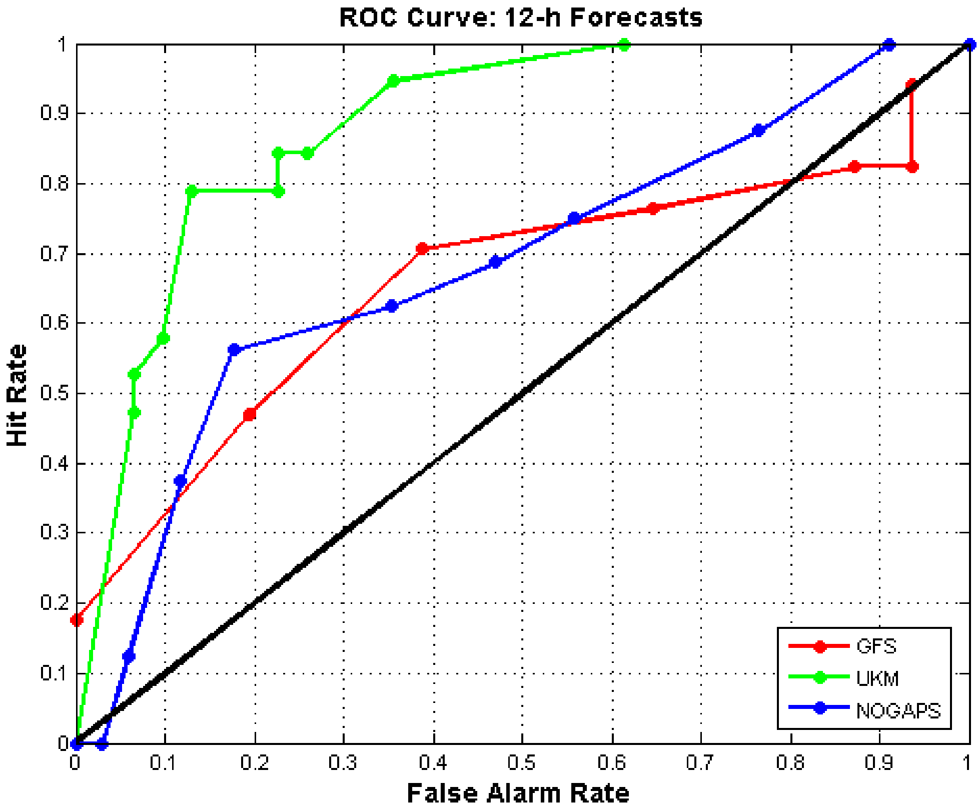

Figure 7 ROC curves for 12-h forecasts based on an independent dataset. The curve for the function applied to GFS is displayed in red, UKMET in green, and NOGAPS in blue.

2. 24-h Forecasts

For the 24-h forecast interval, the discriminant functions applied to each of the three sets model forecasts (Table 3) again include the warm core parameter, but only the GFS function includes vorticity. All functions also include 850-500 hPa shear and the SLP difference. The functions applied to the GFS and NOGAPS models include a thickness parameter while the GFS and UKMET functions include the omega and vapor pressure parameters. The functions for the NOGAPS and UKMET models include SLP minimum.

The discriminant function applied to the UKMET model data again has the highest skill in identifying developing vortices using both dependent data (HSS equal to 0.65 compared to 0.60 for GFS and 0.53 for NOGAPS) and independent data (HSS equal to 0.42 compared to 0.33 for GFS and 0.26 for NOGAPS. The ROC curve (Figure 8) for the UKMET model again has the largest area (AUC equal to 0.64 compared to 0.58 for GFS and .060 for NOGAPS) with an optimal classification threshold of 0.4. Overall, the discriminant analysis applied to the UKMET forecast is marginally more successful in identifying developing vortices than that applied to NOGAPS or GFS.

3. 36-h Forecasts

All three 36-h forecasts resulted in discriminant functions that included the warm core and omega parameters (Table 3). In addition, functions applied to the GFS and NOGAPS models include vorticity, 850-200 hPa shear, and SLP minimum. The functions applied to the NOGAPS and UKMET models also utilize the thickness parameter.

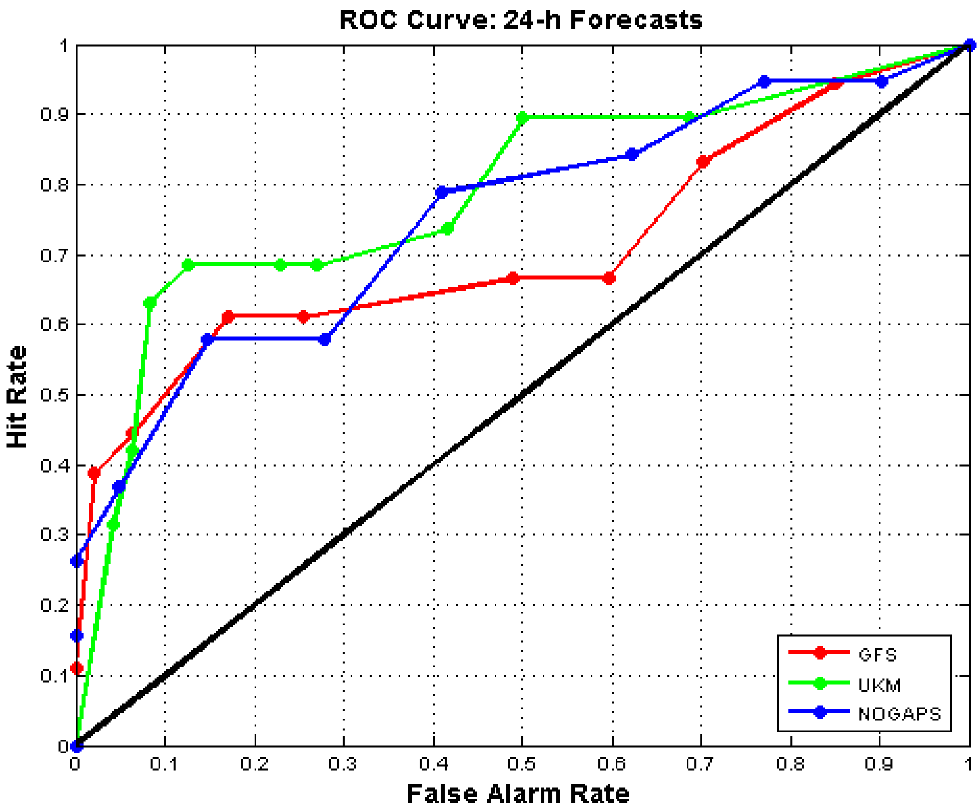

Figure 8   ROC curves as in Figure 7, except for 24-h forecasts.

As for the 12-h and 24-h forecasts, the function applied to the UKMET model data has the most skill in discriminating between developing vortices and false alarms. While the skill scores for the functions using dependent data were not significantly different among the three models (0.51, 0.58, 0.63 for GFS, NOGAPS and UKMET, respectively), the skill scores using independent data had a much larger range (0.19, 0.28, 0.43, respectively). The AUC for the UKMET ROC curve (Figure 9) is 0.60 which is only slightly more than that for NOGAPS (0.59) and GFS (0.57). The optimal threshold for the UKMET function is 0.5. Therefore, the discriminant function applied to UKMET model forecasts again exhibits marginally increased skill in identifying developing vortices.

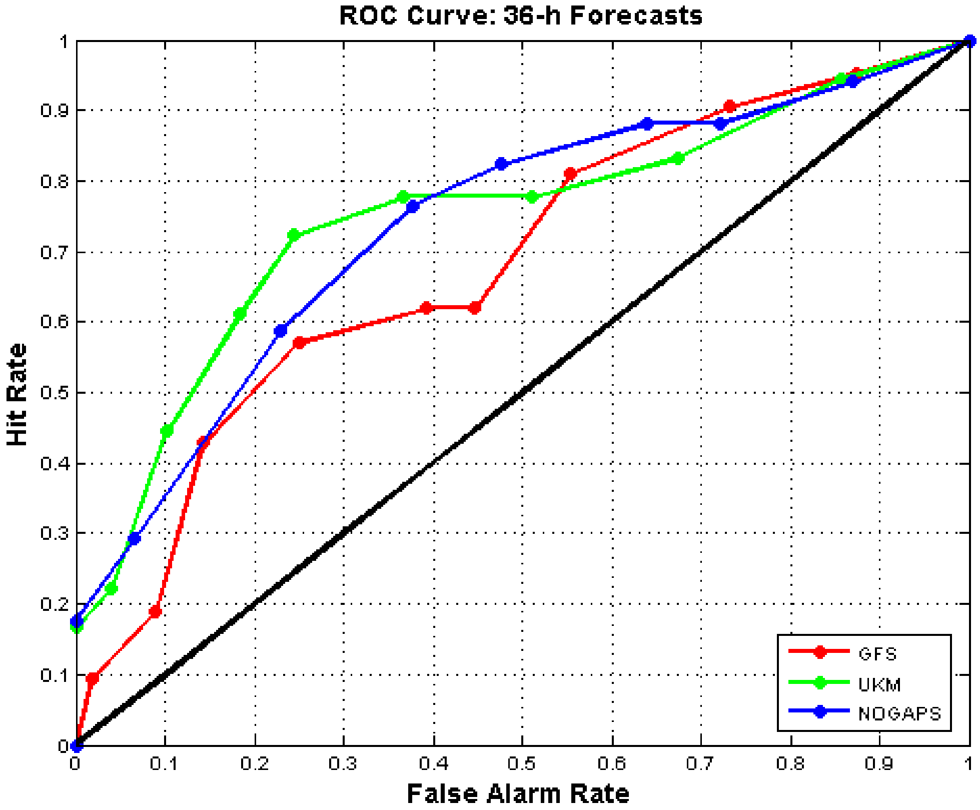

Figure 9 ROC curves as in Figure 7, except for 36-h forecasts.

4. 48-h Forecasts

For the 48-h forecasts, the discriminant functions applied to all models once again include the warm core parameter (Table 3). The functions for the GFS and NOGAPS models include the SLP difference. The functions for the NOGAPS and UKMET models include vapor pressure and SLP minimum. The functions for the GFS and UKMET models include vorticity.

The function applied to the UKMET forecast again attained the highest skill score. The HSS was 0.80 when applied to dependent data and 0.56 when applied to independent data. By comparison, these scores were 0.48 and 0.35 for the GFS function and 0.65 and .034 for the NOGAPS function. The ROC curve for the UKMET function

(Figure 10) also has the largest area. The AUC was 0.75 as compared to 0.60 for the GFS function and 0.55 For the NOGAPS function. The optimal classification threshold for the UKMET function was 0.5. Overall at 48 hours, the methodology applied to forecasts from the UKMET model results in the most accurate discrimination between developing vortices and false alarms.

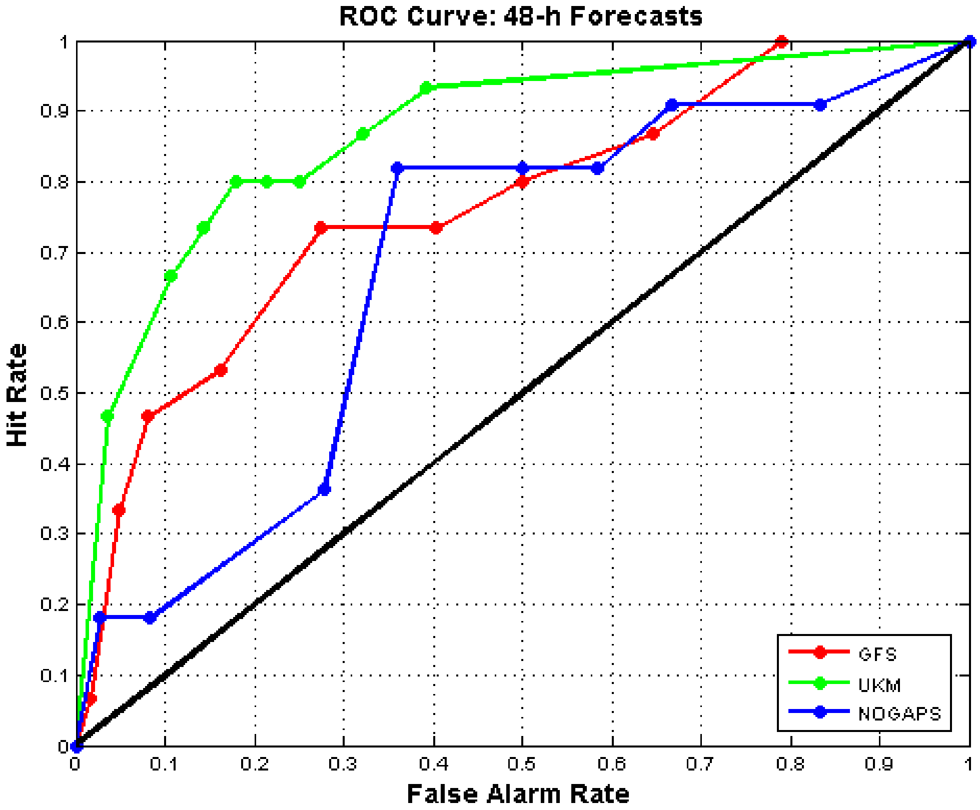

Figure 10 ROC curves, as in Figure 7, except for 48-h forecasts.

5. 60-h Forecasts

All functions for the 60-h forecasts include vorticity and vapor pressure (Table 3). The functions applied to the GFS and NOGAPS forecasts include the SLP difference while the functions applied to the NOGAPS and UKMET forecasts include the thickness parameter and the SLP minimum.

The discriminant function applied to the UKMET model has significantly more skill in identifying developing vortices than the other functions. Using dependent data, the HSS was 0.93 as compared to only 0.13 and 0.39 for the functions applied to the GFS and NOGAPS models. Using independent data, the UKMET score was 0.45 as compared to 0.16 and 0.07 for the functions applied to the GFS and NOGAPS models. While the ROC curves (Figure 11) are not as widely spread as the skill scores, the curve for the UKMET function (with an optimal classification threshold of 0.6) still has an AUC of 0.73 compared to only 0.55 and 0.51 for GFS and NOGAPS, respectively. Overall, the discriminant analysis applied to the UKMET model is significantly more successful in identifying developing vortices.

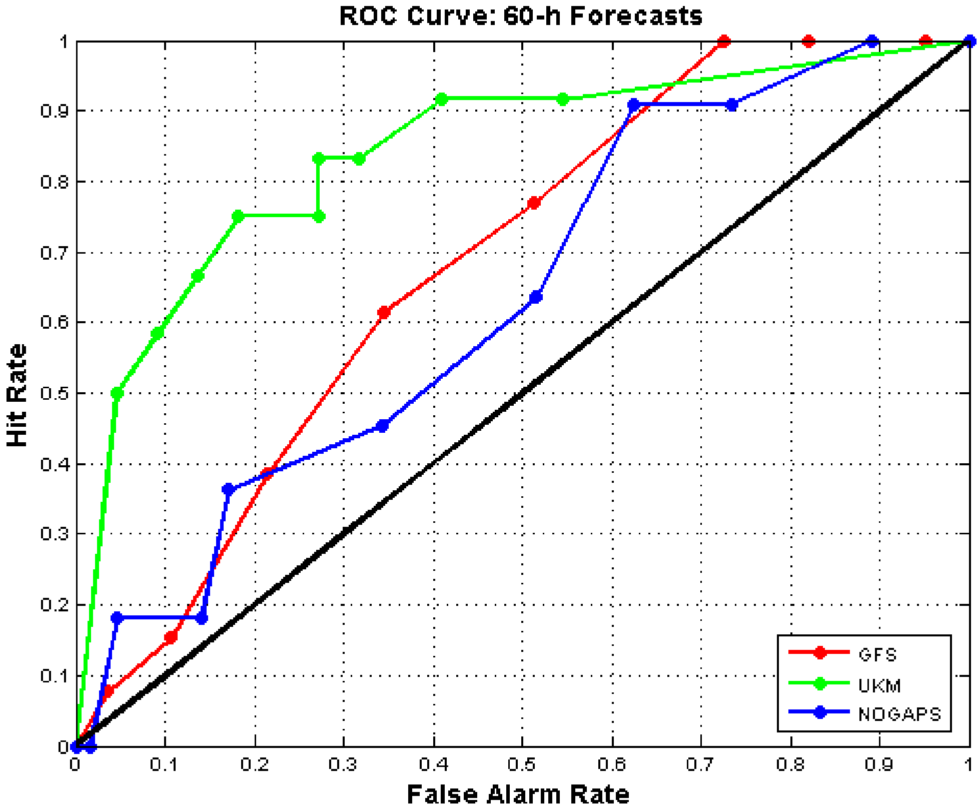

Figure 11 ROC curves, as in Figure 7, except for 60-h forecasts.

6. 72-h Forecasts

Using 72-h model forecasts, all discriminant functions include the warm core and 850-200 hPa shear (Table 3). The functions applied to the GFS and NOGAPS models include the SLP minimum. The functions applied to the GFS and UKMET models include vorticity and 850-500 hPa shear. The functions applied to the GFS and NOGAPS models include vapor pressure.

The function applied to the NOGAPS forecast has more skill than the GFS and UKMET functions. The HSS was 0.67 using dependent data (compared to 0.42 for GFS and 0.61 for UKMET) and 0.40 using independent data (compared to 0.16 for GFS and 0.31 for UKMET). While the skill scores for the functions using both the dependent and independent data spanned a wide range, the ROC curves were closely grouped. The ROC curve (Figure 12) for the discriminant function applied to NOGAPS had the largest AUC (0.60) but this is only slightly more than the curves for the GFS (0.56) or UKMET (0.58) functions. The optimal classification threshold for the NOGAPS function is 0.6. Overall, the function for the NOGAPS forecast has slightly more skill in identifying developing vortices at 72h.

7. 84-h Forecasts

For the 84-h forecasts, the discriminant functions for all models include the warm core parameter and vapor pressure parameters (Table 3). The functions applied to the GFS and NOGAPS models include the 850-200 hPa shear. The functions applied to the NOGAPS and UKMET models include vorticity.

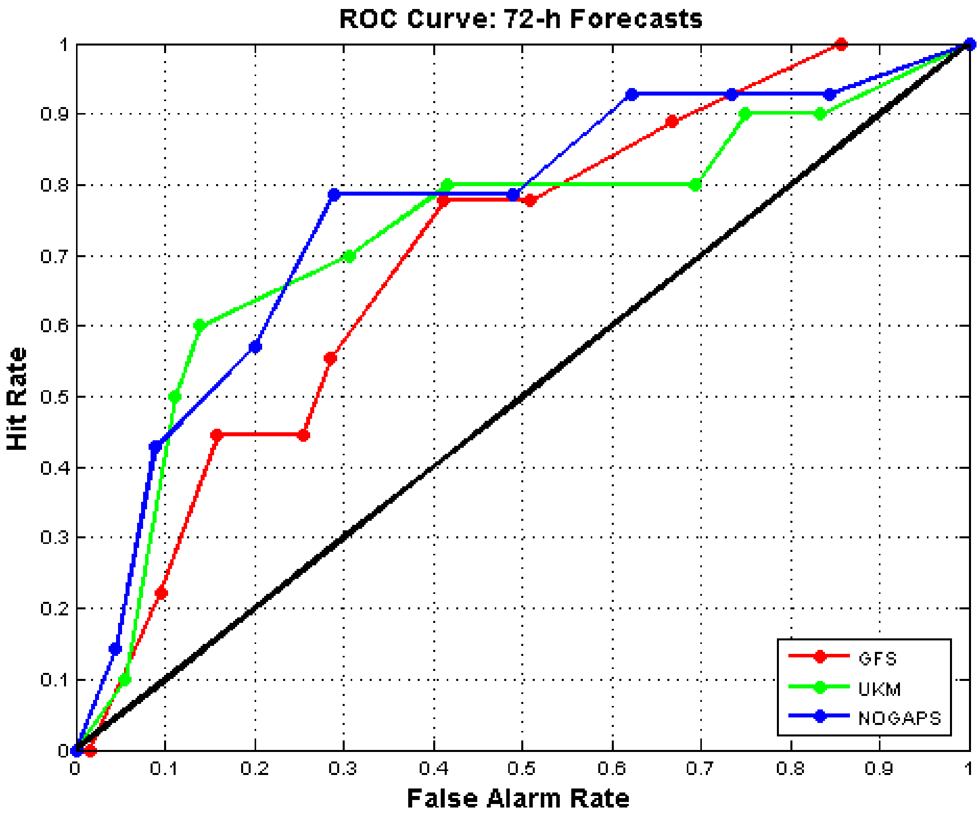

Figure 12 ROC curves as in Figure 7, except for 72-h forecasts.

The discriminant function applied to the UKMET model forecasts has a significantly higher HSS using both dependent / independent data (0.81 / 0.48, respectively, compared to 0.51 / 0.27 for GFS and 0.75 / 0.32 for NOGAPS). The ROC curves (Figure 13) are closely grouped for the three functions, but the UKMET function still has the largest AUC at 0.66 compared to 0.64 for the functions applied to both GFS and NOGAPS. Overall, the function applied to UKMET model data exhibits the most skill at 84h.

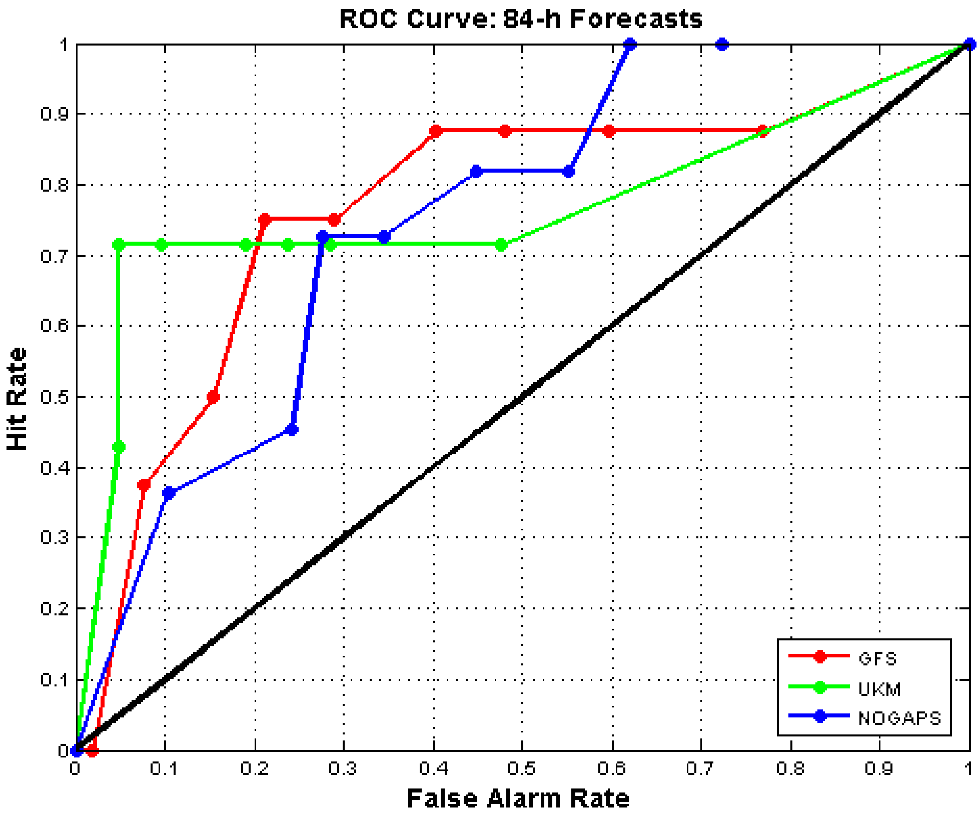

Figure 13 ROC curves as in Figure 7, except for 84-h forecasts.

8. 96-h Forecasts

By 96h, the number of developing cases identified in each model has decreased appreciably. Only one developer was identified in the UKMET 96-h forecast which results in an unrealistic discriminant function for UKMET that includes only one parameter. Although the function has a perfect skill score using the dependent data, when that one case is removed, the function has a skill score and AUC of zero using ‘independent’ data. The corresponding ROC curve is therefore not included in Figure 14. The NOGAPS and GFS forecasts still have enough developers to make the discriminant analysis well-posed, however, as the forecast interval increases, the resulting statistics are presumed to be less meaningful given the decrease in the size of the data set.

The only parameters included in the discriminant functions for both the GFS and NOGAPS models are omega and the SLP difference. The discriminant function applied to the GFS model (with scores of 0.50 and 0.38) exhibits more skill in identifying developing vortices than that of NOGAPS (with scores of .32 and 0.21). The ROC curve (Figure 14) for the GFS function also has a slightly larger AUC (0.62) than that of NOGAPS (0.55). In summary, the methodology applied to the GFS forecast is the most successful in identifying developing vortices at 96h.

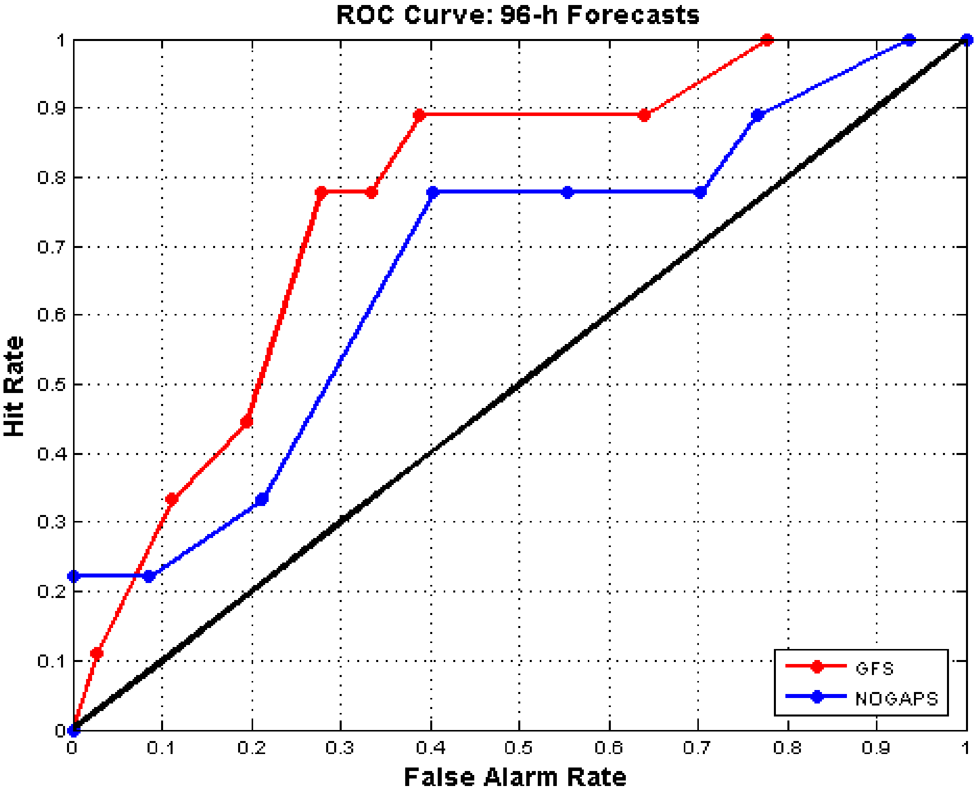

Figure 14 ROC curves as in Figure 7, except for 96-h forecasts and the curve for the UKMET function is omitted.

9. 108-h Forecasts

The NOGAPS 108-h forecast had only one developing system, therefore the methodology does not provide realistic results. This ROC curve is not included in Figure 15. The discriminant function applied to the UKMET model, which is based on significantly fewer cases than the GFS function, attains a skill score of 1 using independent data while the latter attains a skill score of 0.60. The score for the UKMET function, however, decreases to 0.31 using independent data, which is equal to that for the GFS function. The UKMET function has the largest AUC (Figure 15) at 0.67, which is only slightly larger than the AUC for the function applied to the GFS model (.58). Overall, the functions applied to UKMET and GFS model data display roughly equivalent skill at 108h.

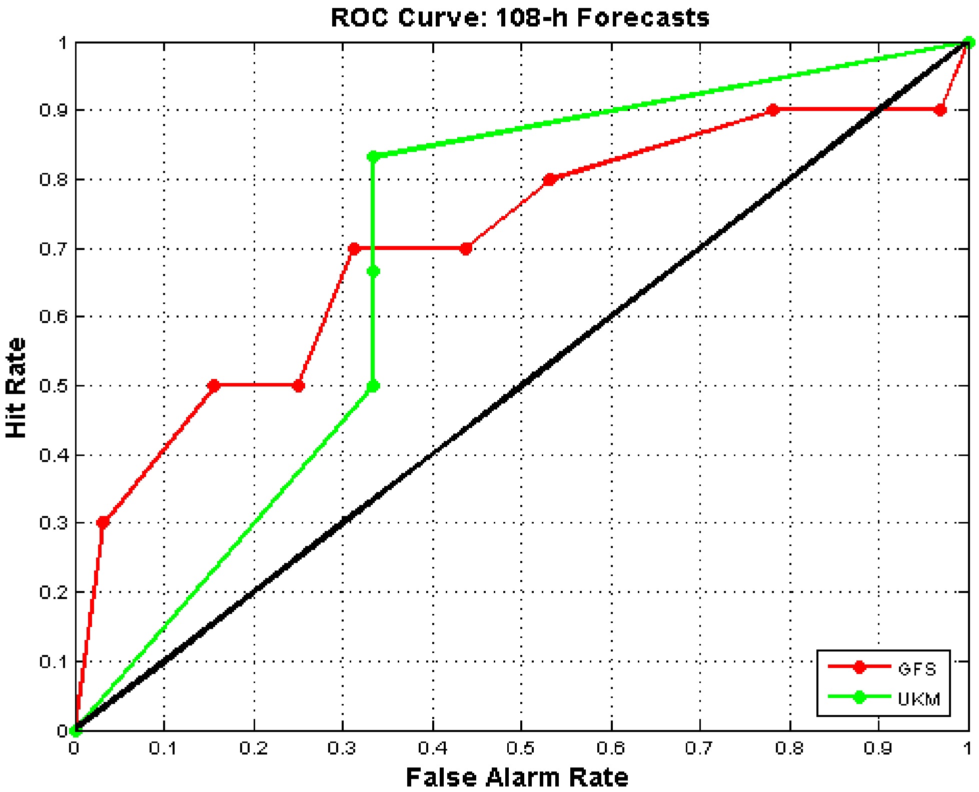

Figure 15 ROC curves as in Figure 7, except for 108-h forecasts and the curve for the NOGAPS function is omitted.

10. 120-h Forecasts

Very few 120-h forecasts of developers exist in any of the models. Since there are only two developers in the NOGAPS forecast, the methodology applied to this model is not meaningful. The ROC curve for the NOGAPS function is therefore not included in Figure 16. The discriminant functions applied to the GFS and UKMET forecasts include the warm core, 850-500 hPa shear, and omega parameters (Table 3). The function applied to the UKMET model has higher skill scores (0.72 and 0.42) than the function applied to the GFS model (0.55 and 0.10) and the ROC curve (Figure 16) for the UKMET function has a larger AUC (0.65) than that of the GFS function (0.55).

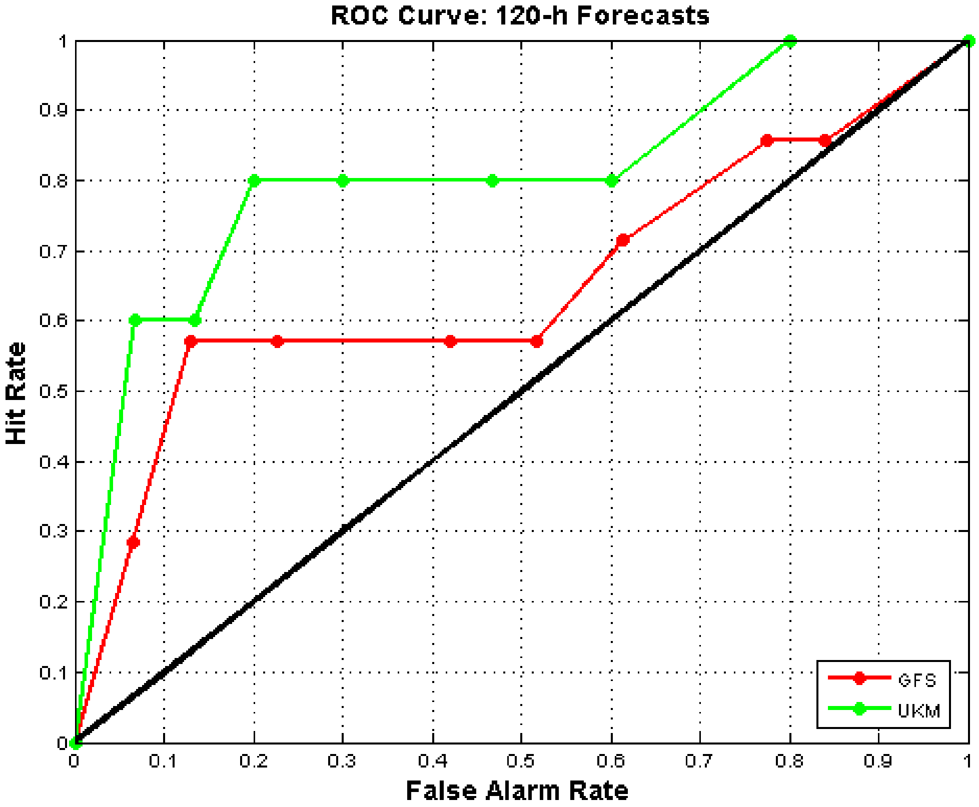

Figure 16 ROC curves as in Figure 7, except for 120-h forecasts and the curve for the NOGAPS function is omitted.

C. CLASSIFICATION EXAMPLES

In this section, two cases are examined to provide an example of how the methodology would be interpreted with respect to a single tropical vortex that is forecast to exceed vorticity and warm core thresholds.

1. Correctly Classified False Alarm

This section examines the model data, statistics, and classification of a case from the UKMET 48-h model. The vortex, which was tracked in the TCVTP from 17°N, 15°W at 1200UTC 7 July 2005, was assigned the ID "UKM_2005070712_17_015" by the database. The 48-h UKMET forecast to be discussed was initiated at 1200UTC 14 July 2005. The 48-h vorticity and warm core values for this vortex are identified on Figure 17 with a blue arrow. The sequence of forecast tracks for this vortex is shown in Figure 18. The 48-h track forecast is illustrated in Figure 19.

The UKMET forecast and analyzed values for the six parameters used in the 48-h discriminant function (Tables 3 and 4) are compared in Figures 20-25. Figure 20 illustrates that the 48-h forecast relative vorticity was *higher* than the analyzed relative vorticity. Figure 21 illustrates that the 48-h forecast warm core was *higher* than the analyzed warm core. Figure 22 illustrates that the 48-h forecast wind shear was *lower* than the analyzed wind shear. Figure 23 illustrates that the 48-h forecast vertical motion was *higher* than the analyzed vertical motion. Figure 24 illustrates that the 48-h forecast vapor pressure was *higher* than the analyzed vapor pressure. Figure 25 illustrates that the 48-h forecast sea-level pressure was *lower* than the analyzed sea-level pressure.

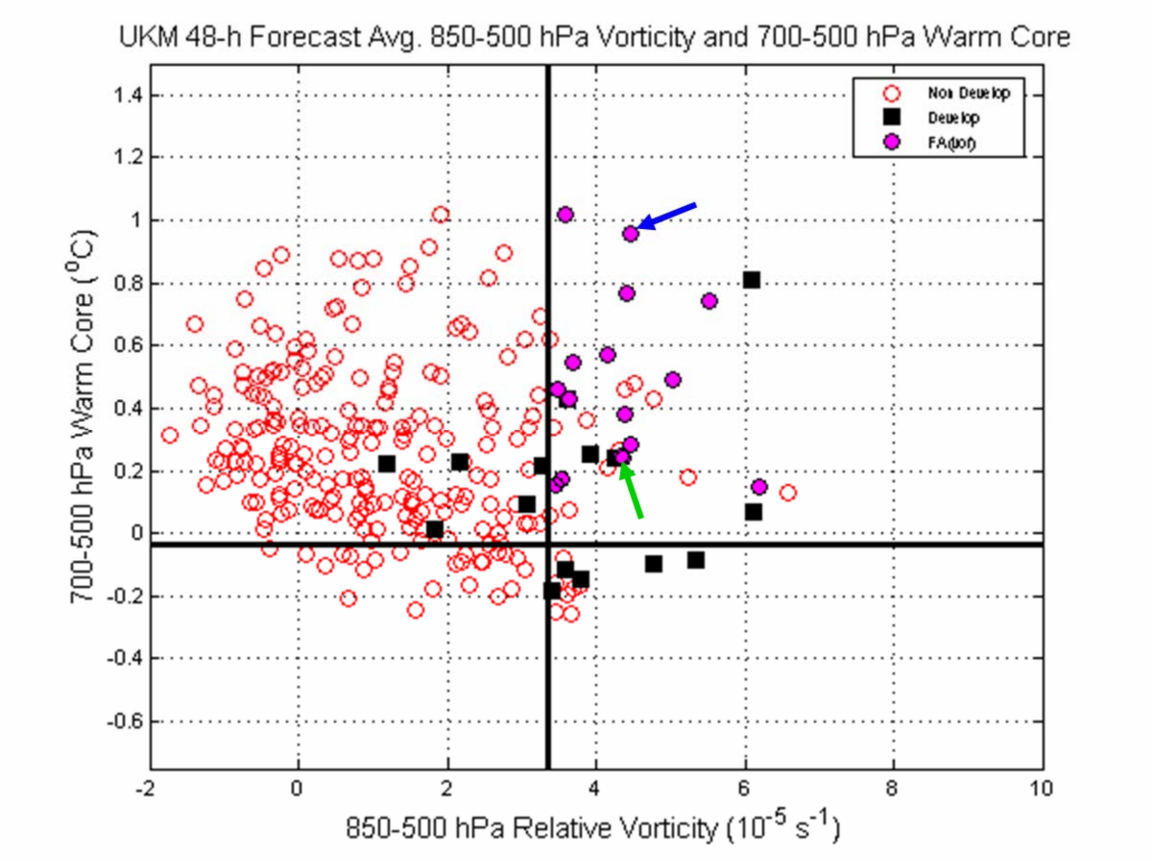

Figure 17 Scatterplot of 850-500 hPa relative vorticity and 700-500 hPa warm core for all vortices in the TCVTP database for the UKMET model at the 48-h forecast interval. The case UKM_2005070712_17_015 is highlighted with a blue arrow. The case UKM_2005091900_018_002 is highlighted with a green arrow.

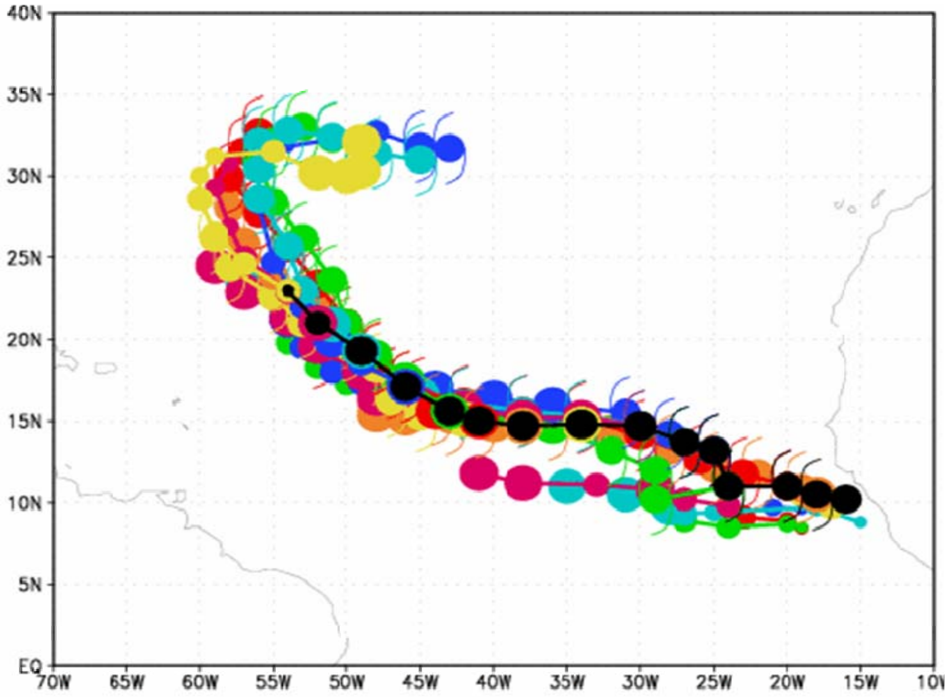

Figure 18 The analyzed track (black) and all UKMET forecast tracks (colors) for the case UKM_2005070712_17_015.

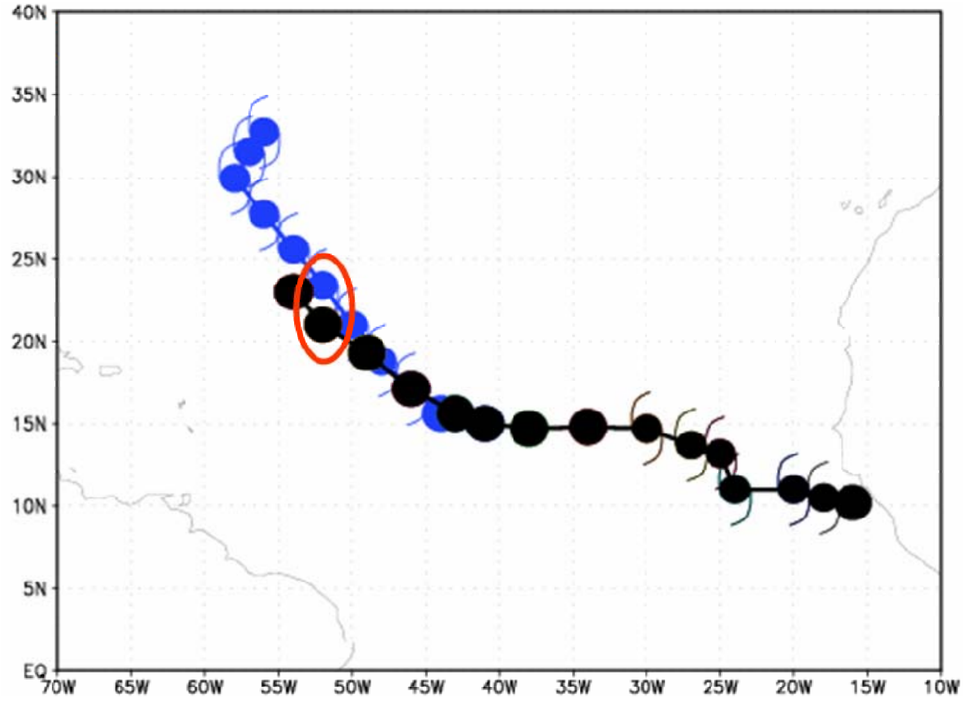

Figure 19 As in Figure 18, except with the UKMET forecast track initiated at 1200 UTC 14 July 2005 (blue) and the 48-h analyzed and forecast positions circled in red.

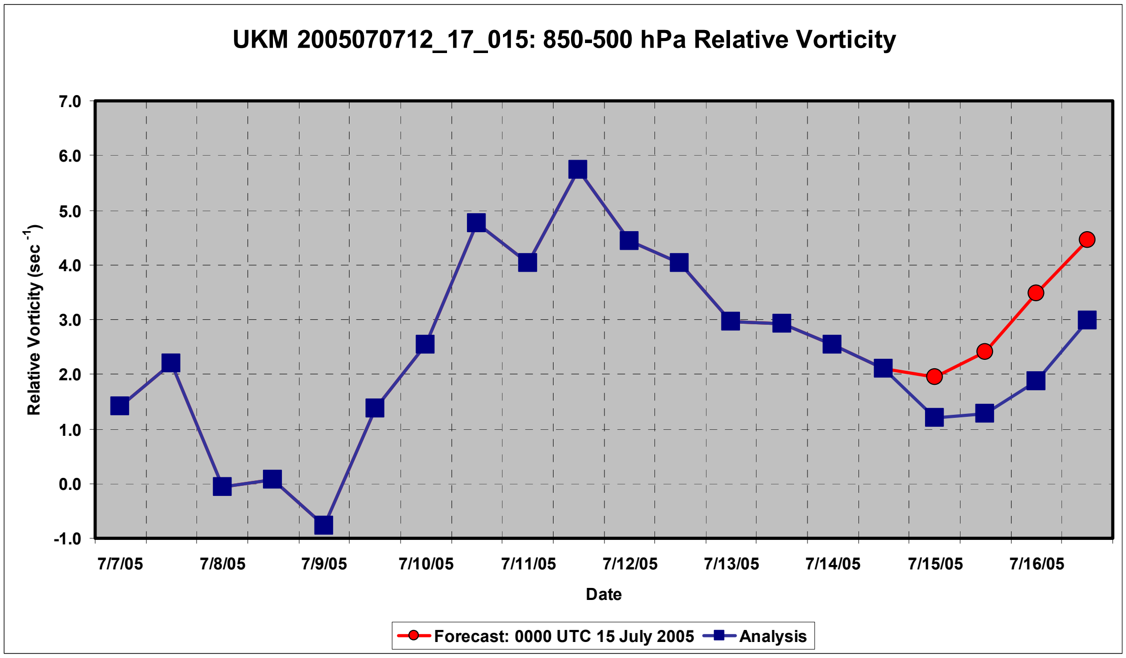

Figure 20 Average relative vorticity (10^{-5} s^{-1}) between 850 and 500 hPa for case UKM_2005070712_17_015. The UKMET 48-h forecast values from 1200 UTC 14 July 2005 are plotted with red circles, while analyzed values are plotted with blue squares.

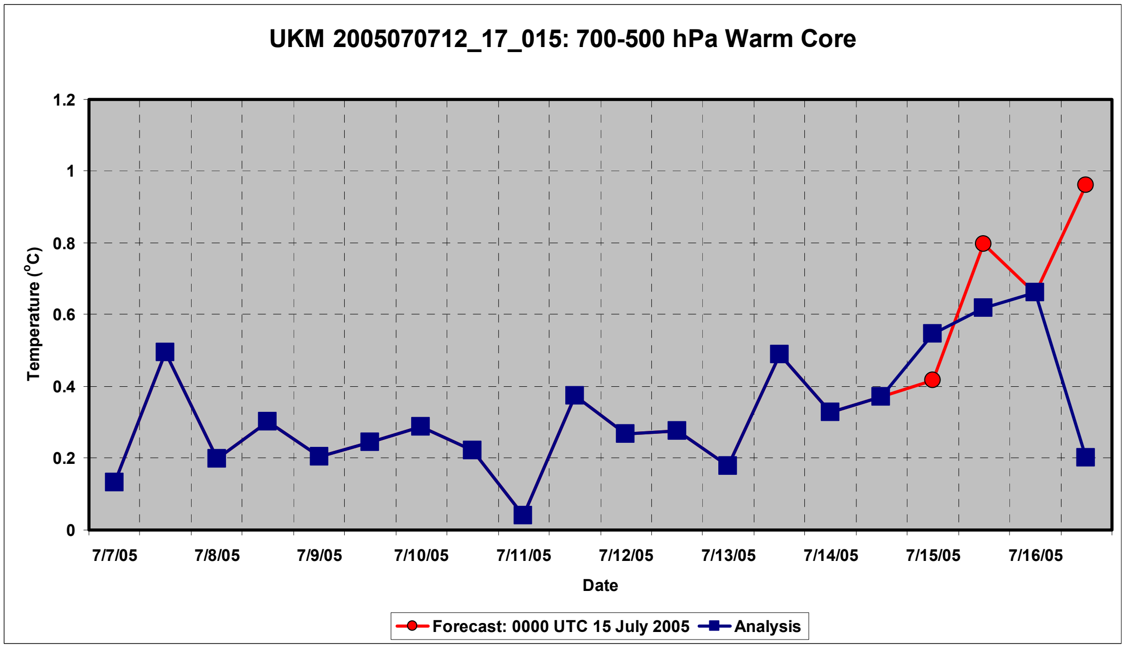

Figure 21 As in Figure 20, except for warm core (°C) at 700-500 hPa.

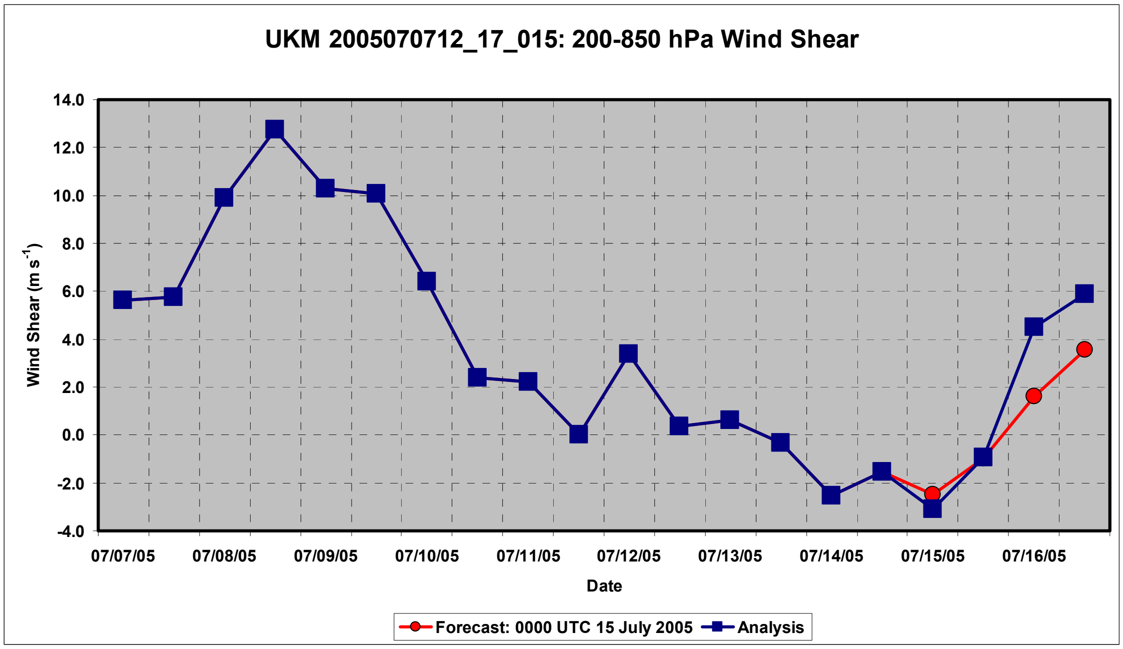

Figure 22 As in Figure 20, except for vertical wind shear (m s^{-1}) between 200 and 850 hPa.

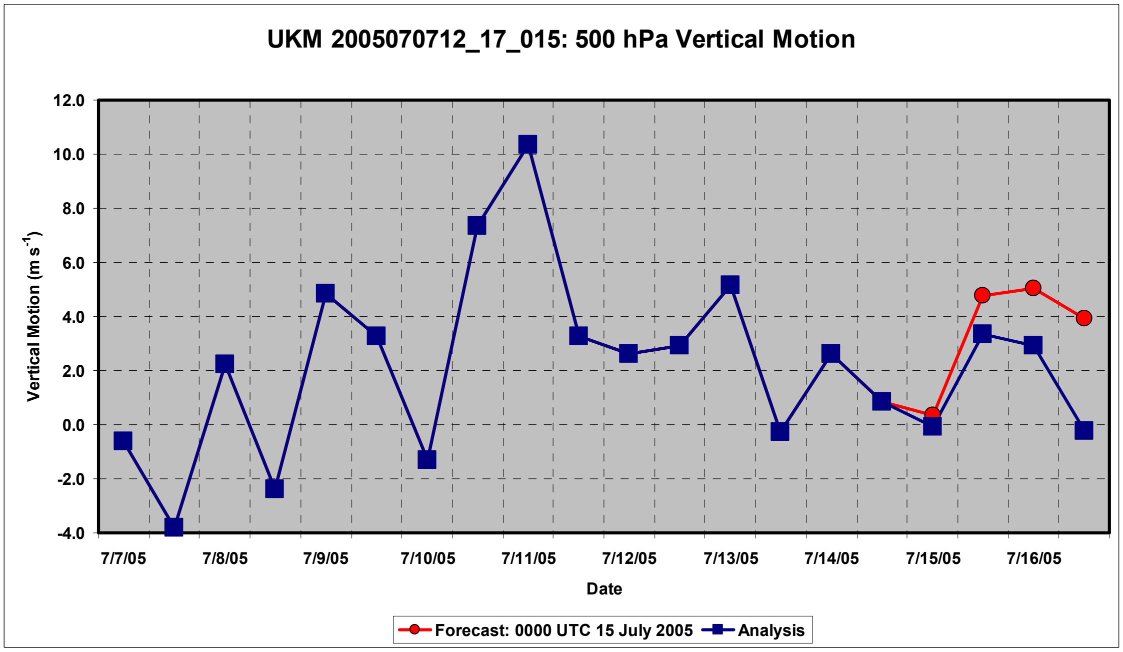

Figure 23 As in Figure 20, except for vertical motion (m s^{-1} * 10) at 500 hPa.

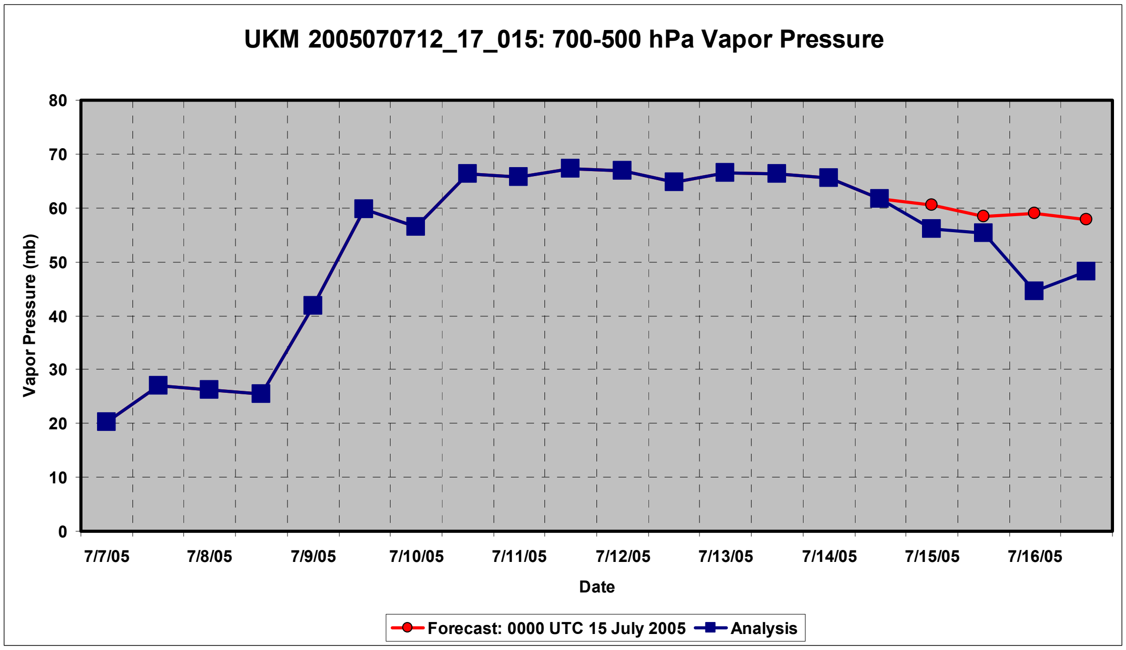

Figure 24 As in Figure 20, except for vapor pressure (mb) between 700 and 500 hPa.

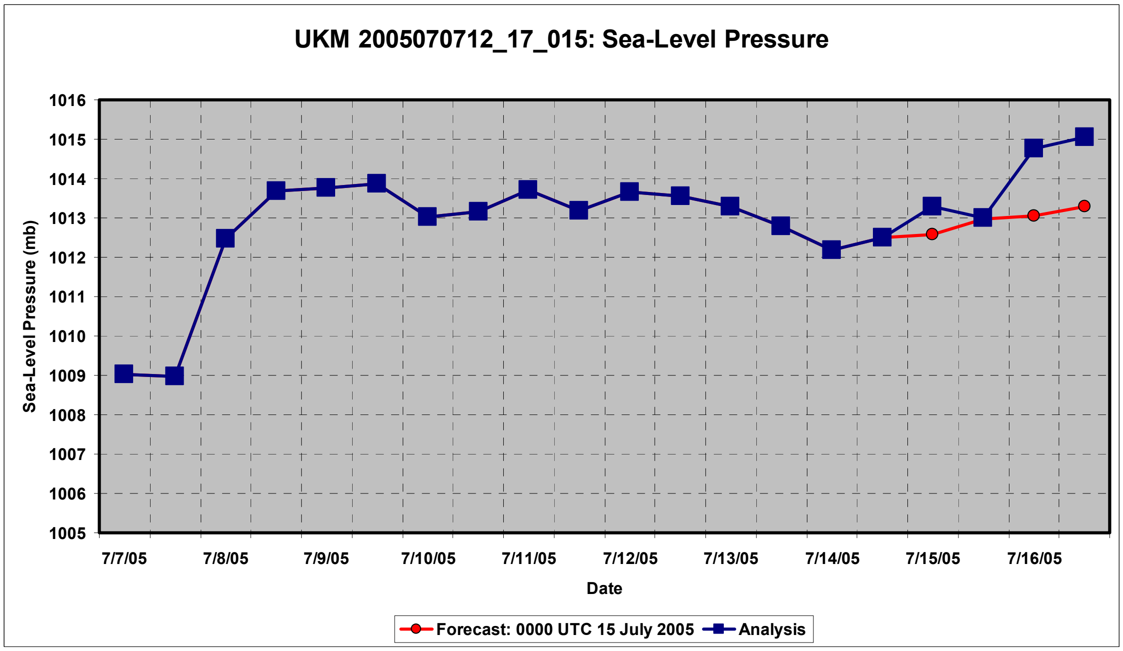

Figure 25 As in Figure 20, except for sea-level pressure (mb).

Table 9 is a list of the values of the six parameters for this case (Tables 3 and 4) compared to the overall mean values for the developer and false-alarm classifications.

The values of four of the six parameters for this case were closer to the mean values for false alarms. As defined by Equation (6) in Chapter II, Section D, the distance between each value and the midpoint of the two classification groups for each parameter contributes to the computation of the probabilities of group membership. As calculated by the discriminant analysis, the probability that this case belongs to Group 1 is 0.0003 and the probability that it belongs to Group 2 is .9997. The discriminant function therefore correctly classified this case as a false alarm.

Table 9 Six parameters for case UKM_2005070712_17_015 (third row) compared to the mean values for developers (first row) and false alarms (second row). The fourth and fifth rows contain the differences between the values for this case and the mean values for developers and false alarms, respectively. The smaller differences are highlighted.

Parameter (as in Table 4)	1	2	4	6	7	9
Mean for developers	3.76	0.13	0.85	2.05	64.73	1010.4
Mean for false alarms	4.3	0.41	0.34	1.8	60.4	1012.2
UKM_2005070712_17_015	4.464	0.96	3.54	3.94	57.82	1013.3
Difference from developers	0.70	0.83	2.7	1.9	-6.9	2.9
Difference from false alarms	0.17	0.58	3.3	2.2	-2.66	1.12

2. Incorrectly Classified False Alarm

This section examines a tropical vortex that was initially identified in the UKMET 48-h forecast at 18°N, 2°W at 0000UTC 19 September 2005 ("UKM_20050919_018_002"). The 48-h UKMET forecast to be examined was initiated at 1200 UTC 23 September 2005. Vorticity and warm core values for this vortex are identified on Figure 17 with a green arrow. The sequence of forecast tracks for this vortex is shown in Figure 26. The 48-h forecast track is illustrated in Figure 27.

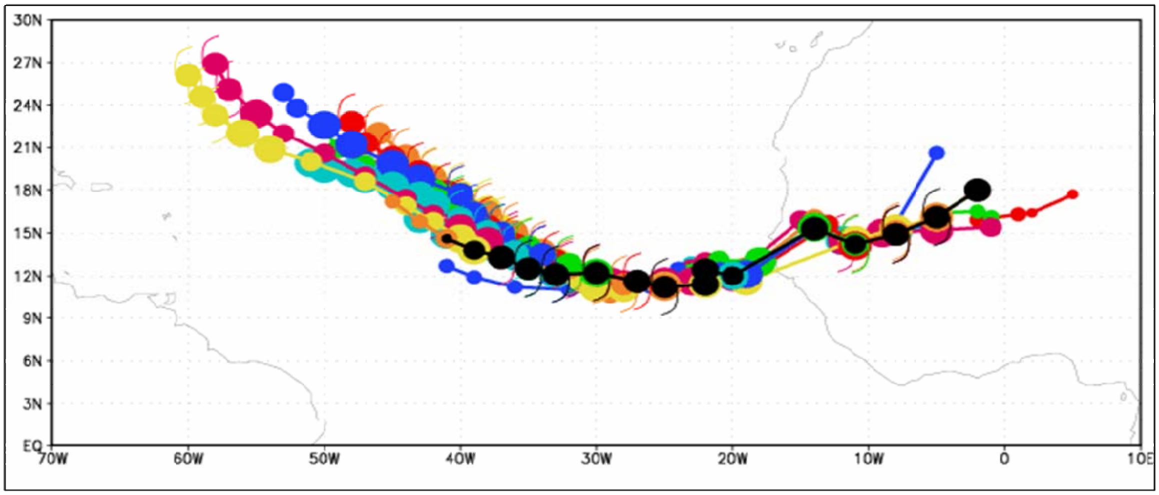

Figure 26 The analyzed track (black) and all UKMET forecast tracks (colors) for the case UKM_20050919_018_002.

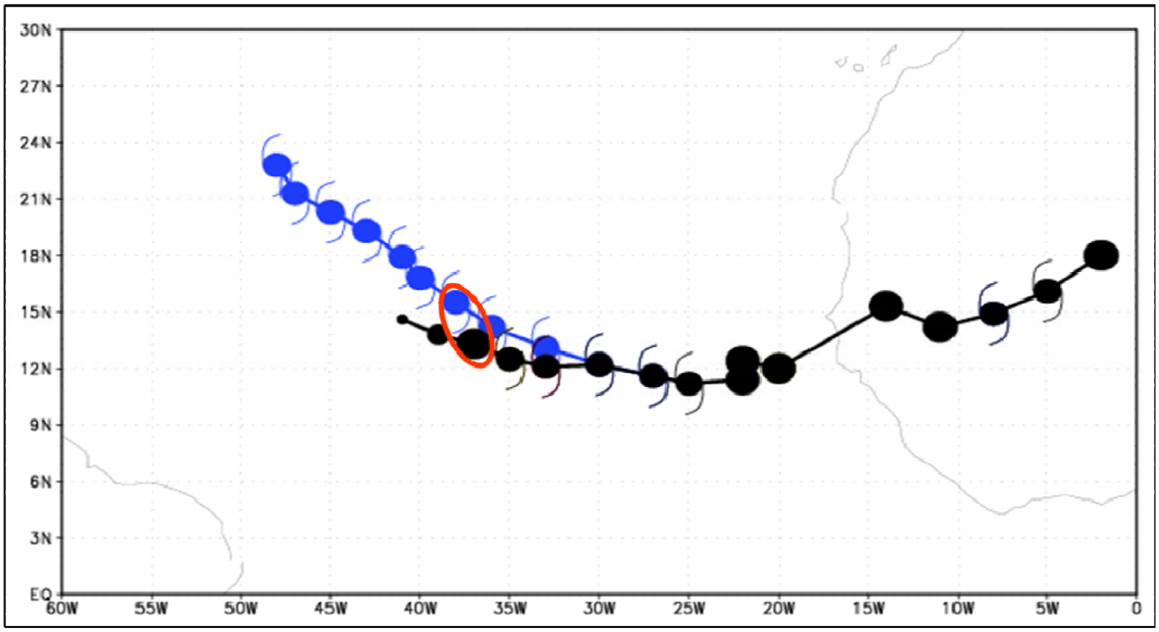

Figure 27 The analyzed track (black) and UKMET forecast track initiated at 1200 UTC 23 September 2005 (blue) for case UKM_20050919_018_002. The 48-h analyzed and forecast positions are circled in red.

The UKMET forecast and analyzed values for the six parameters used in the 48-h discriminant function (Tables 3 and 4) are compared in Figures 28-33. Figure 28 illustrates that the 48-h forecast relative vorticity was *higher* than the analyzed relative vorticity. Figure 29 illustrates that the 48-h forecast warm core was *lower* than the analyzed warm core. Figure 30 illustrates that the 48-h forecast wind shear was *lower* than the analyzed wind shear. Figure 31 illustrates that the 48-h forecast vertical motion was *higher* than the analyzed vertical motion. Figure 32 illustrates that the 48-h forecast vapor pressure was *higher* than the analyzed vapor pressure. Figure 33 illustrates that the 48-h forecast sea-level pressure was *equal to* the analyzed sea-level pressure.

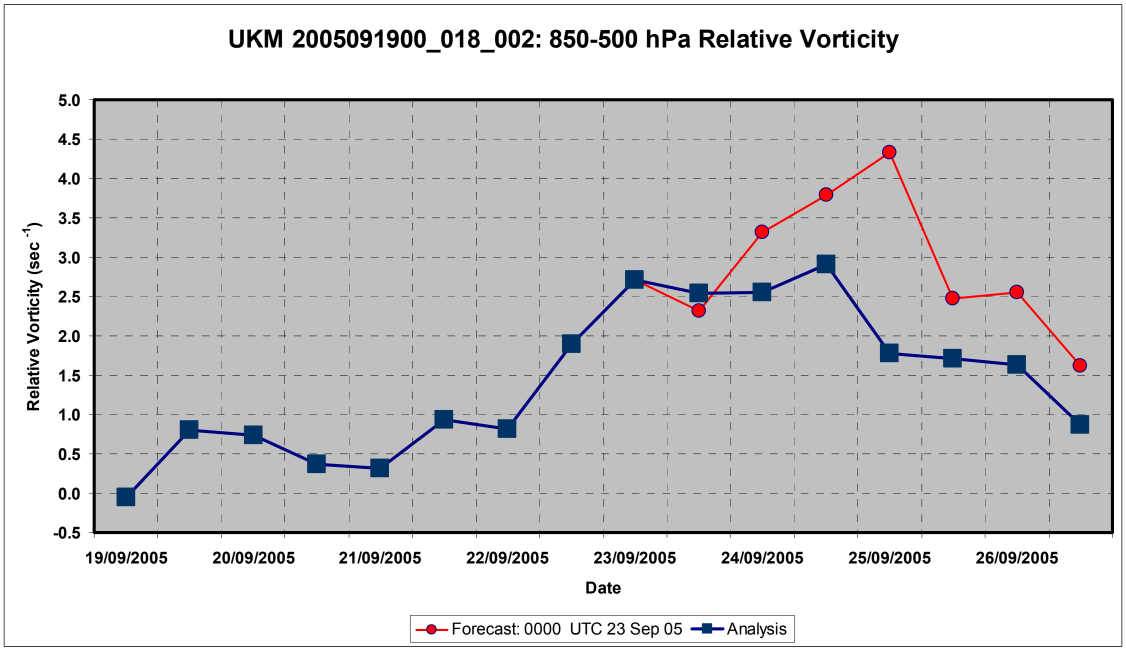

Figure 28 As in Figure 20, except for case UKM_20050919_018 _002. The UKMET 48-h forecast values from 1200 UTC 23 September 2005 are plotted with red circles while analyzed values are plotted with blue squares.

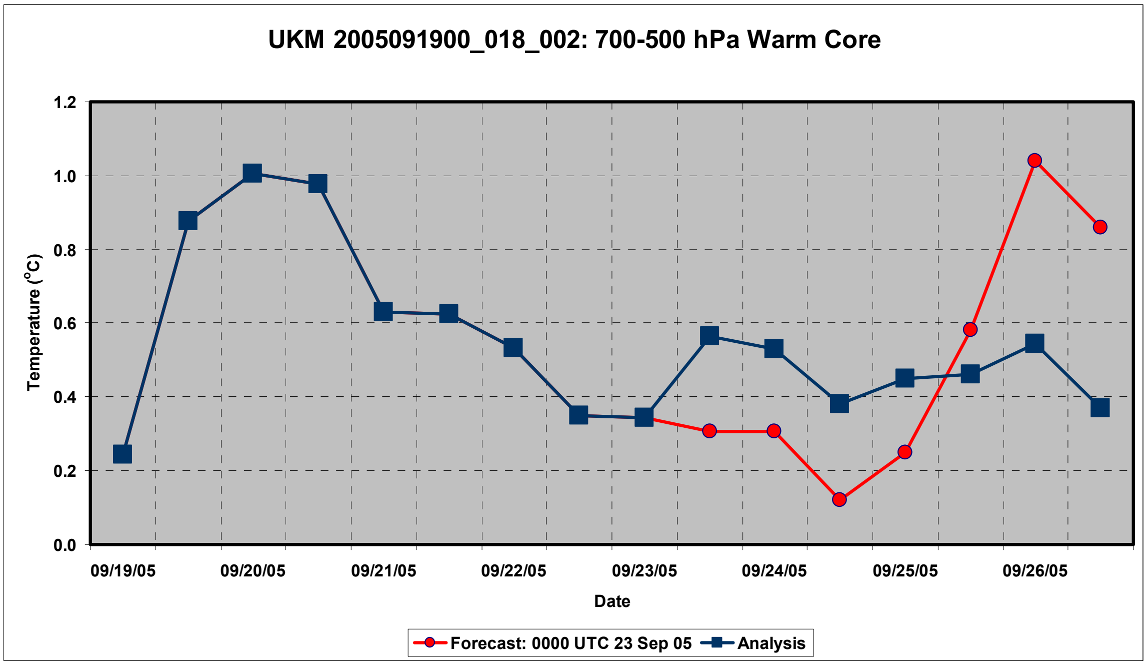

Figure 29 As in Figure 28, except for warm core (°C) at 700-500 hPa.

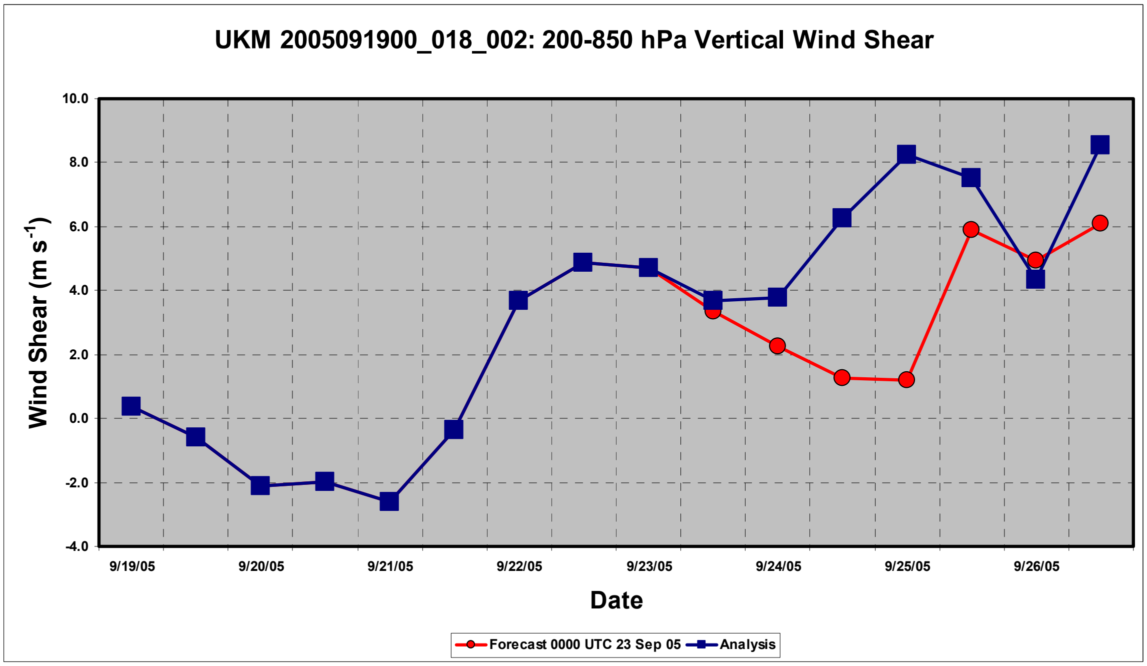

Figure 30 As in Figure 28, except for vertical wind shear (m s^{-1}) between 200 and 850 hPa.

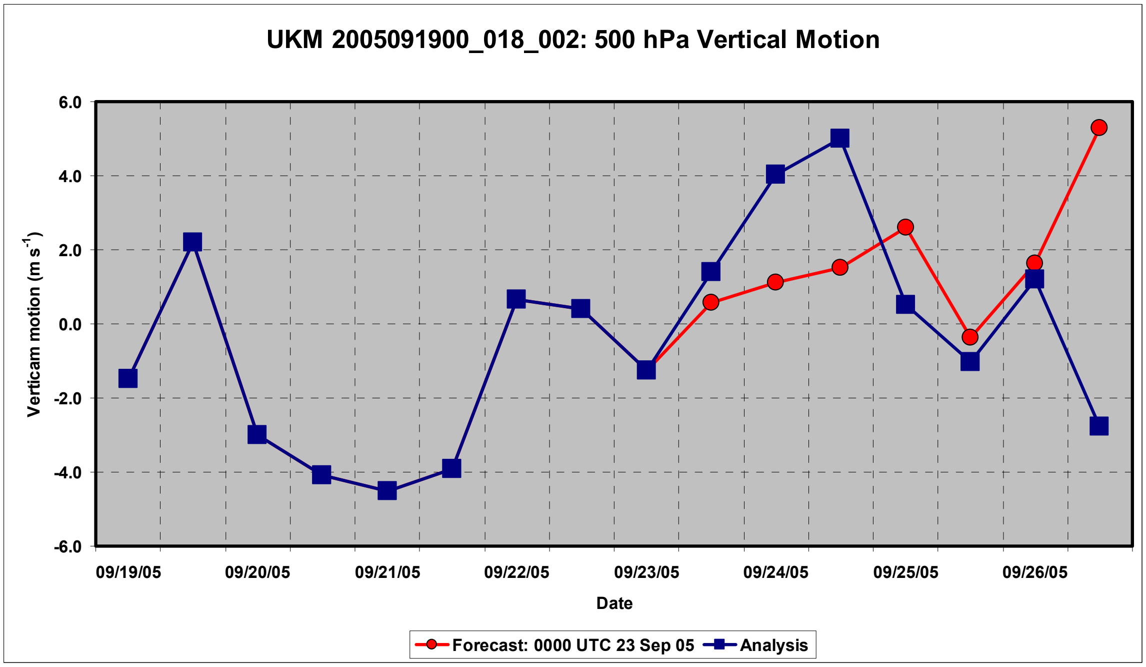

Figure 31 As in Figure 28, except for vertical motion (m s^{-1} * 10) at 500 hPa.

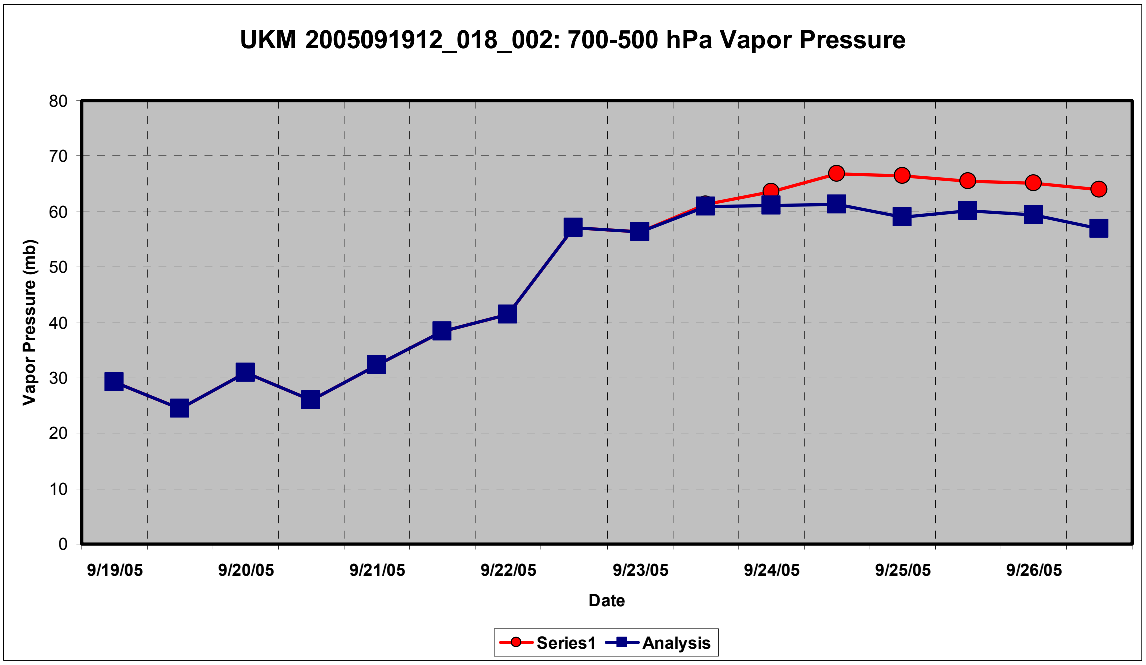

Figure 32 As in Figure 28, except for vapor pressure(mb) between 700 and 500 hPa.

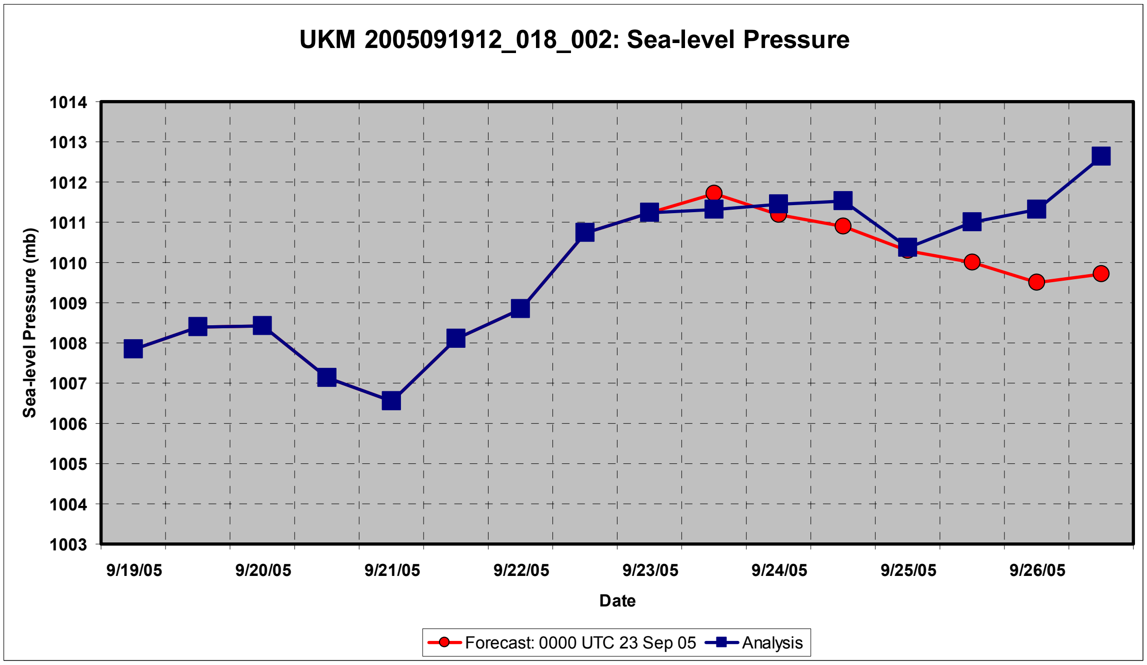

Figure 33 As in Figure 28, except for sea-level pressure (mb).

Table 10 is a list of the values of the six parameters for this case compared to the overall mean values for the developer and false-alarm classifications. Values of five of the six parameters for this case were closer to the mean values for developers than to the mean values for false alarms. As calculated by the discriminant analysis, the probability that this case belongs to Group 1 is 0.84 and the probability that it belongs to Group 2 is 0.16. The discriminant function therefore incorrectly classified this case as a developer. The cause of this misclassification can be seen in Figures 28, 30, and 31 which demonstrate that through the 48-h forecast there was a strong indication that the vortex would develop into a tropical cyclone. While the model would eventually weaken the vortex beyond 48h, it did so 12h after the actual vortex weakened.

Table 10 Six parameters for case UKM_20050919_018_002 (third row) compared to the mean values for developers (first row) and false alarms (second row). The fourth and fifth rows contain the differences between the values for this case and the mean values for developers and false alarms, respectively. The smaller differences is highlighted.

Parameter (as in Table 4)	1	2	4	6	7	9
Mean for developers	3.76	0.13	0.85	2.05	64.73	1010.4
Mean for false alarms	4.3	0.41	0.34	1.8	60.4	1012.2
UKM_20050919_018_002	4.33	0.25	1.19	2.6	66.4	1010.3
Difference from developers	0.57	0.12	0.34	0.56	1.63	-0.09
Difference from false alarms	0.032	-0.16	0.88	0.82	6.2	-1.99

THIS PAGE INTENTIONALLY LEFT BLANK

IV. CONCLUSIONS AND RECOMMENDATIONS

As the NHC and JTWC issue tropical cyclone advisories for longer forecast periods, the necessity to predict tropical cyclone formation becomes more important. Many of the processes that are believed to control the timing of tropical cyclone formation occur in the mesoscale. Therefore, it is a matter of current debate as to whether global model forecasts contain valuable information with regard to tropical cyclone formation. However, the current circumstances are such that the global models are the only numerical data routinely available to forecasters for this type of prediction. Therefore, the goal of this study was to use the global model data available in the TCVTP database to develop a tool to aid in the prediction of tropical cyclone formation.

After a preliminary examination of forecasts from the three models, it became clear that the models could not effectively distinguish developing vortices from the large number of non-developing vortices (Appendix B). As a result, the focus was shifted to only those cases in which a model forecasted a vortex to exceed vorticity and warm-core thresholds for tropical cyclone formation. Hence, the objective was to develop a procedure for determining which model-predicted tropical cyclones will actually develop and which are false alarms.

In this study, nine parameters relevant to tropical cyclone formation were subjected to a linear discriminant analysis. The nine parameters derived from global model output do not define all tropical cyclone characteristics. Vortices are identified in which vorticity and warm core thresholds are exceeded, but in which other parameters (e.g., wind speed) suggest that the vortex is not a tropical cyclone. Correct forecasts of vorticity and warm core parameters for these types of vortices are not considered false alarms since the forecasts did verify in the correct category.

The discriminant analysis was performed on the nine parameters from each model at each forecast period (30 analyses in total) to determine the combination of parameters that best discriminates between a vortex that was correctly forecast to intensify into a tropical cyclone (developer) and a vortex that was forecast to intensify into a tropical cyclone, but did not (false alarm). The performance of the resulting discriminant functions were then assessed using the Heidke Skill Score and Receiver Operating Characteristic curves.

A. CONCLUSIONS

The primary conclusion of this thesis is that linear discriminant analysis applied to the parameters defined in the TCVTP database provides a valid method of discriminating between developers and false alarms in the global model data. The resulting discriminant functions exhibited various levels of skill. In 27 of 30 cases, the discriminant function performed better than a random forecast as measured by the HSS and the area under the ROC curve. It is important to note that the VORTRACK system and the TCVTP database make this type of data analysis quick and simple to complete.

Efforts to reduce the number of parameters considered in the analysis (by considering PDFs, for example), did not yield profitable results. The discriminant functions resulting from each of the thirty analyses used different combinations of the nine parameters (Table 3). It is therefore concluded that all possible combinations of all available parameters should be considered in a discriminant analysis.

Some challenges remain to performing this type of data analysis. Models undergo frequent updates. Each time changes are made to the model, a new, and *sufficient*, training sample would be required before the discriminant analysis could yield meaningful results. Additionally, the small number of developing vortices identified and tracked by the TCVTP at the longer forecast intervals poses a problem. For example, not enough developing vortices were tracked in the 2005 UKMET forecasts for the discriminant analysis to produce meaningful results beyond 84h.

The discriminant function applied to the UKMET model outperformed those applied to NOGAPS and GFS in eight of the 10 forecast periods. This superiority is at least partially attributable to a low false-alarm rate associated with the UKMET model. However, the UKMET model also has a tendency for a low probability of detection which is responsible for the lack of cases at the longer forecast intervals. The GFS is the only model in which the TCVTP identifies sufficient vortices at all forecast intervals. However, the HSS and ROC curves for GFS suffer as a result of its tendency to over-predict formation (i.e., higher false-alarm rate).

B. RECOMMENDATIONS FOR FUTURE WORK

This analysis should be replicated for different datasets to include additional geographic regions and time periods. If future analysis demonstrates that the models are becoming capable of discriminating between developers and false alarms, the methodology should be redirected toward that important forecast problem.

Two extensions to the discriminant analysis may lead to improved results. First, all parameters in this study were considered in a static sense. However, the time variability, or trend, of parameters could be incorporated and may have great potential to increase the skill of the discriminant analysis. Second, the analysis could consider combinations of parameters from multiple models that would result in an ‘ensemble’ discriminant function. For example, the discriminant function for the 12-h forecast period may include the vorticity parameter from the GFS model, the warm-core parameter from the NOGAPS model, and the vapor pressure parameter from the UKMET model. However, the probability of detection for the UKMET and GFS models would need to increase for an ensemble approach to be useful at longer forecast intervals.

APPENDIX A. SCATTERPLOTS FOR GFS 12-H FORECAST

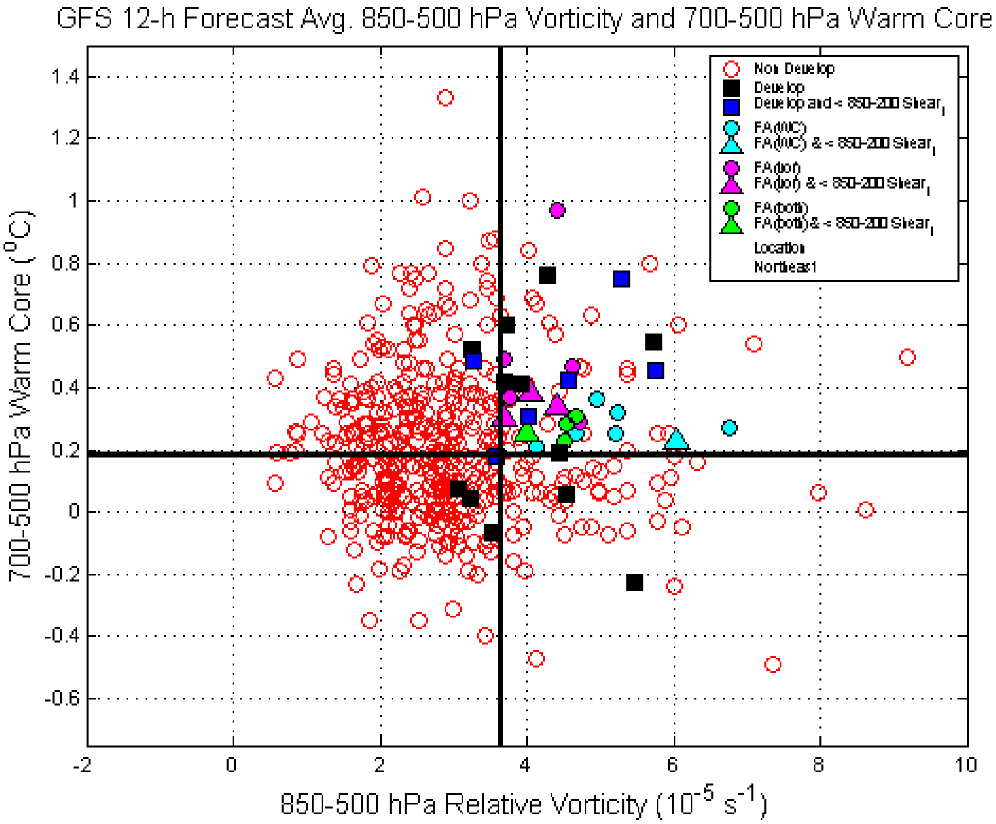

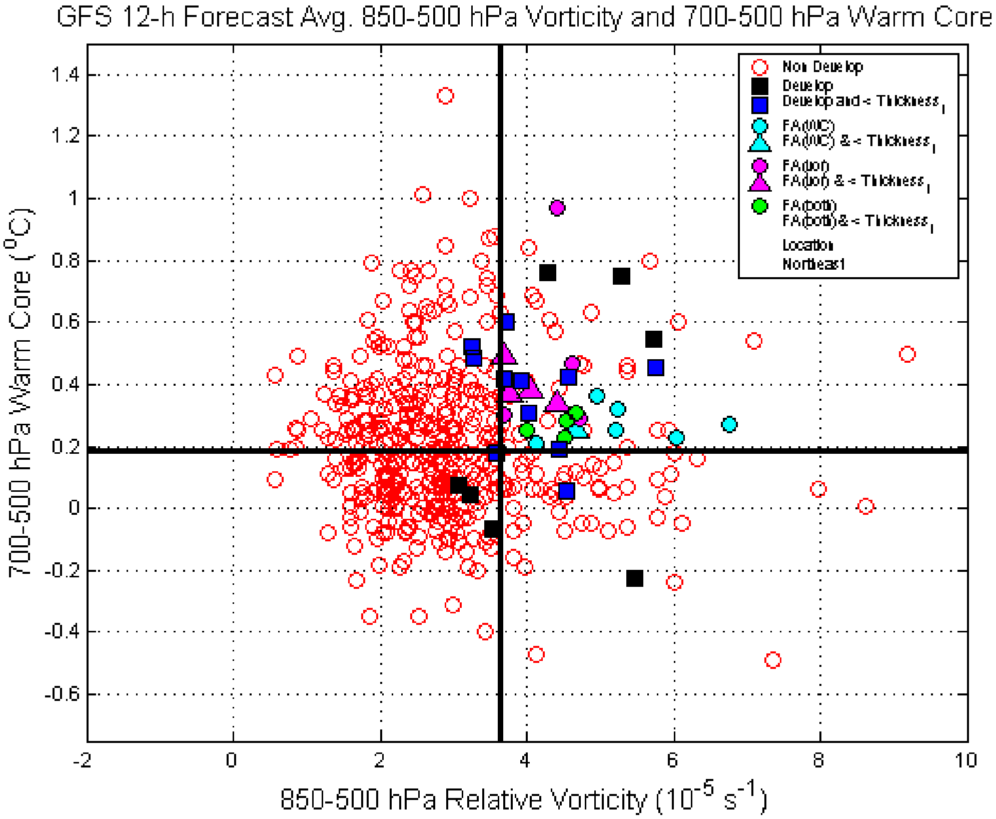
GFS 12-h Forecast Avg. 850-500 hPa Vorticity and 700-500 hPa Warm Core

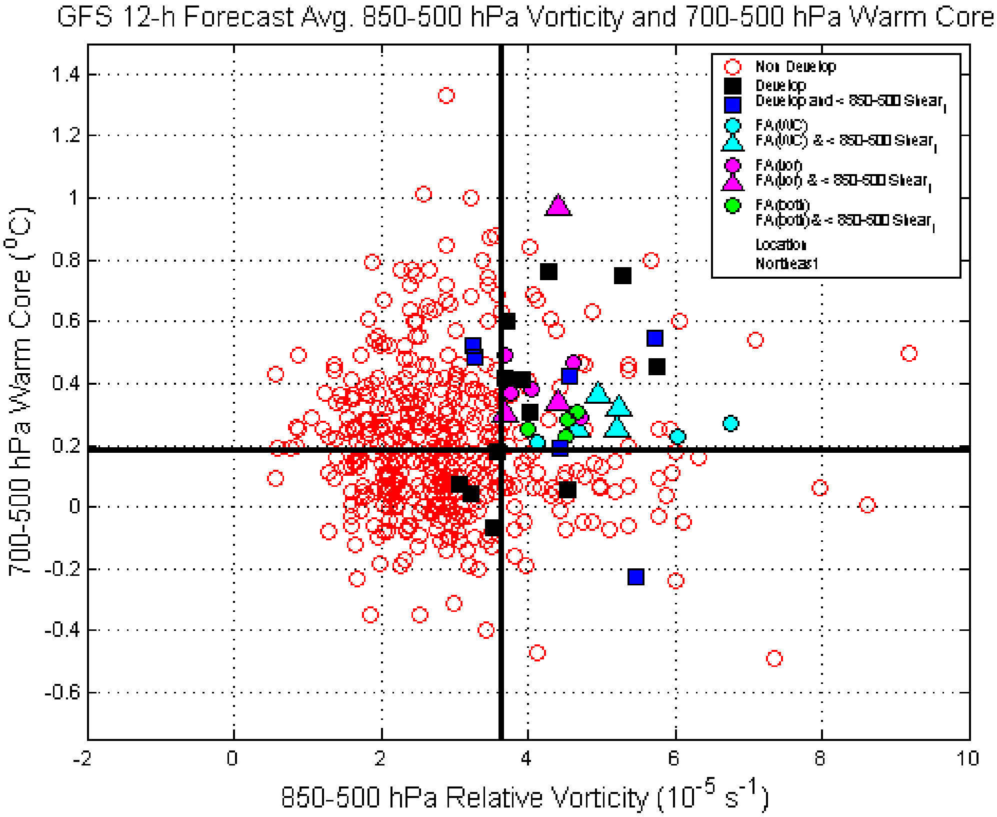
GFS 12-h Forecast Avg. 850-500 hPa Vorticity and 700-500 hPa Warm Core

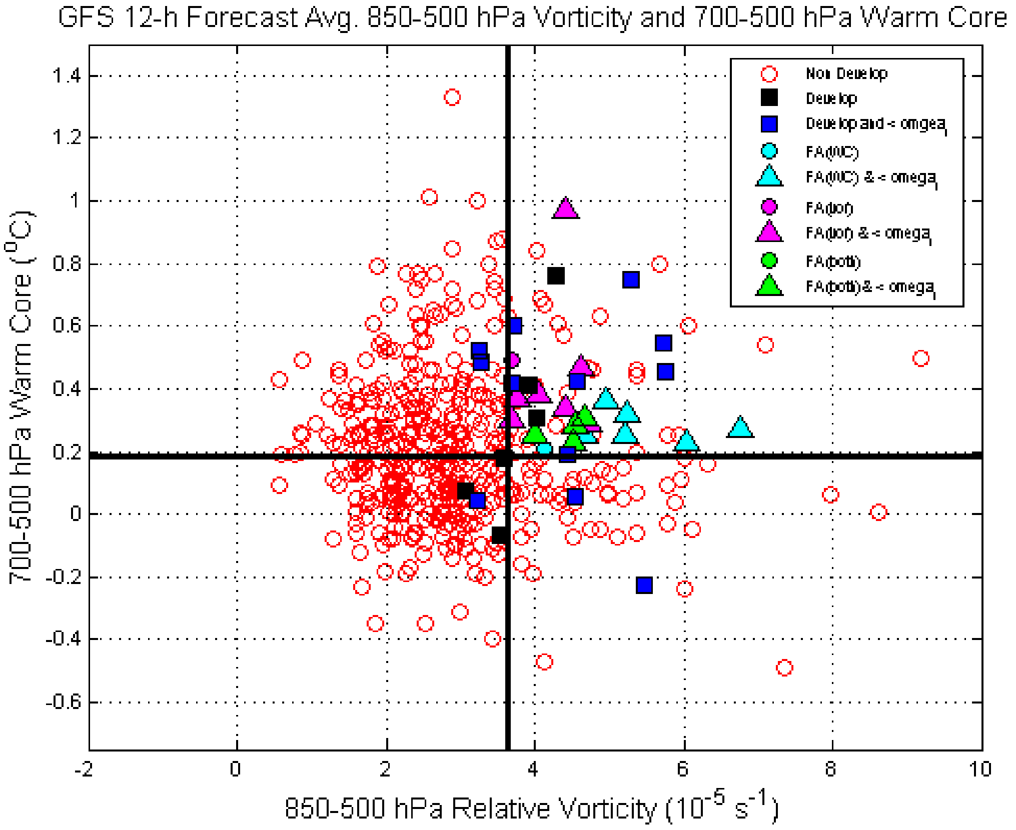
GFS 12-h Forecast Avg. 850-500 hPa Vorticity and 700-500 hPa Warm Core

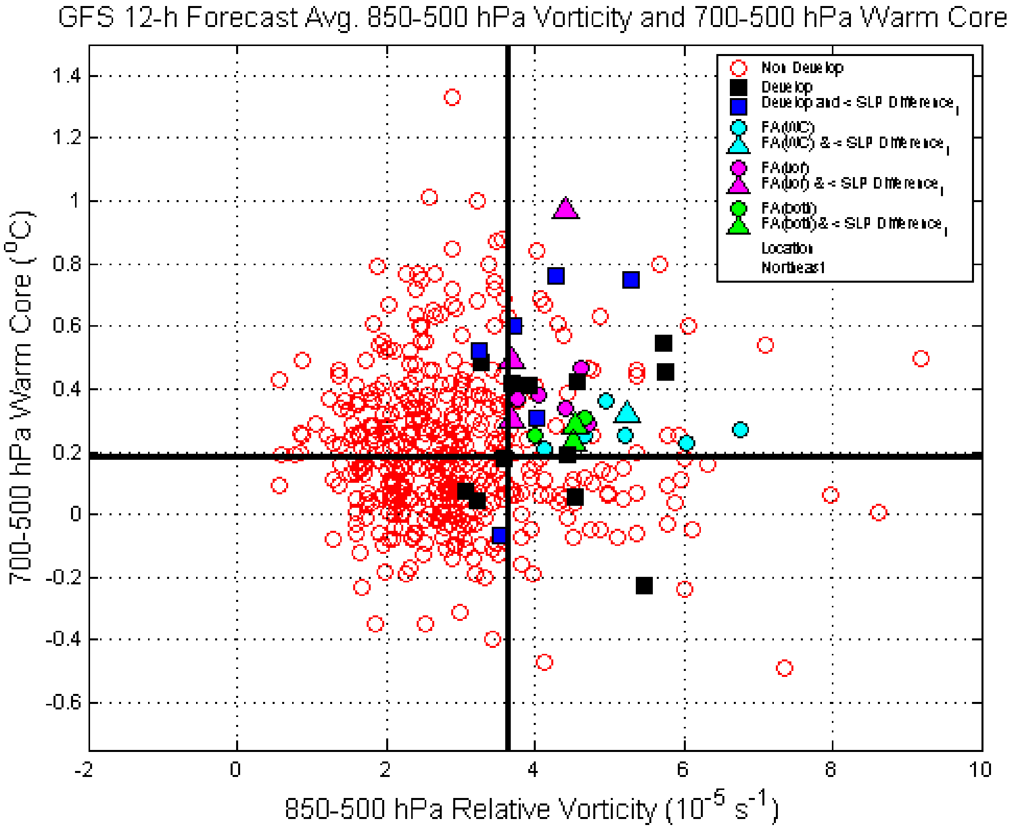
GFS 12-h Forecast Avg. 850-500 hPa Vorticity and 700-500 hPa Warm Core

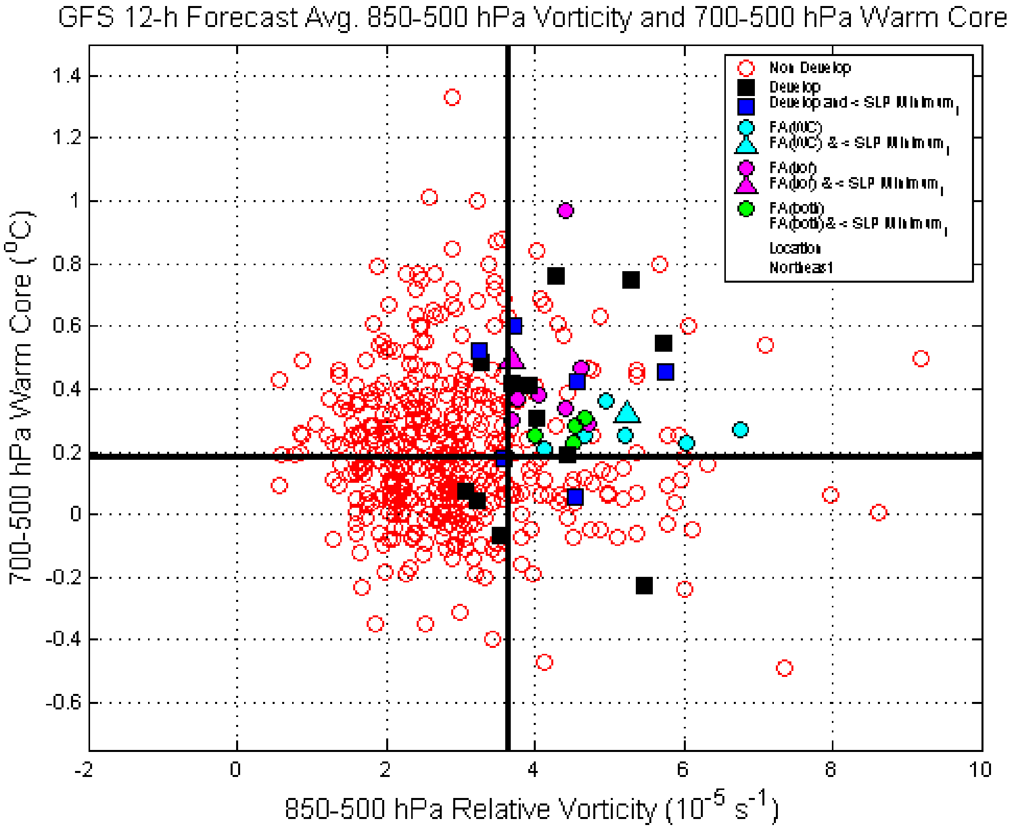
GFS 12-h Forecast Avg. 850-500 hPa Vorticity and 700-500 hPa Warm Core
700-500 hPa Warm Core (^{o}C)
850-500 hPa Relative Vorticity (10^{-5} s^{-1})
1.4
1.2
1
0.8
0.6
0.4
0.2
0
-0.2
-0.4
-0.6
-2
0
2
4
6
8
10
Non Develop
Develop
Develop and < SLP Minimum$_1$
FA(WC)
FA(WC) & < SLP Minimum$_1$
FA(vort)
FA(vort) & < SLP Minimum$_1$
FA(both)
FA(both)& < SLP Minimum$_1$
Location
Northeast1

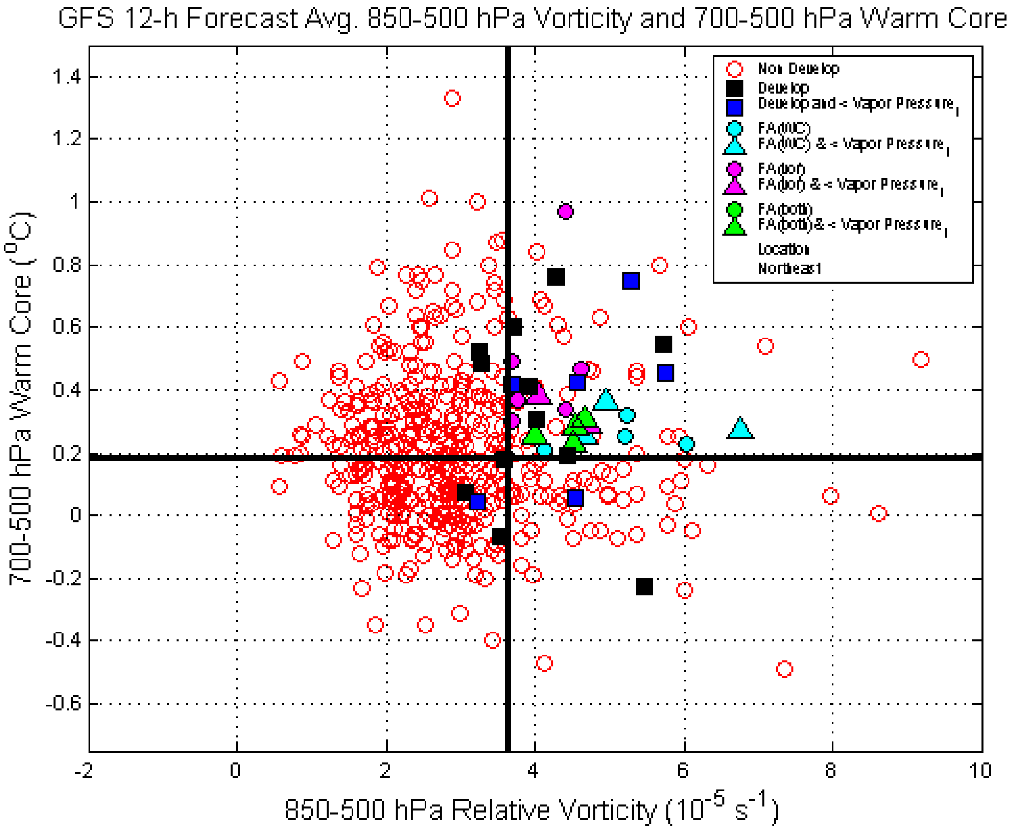
GFS 12-h Forecast Avg. 850-500 hPa Vorticity and 700-500 hPa Warm Core
700-500 hPa Warm Core (^{o}C)
850-500 hPa Relative Vorticity (10^{-5} s^{-1})
1.4
1.2
1
0.8
0.6
0.4
0.2
0
-0.2
-0.4
-0.6
-2
0
2
4
6
8
10
Non Develop
Develop
Develop and < Vapor Pressure$_1$
FA(WC)
FA(WC) & < Vapor Pressure$_1$
FA(vort)
FA(vort) & < Vapor Pressure$_1$
FA(both)
FA(both)& < Vapor Pressure$_1$
Location
Northeast1

APPENDIX B. SCATTERPLOTS INCLUDING OMEGA

GFS 12-h Forecast Avg. 850-500 hPa Vorticity and 700-500 hPa Warm Core

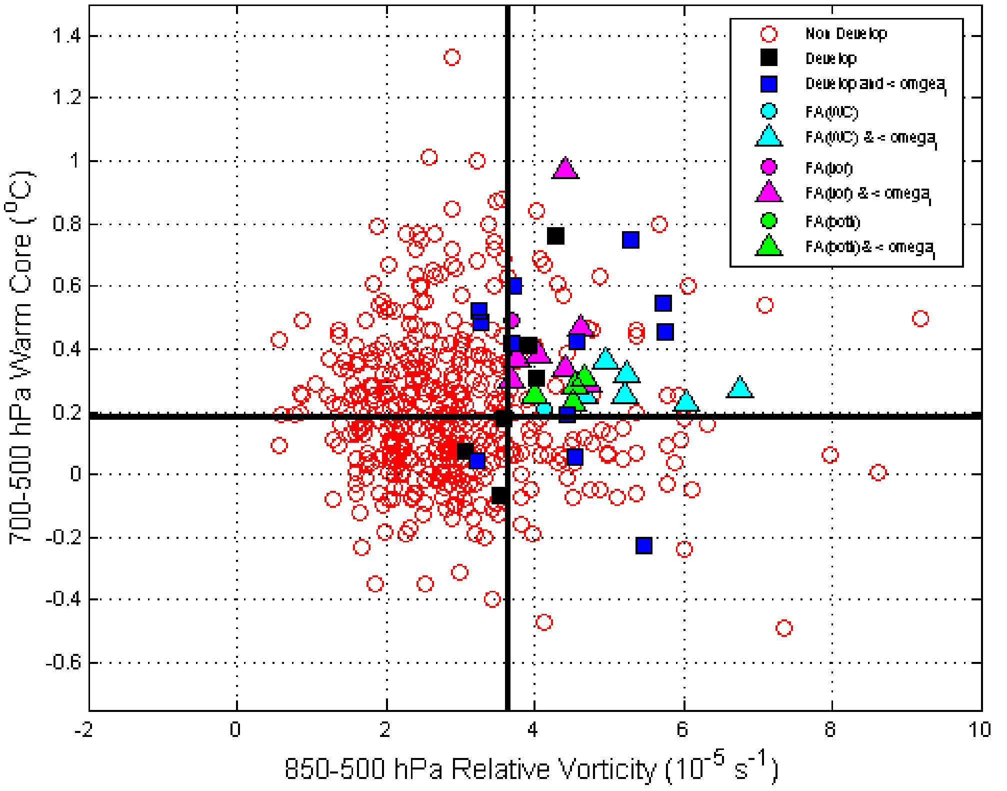

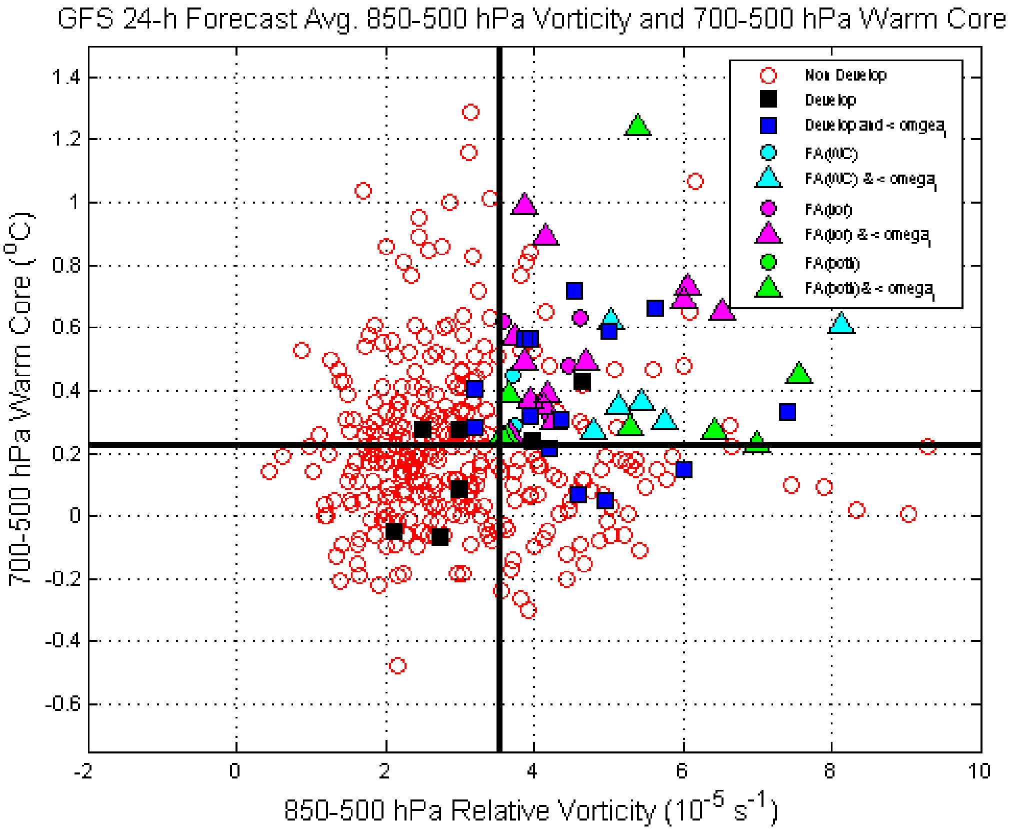
GFS 24-h Forecast Avg. 850-500 hPa Vorticity and 700-500 hPa Warm Core
700-500 hPa Warm Core (^oC)
850-500 hPa Relative Vorticity (10^{-5} s^{-1})
1.4
1.2
1
0.8
0.6
0.4
0.2
0
-0.2
-0.4
-0.6
-2
0
2
4
6
8
10
Non Develop
Develop
Develop and < omega_t
FA(WC)
FA(WC) & < omega_t
FA(vor)
FA(vor) & < omega_t
FA(both)
FA(both)& < omega_t

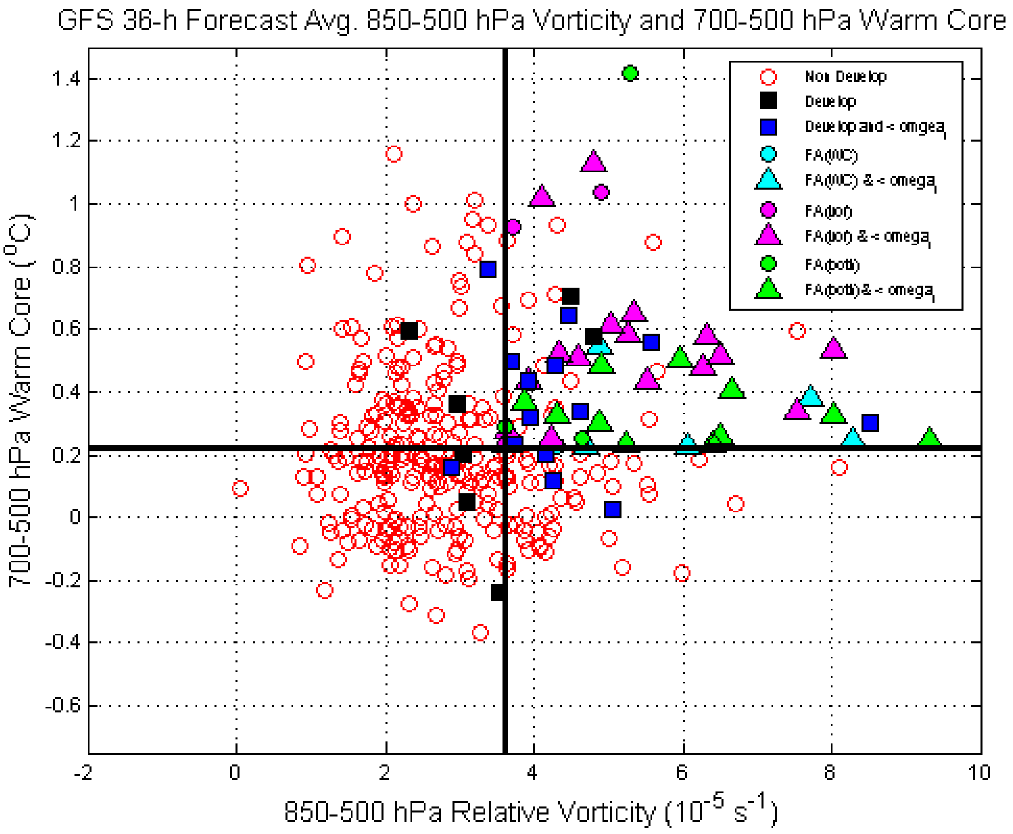
GFS 36-h Forecast Avg. 850-500 hPa Vorticity and 700-500 hPa Warm Core
700-500 hPa Warm Core (^oC)
850-500 hPa Relative Vorticity (10^{-5} s^{-1})
1.4
1.2
1
0.8
0.6
0.4
0.2
0
-0.2
-0.4
-0.6
-2
0
2
4
6
8
10
Non Develop
Develop
Develop and < omega_t
FA(WC)
FA(WC) & < omega_t
FA(vor)
FA(vor) & < omega_t
FA(both)
FA(both)& < omega_t

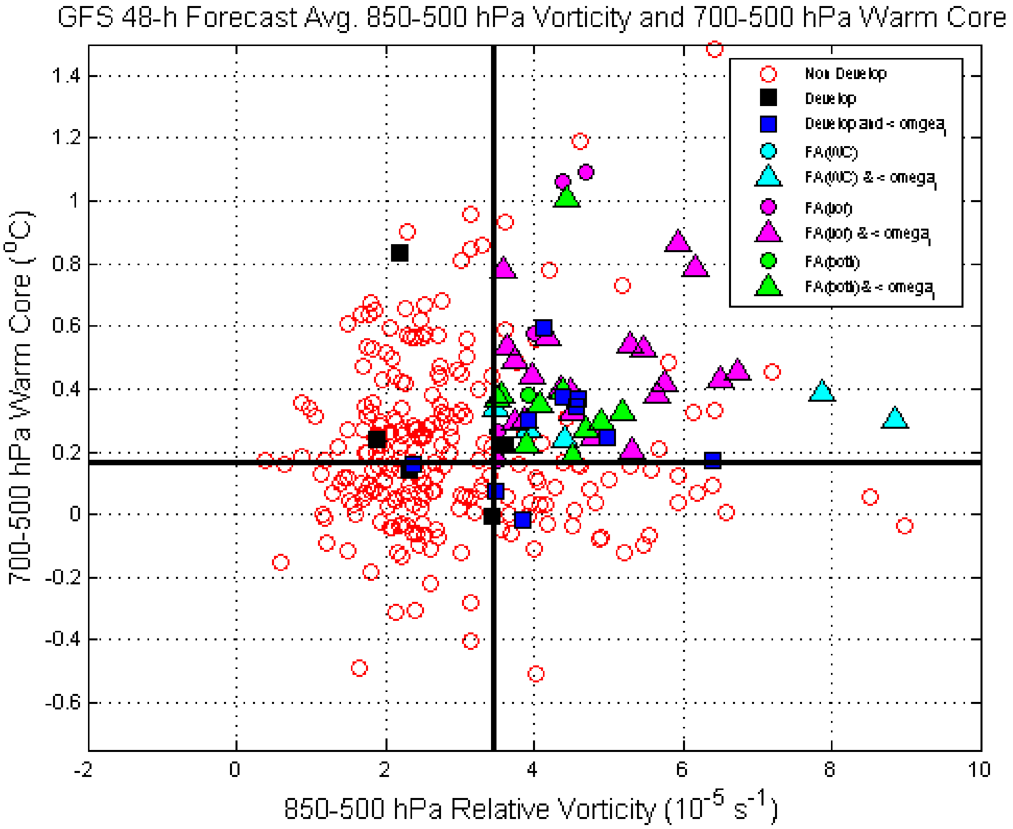
GFS 48-h Forecast Avg. 850-500 hPa Vorticity and 700-500 hPa Warm Core
700-500 hPa Warm Core (^{o}C)
850-500 hPa Relative Vorticity (10^{-5} s^{-1})
1.4
1.2
1
0.8
0.6
0.4
0.2
0
-0.2
-0.4
-0.6
-2
0
2
4
6
8
10
Non Develop
Develop
Develop and < omga$_t$
FA(WC)
FA(WC) & < omega$_t$
FA(vort)
FA(vort) & < omega$_t$
FA(both)
FA(both) & < omega$_t$

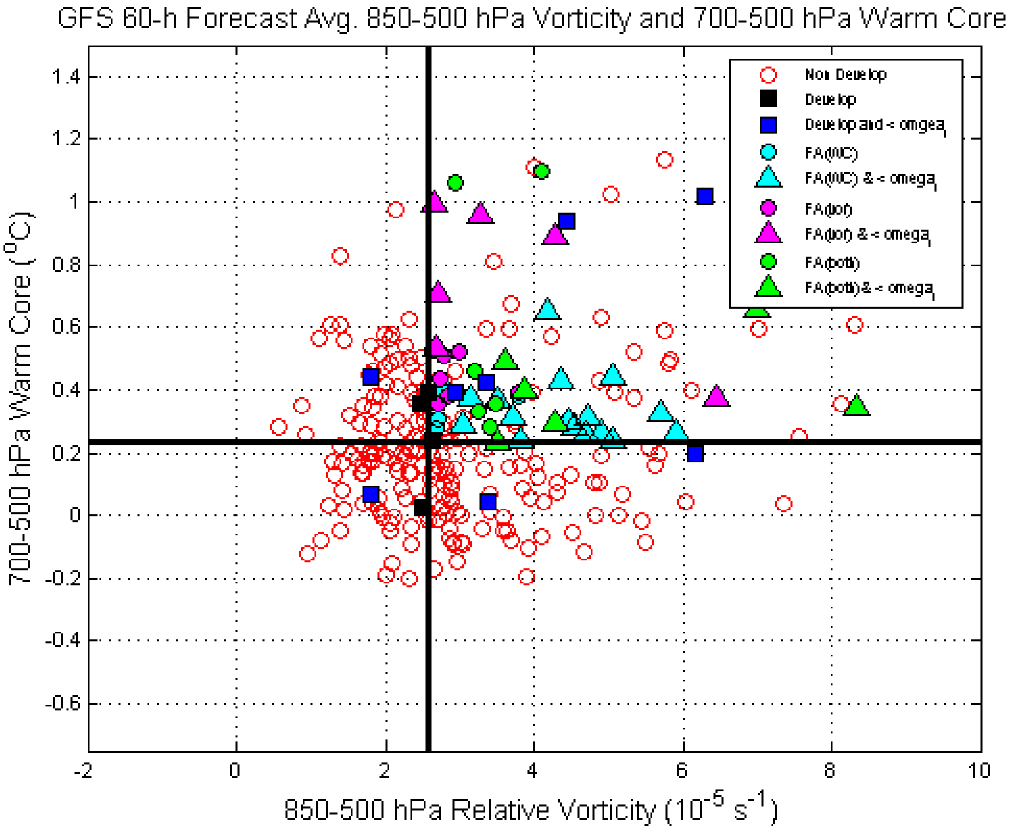
GFS 60-h Forecast Avg. 850-500 hPa Vorticity and 700-500 hPa Warm Core
700-500 hPa Warm Core (^{o}C)
850-500 hPa Relative Vorticity (10^{-5} s^{-1})
1.4
1.2
1
0.8
0.6
0.4
0.2
0
-0.2
-0.4
-0.6
-2
0
2
4
6
8
10
Non Develop
Develop
Develop and < omega$_t$
FA(WC)
FA(WC) & < omega$_t$
FA(vort)
FA(vort) & < omega$_t$
FA(both)
FA(both) & < omega$_t$

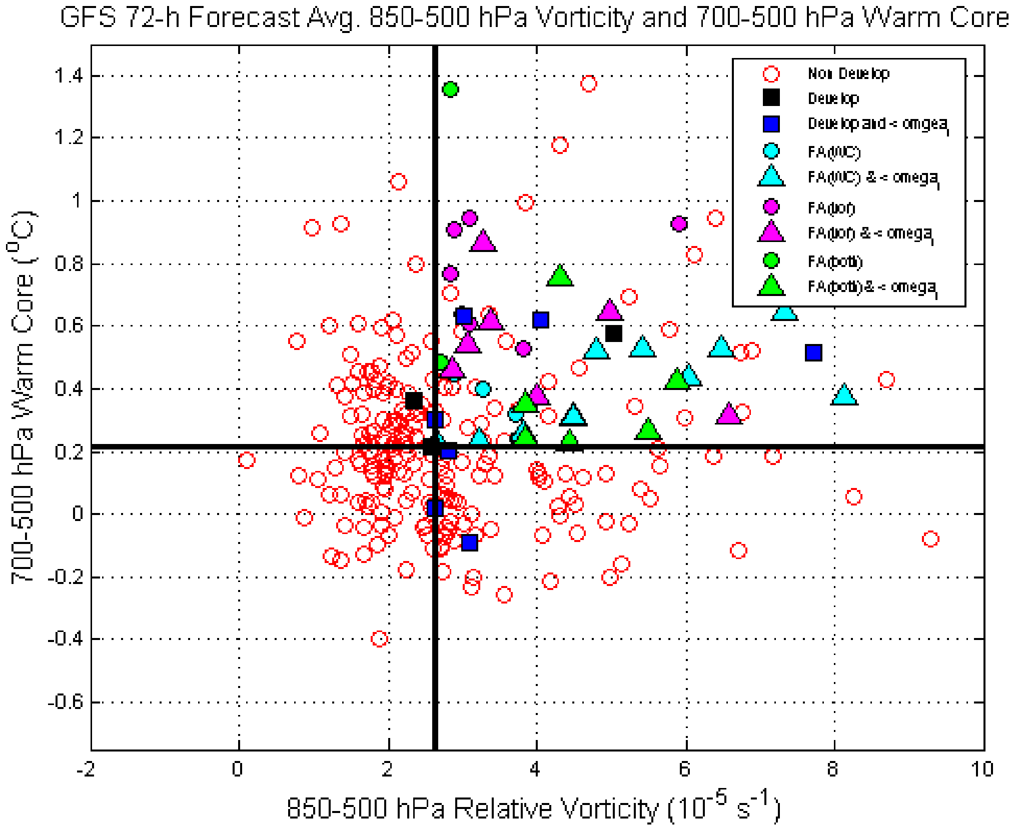
GFS 72-h Forecast Avg. 850-500 hPa Vorticity and 700-500 hPa Warm Core
700-500 hPa Warm Core (^{o}C)
850-500 hPa Relative Vorticity (10^{-5} s^{-1})
1.4
1.2
1
0.8
0.6
0.4
0.2
0
-0.2
-0.4
-0.6
-2
0
2
4
6
8
10
Non Develop
Develop
Develop and < omega
FA(WC)
FA(WC) & < omega
FA(vort)
FA(vort) & < omega
FA(both)
FA(both) & < omega

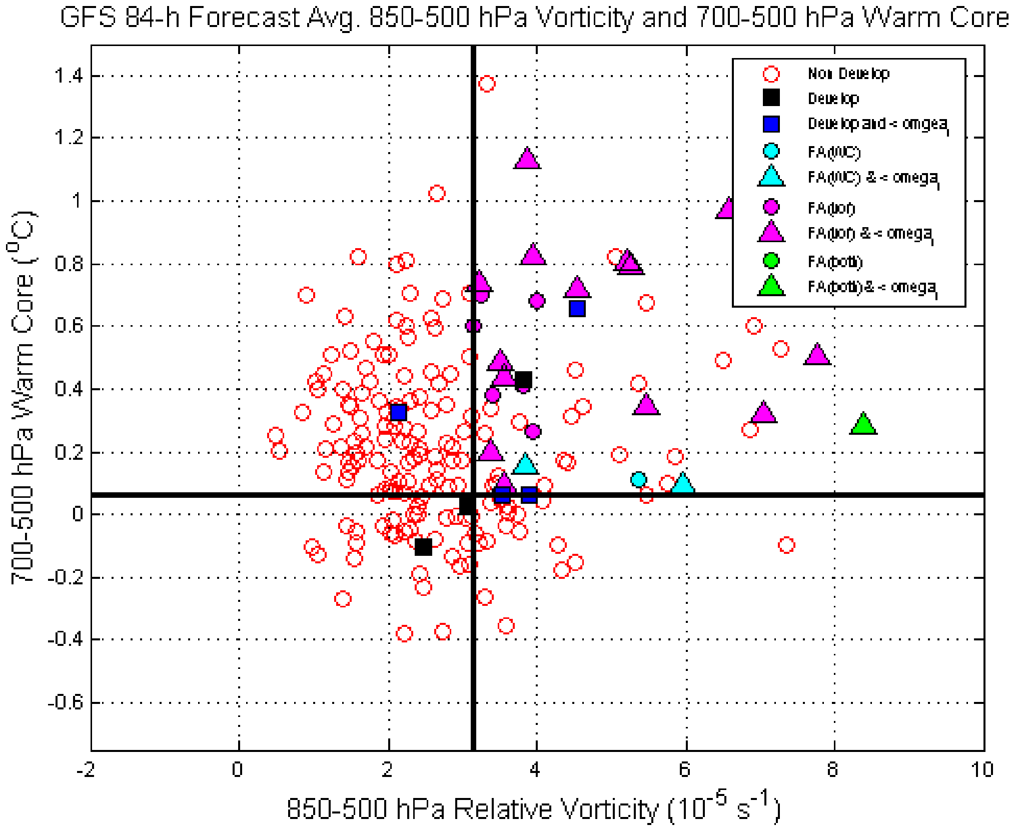
GFS 84-h Forecast Avg. 850-500 hPa Vorticity and 700-500 hPa Warm Core
700-500 hPa Warm Core (^{o}C)
850-500 hPa Relative Vorticity (10^{-5} s^{-1})
1.4
1.2
1
0.8
0.6
0.4
0.2
0
-0.2
-0.4
-0.6
-2
0
2
4
6
8
10
Non Develop
Develop
Develop and < omega
FA(WC)
FA(WC) & < omega
FA(vort)
FA(vort) & < omega
FA(both)
FA(both) & < omega

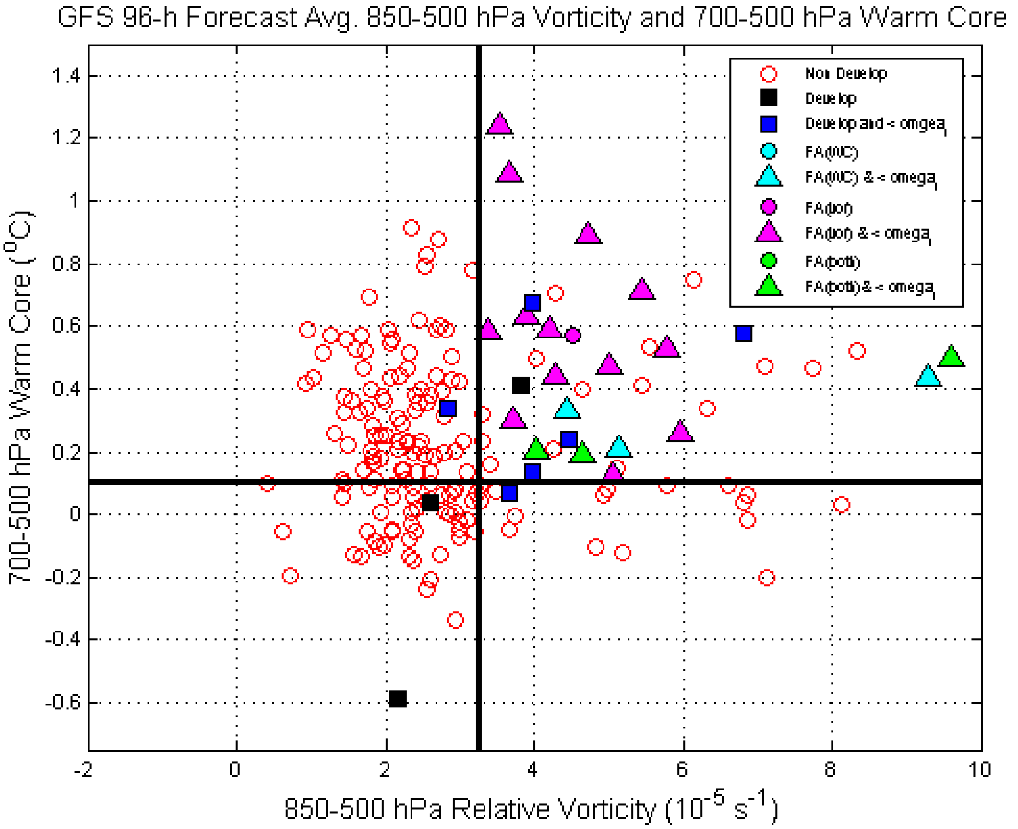
GFS 96-h Forecast Avg. 850-500 hPa Vorticity and 700-500 hPa Warm Core
700-500 hPa Warm Core (^oC)
850-500 hPa Relative Vorticity (10^{-5} s^{-1})
1.4
1.2
1
0.8
0.6
0.4
0.2
0
-0.2
-0.4
-0.6
-2
0
2
4
6
8
10
Non Develop
Develop
Develop and < omega
FA(WC)
FA(WC) & < omega
FA(vor)
FA(vor) & < omega
FA(both)
FA(both) & < omega

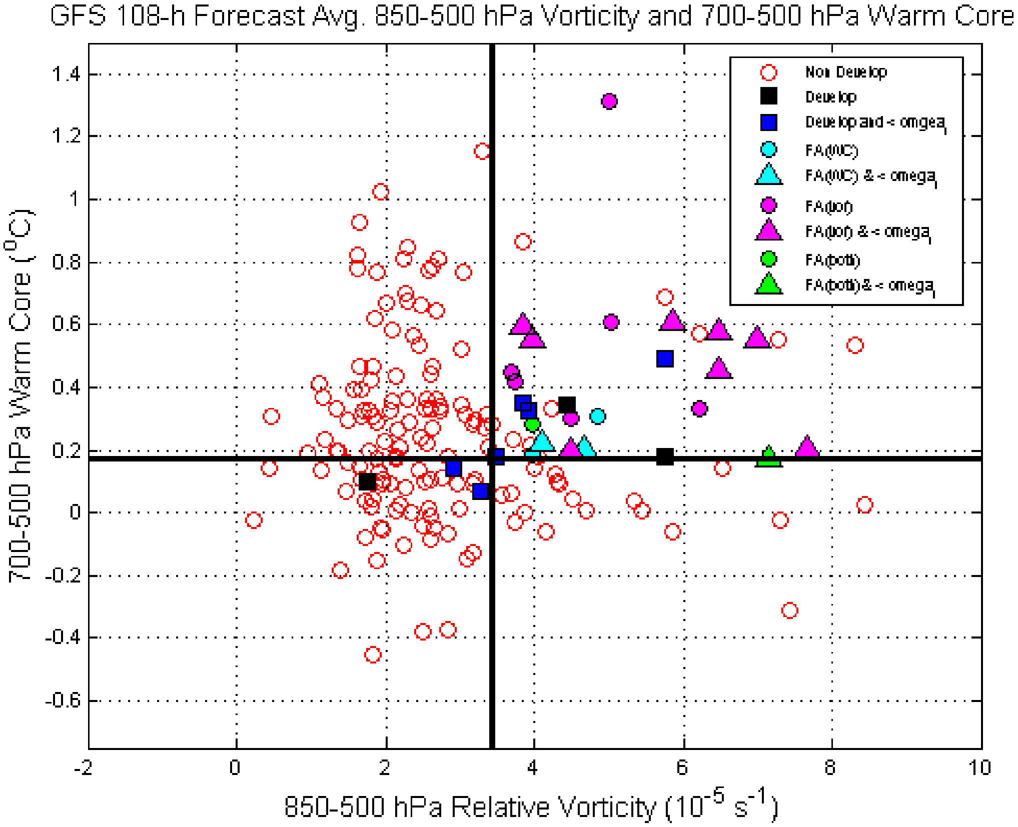
GFS 108-h Forecast Avg. 850-500 hPa Vorticity and 700-500 hPa Warm Core
700-500 hPa Warm Core (^oC)
850-500 hPa Relative Vorticity (10^{-5} s^{-1})
1.4
1.2
1
0.8
0.6
0.4
0.2
0
-0.2
-0.4
-0.6
-2
0
2
4
6
8
10
Non Develop
Develop
Develop and < omega
FA(WC)
FA(WC) & < omega
FA(vor)
FA(vor) & < omega
FA(both)
FA(both) & < omega

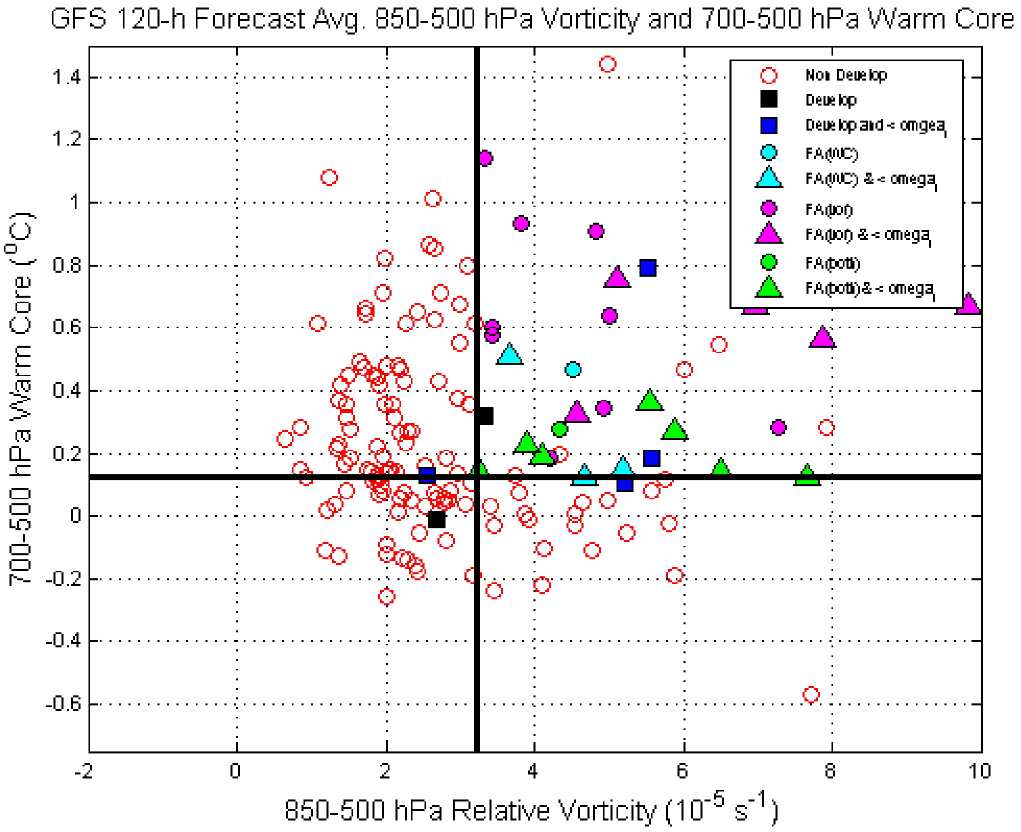
GFS 120-h Forecast Avg. 850-500 hPa Vorticity and 700-500 hPa Warm Core

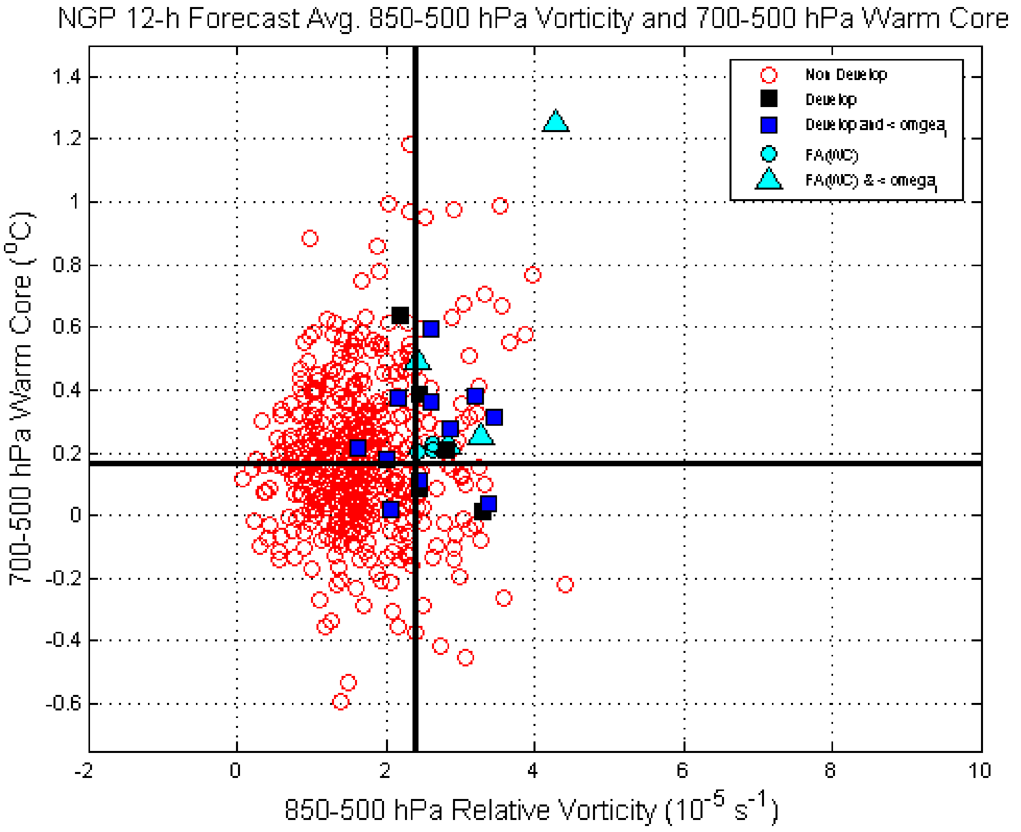
NGP 12-h Forecast Avg. 850-500 hPa Vorticity and 700-500 hPa Warm Core

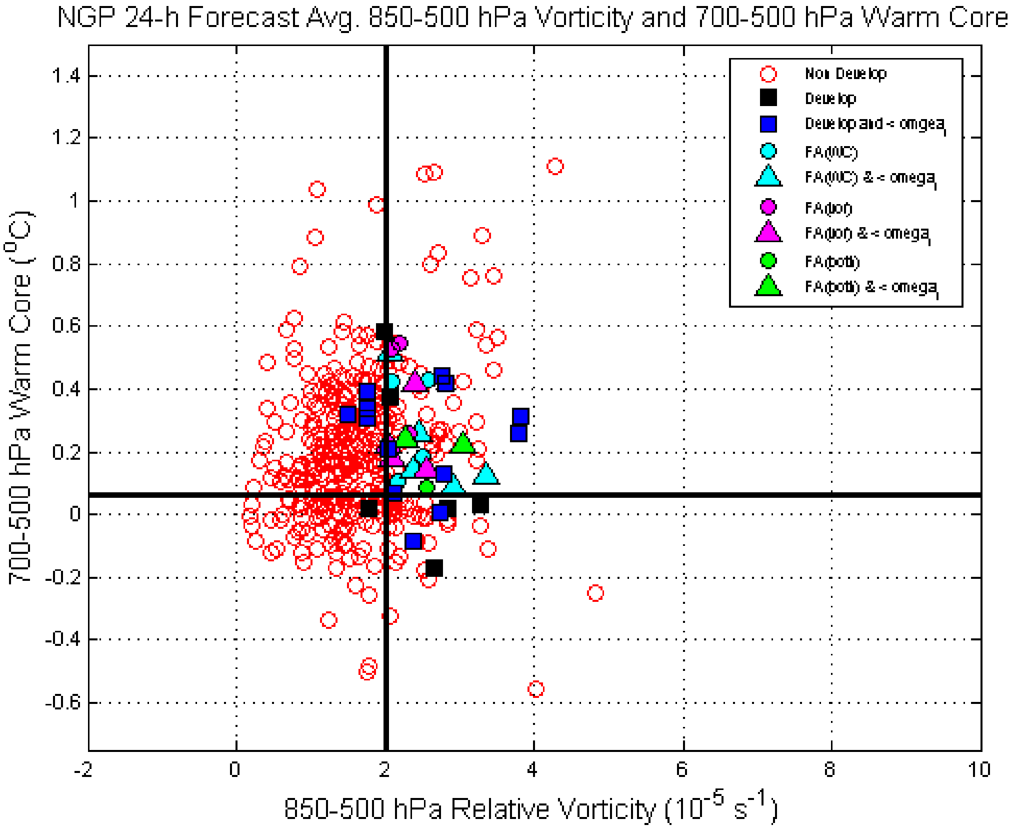
NGP 24-h Forecast Avg. 850-500 hPa Vorticity and 700-500 hPa Warm Core

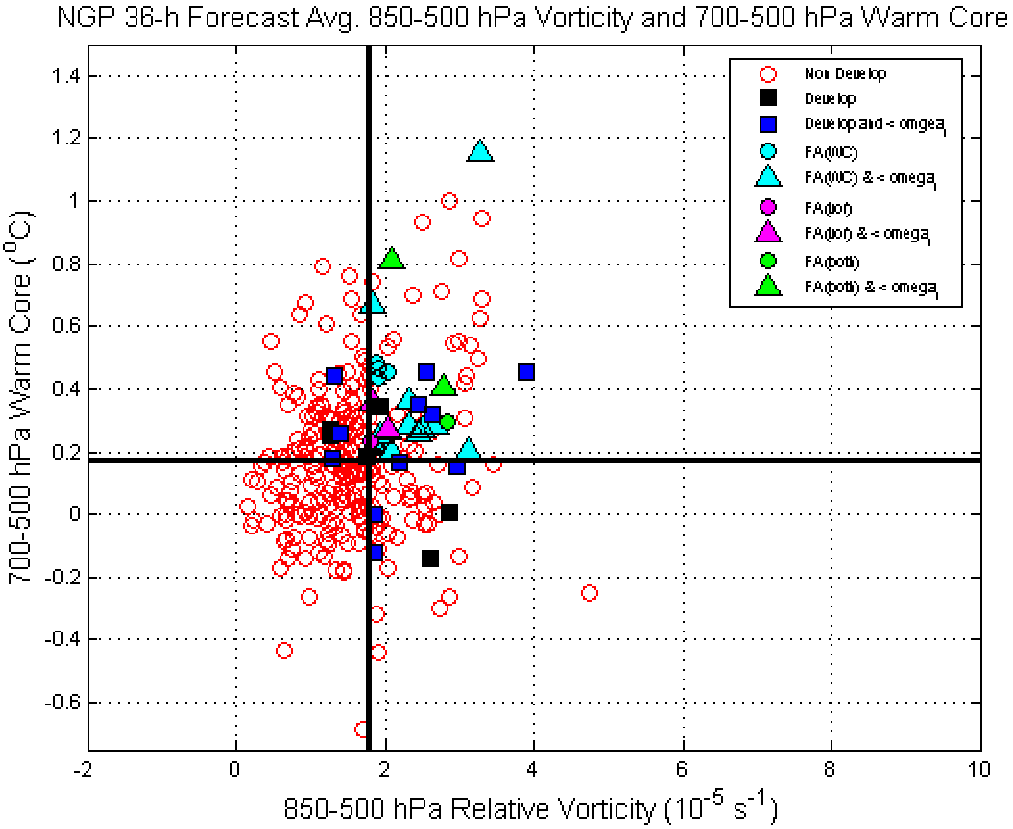
NGP 36-h Forecast Avg. 850-500 hPa Vorticity and 700-500 hPa Warm Core

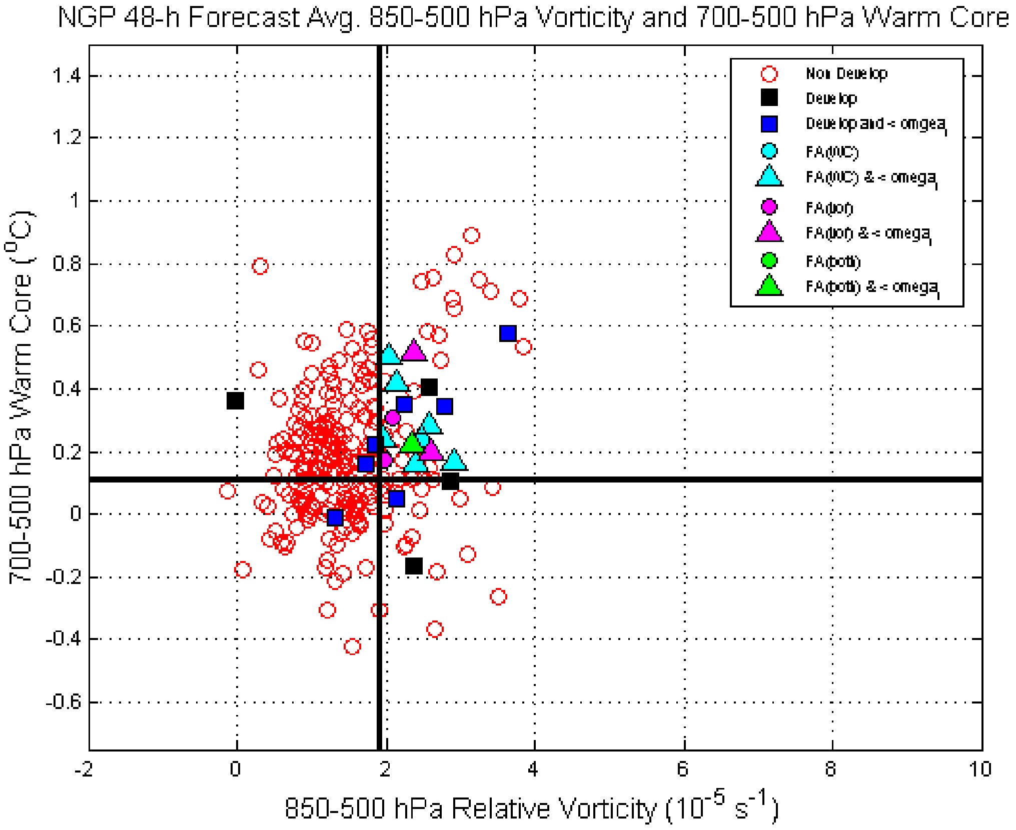

NGP 48-h Forecast Avg. 850-500 hPa Vorticity and 700-500 hPa Warm Core

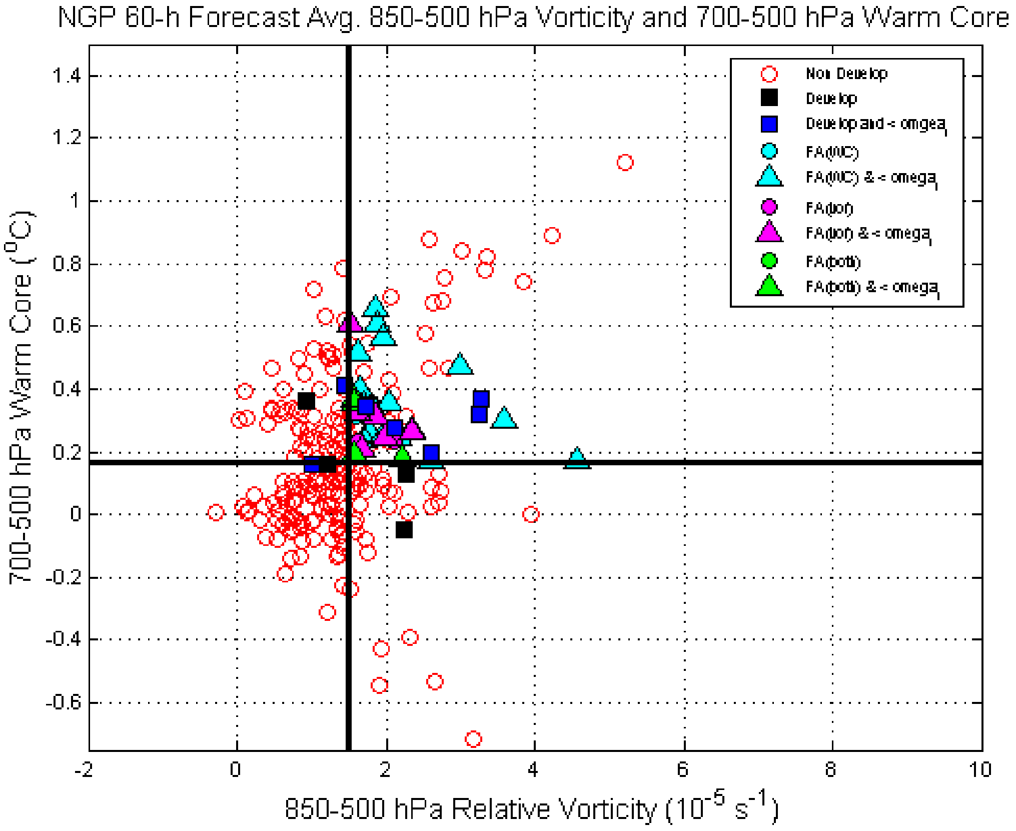

NGP 60-h Forecast Avg. 850-500 hPa Vorticity and 700-500 hPa Warm Core

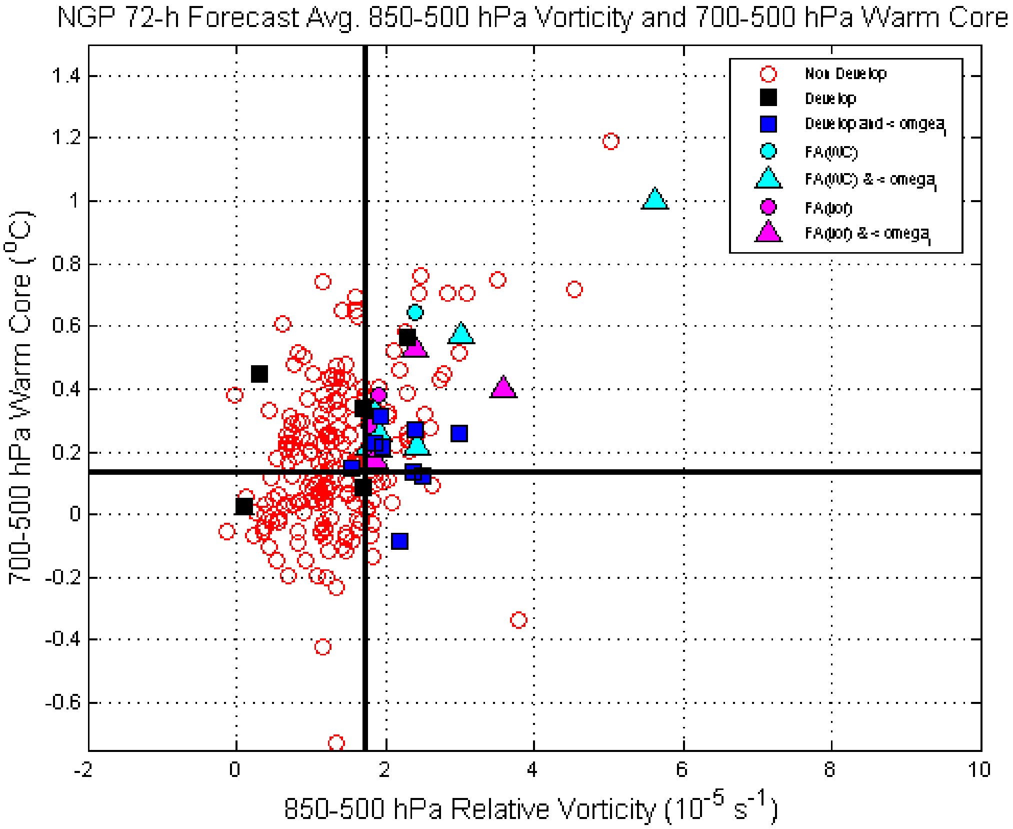

NGP 72-h Forecast Avg. 850-500 hPa Vorticity and 700-500 hPa Warm Core

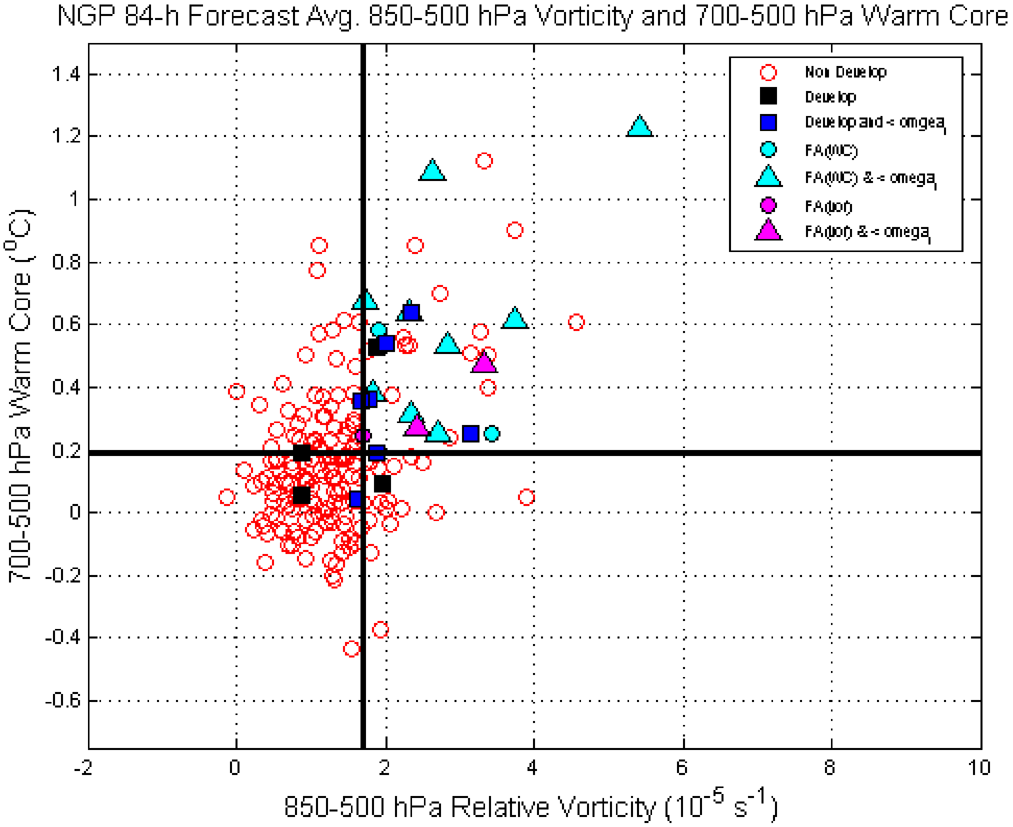

NGP 84-h Forecast Avg. 850-500 hPa Vorticity and 700-500 hPa Warm Core

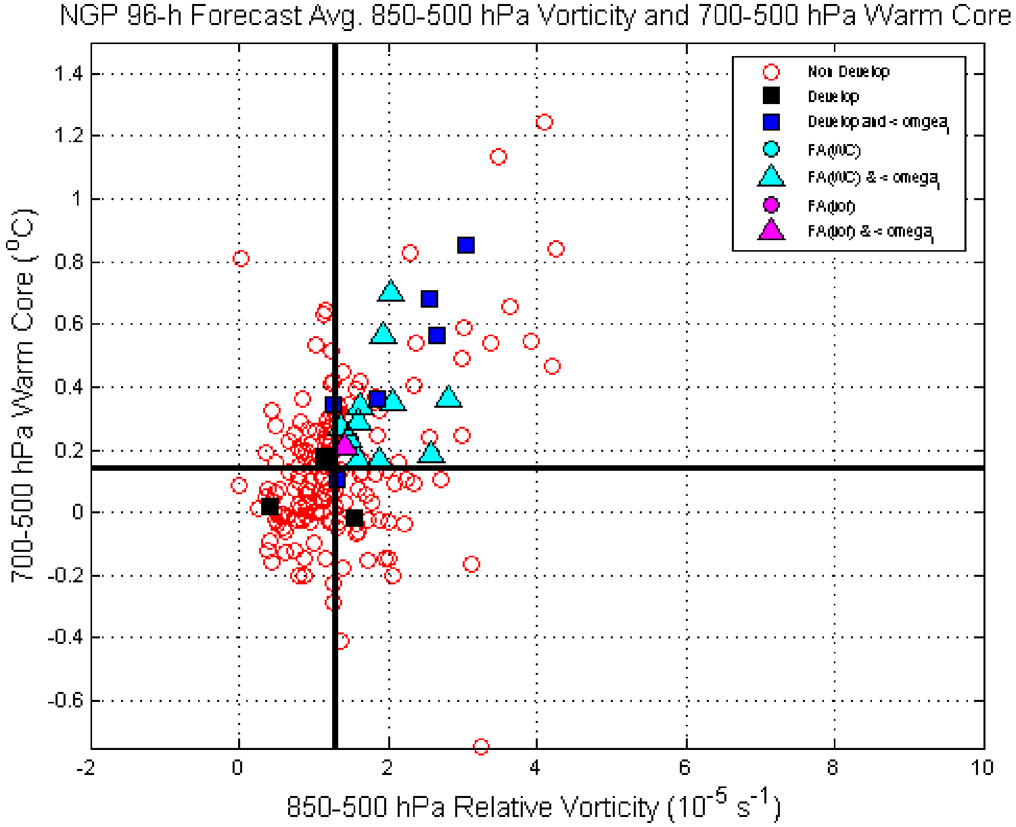
NGP 96-h Forecast Avg. 850-500 hPa Vorticity and 700-500 hPa Warm Core
700-500 hPa Warm Core (^oC)
850-500 hPa Relative Vorticity (10^{-5} s^{-1})
1.4
1.2
1
0.8
0.6
0.4
0.2
0
-0.2
-0.4
-0.6
-2
0
2
4
6
8
10
Non Develop
Develop
Develop and < omgea$_t$
FA(WC)
FA(WC) & < omega$_t$
FA(vor)
FA(vor) & < omega$_t$

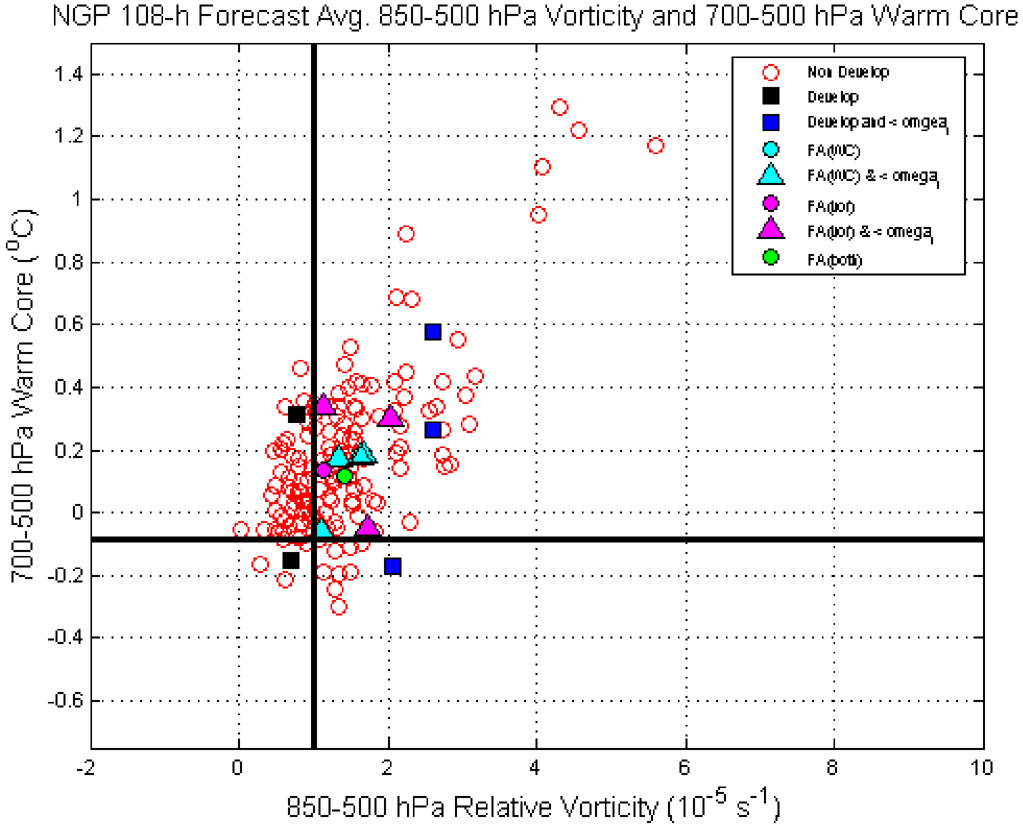
NGP 108-h Forecast Avg. 850-500 hPa Vorticity and 700-500 hPa Warm Core
700-500 hPa Warm Core (^oC)
850-500 hPa Relative Vorticity (10^{-5} s^{-1})
1.4
1.2
1
0.8
0.6
0.4
0.2
0
-0.2
-0.4
-0.6
-2
0
2
4
6
8
10
Non Develop
Develop
Develop and < omgea$_t$
FA(WC)
FA(WC) & < omega$_t$
FA(vor)
FA(vor) & < omega$_t$
FA(both)

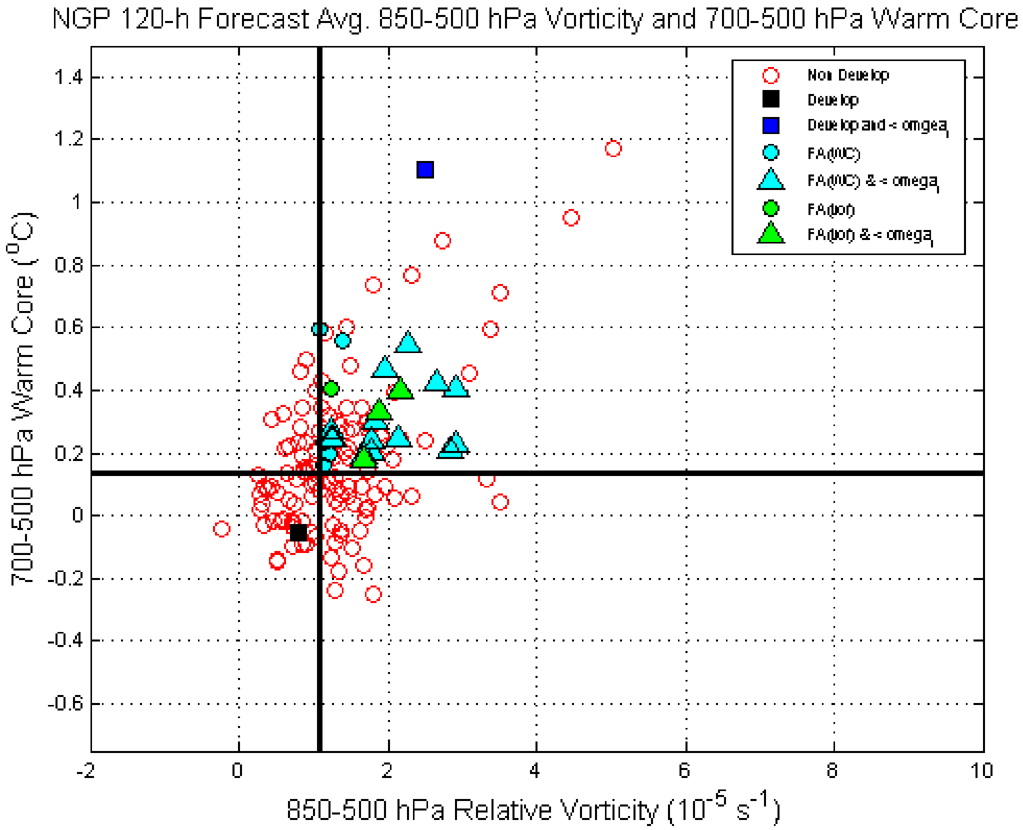
NGP 120-h Forecast Avg. 850-500 hPa Vorticity and 700-500 hPa Warm Core

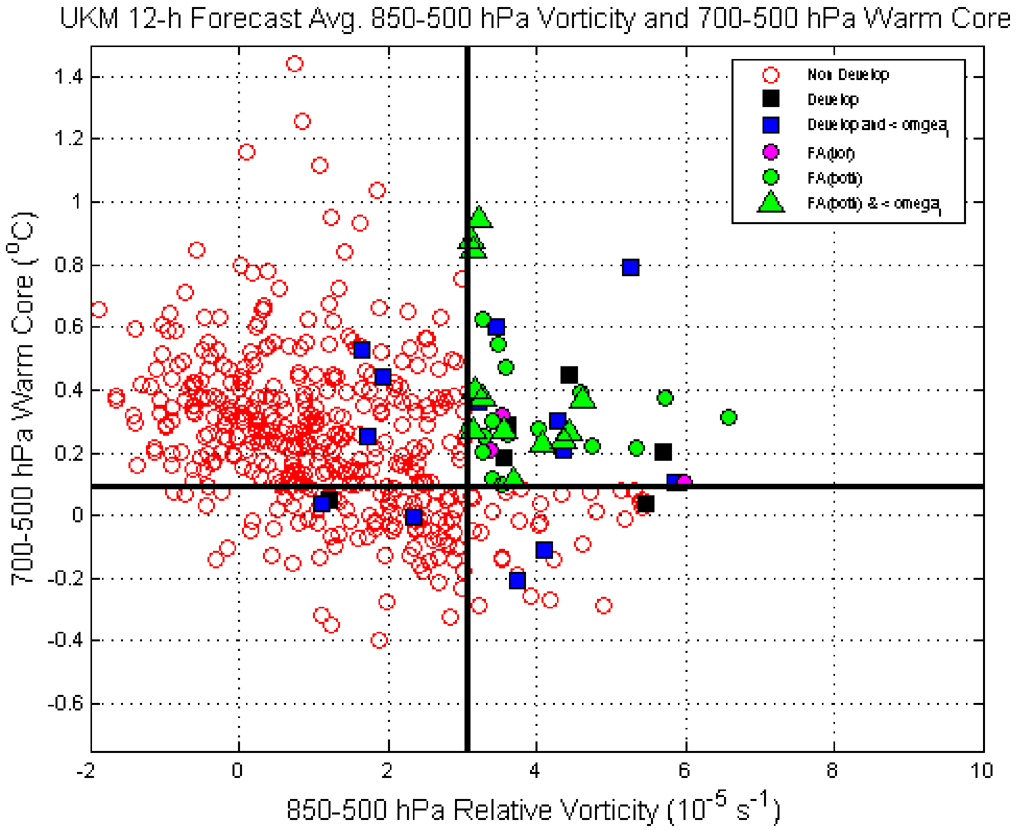
UKM 12-h Forecast Avg. 850-500 hPa Vorticity and 700-500 hPa Warm Core

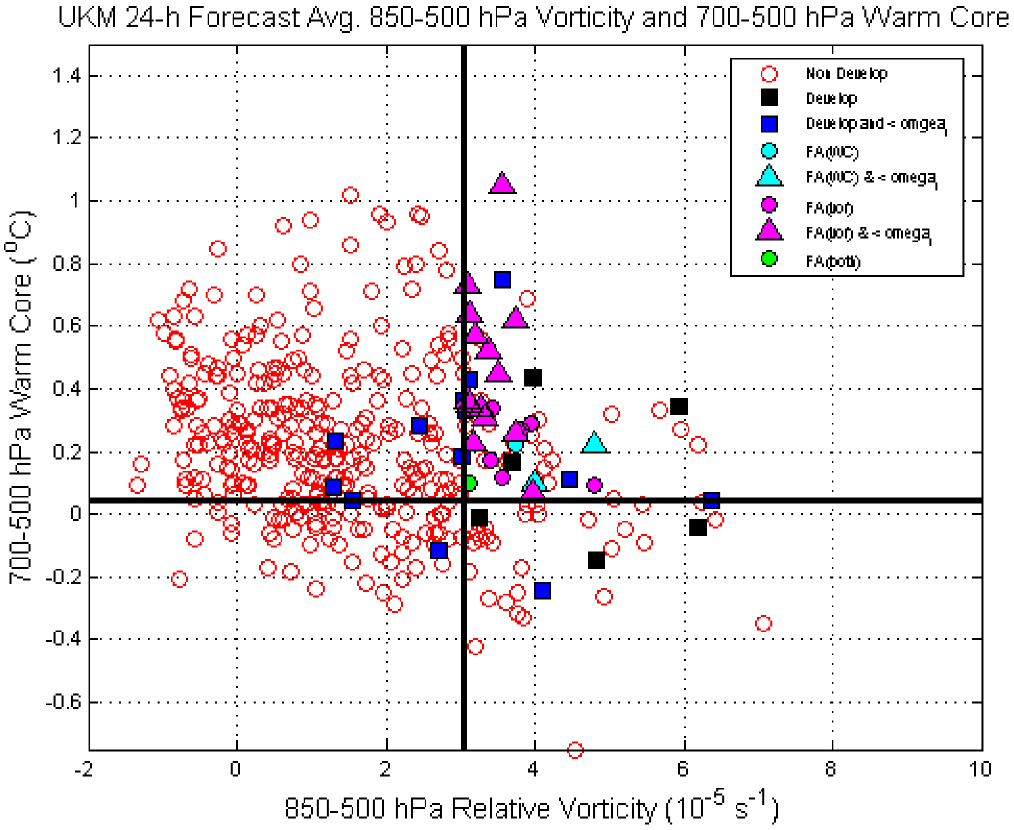
UKM 24-h Forecast Avg. 850-500 hPa Vorticity and 700-500 hPa Warm Core

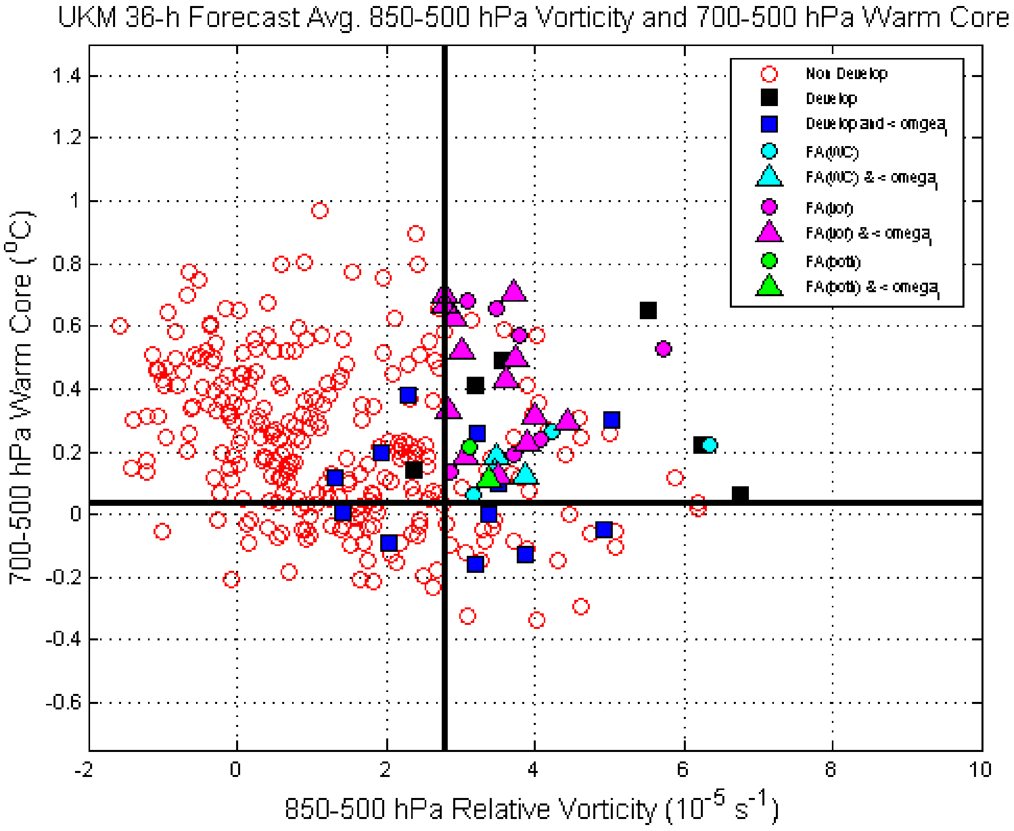
UKM 36-h Forecast Avg. 850-500 hPa Vorticity and 700-500 hPa Warm Core

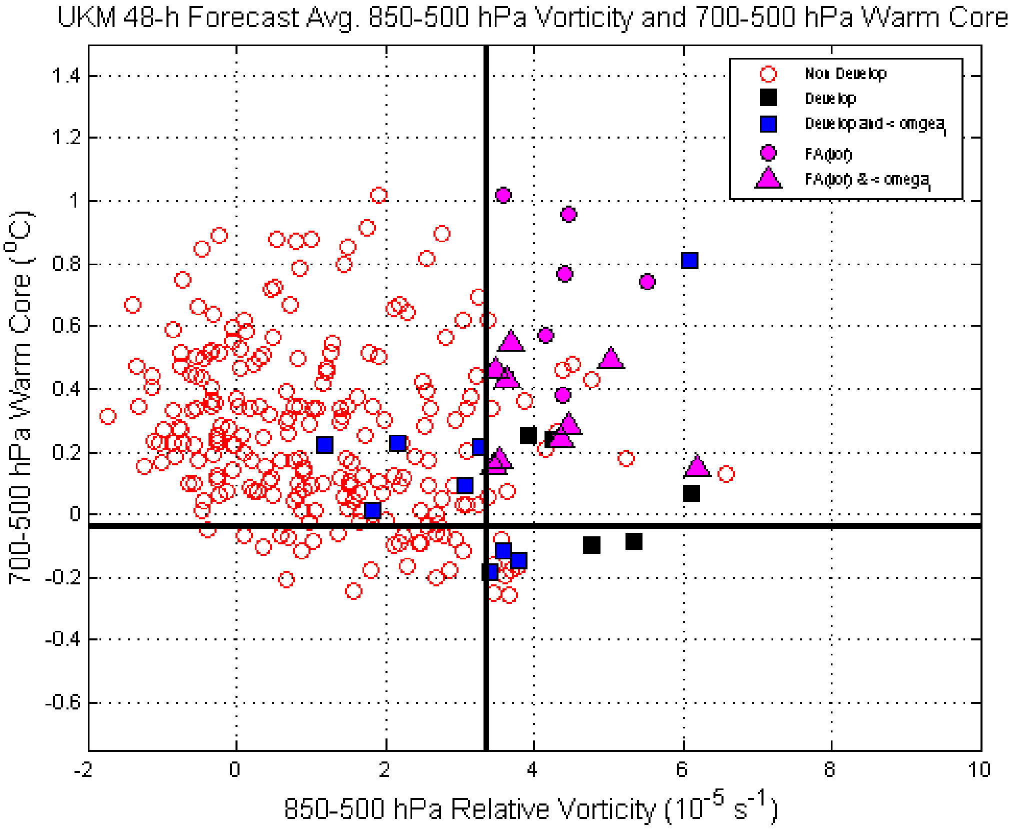
UKM 48-h Forecast Avg. 850-500 hPa Vorticity and 700-500 hPa Warm Core

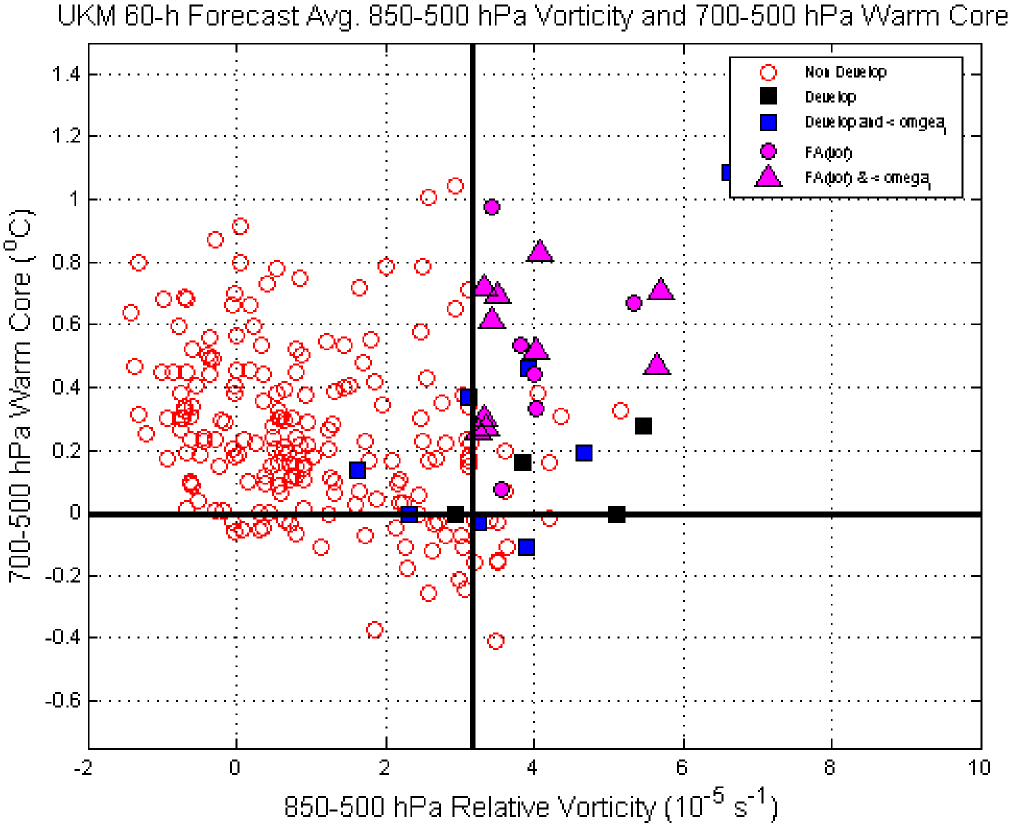
UKM 60-h Forecast Avg. 850-500 hPa Vorticity and 700-500 hPa Warm Core

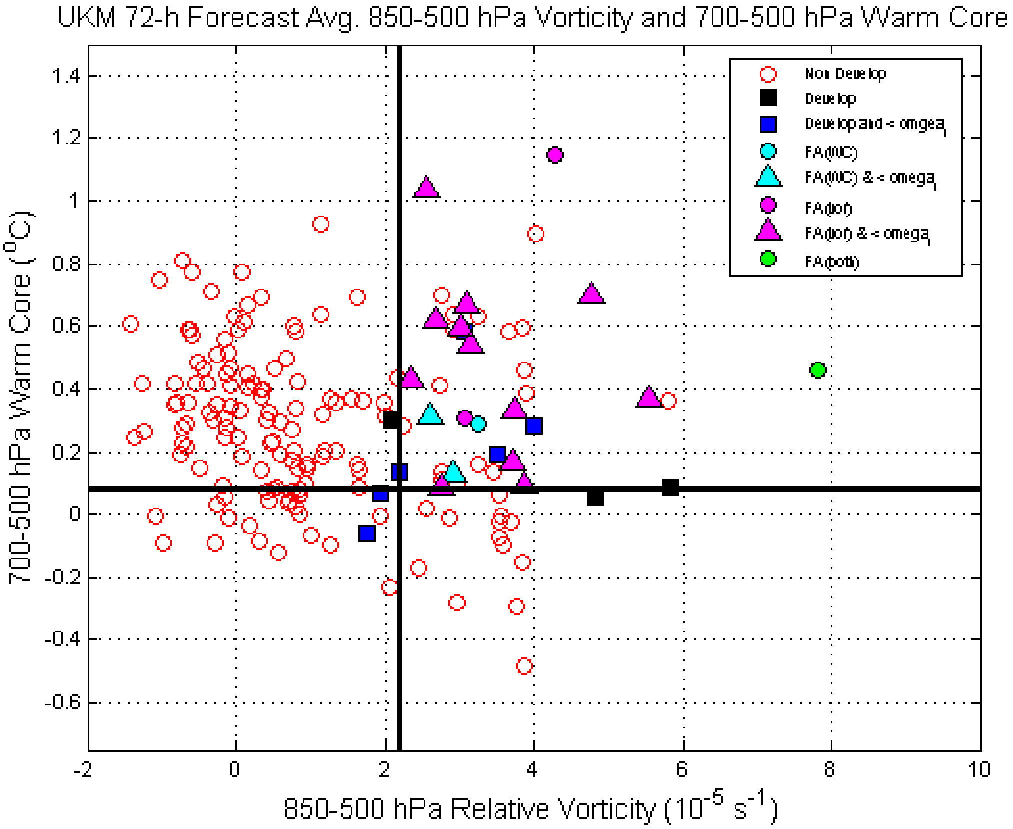
UKM 72-h Forecast Avg. 850-500 hPa Vorticity and 700-500 hPa Warm Core

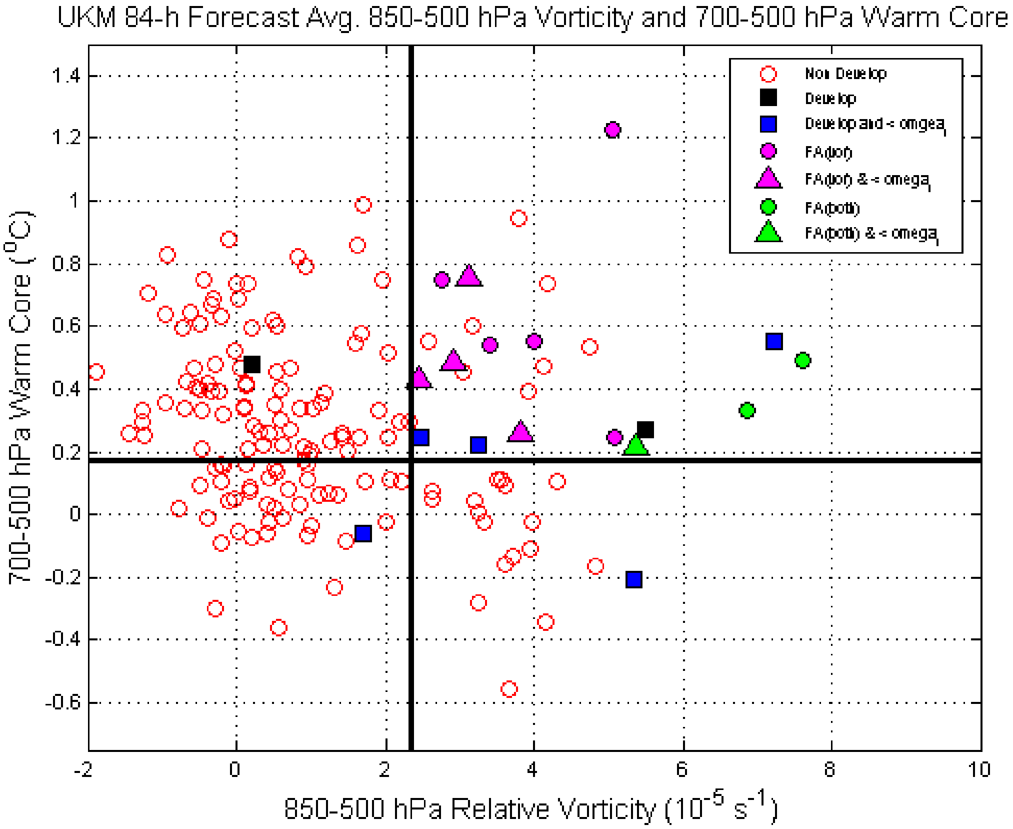
UKM 84-h Forecast Avg. 850-500 hPa Vorticity and 700-500 hPa Warm Core

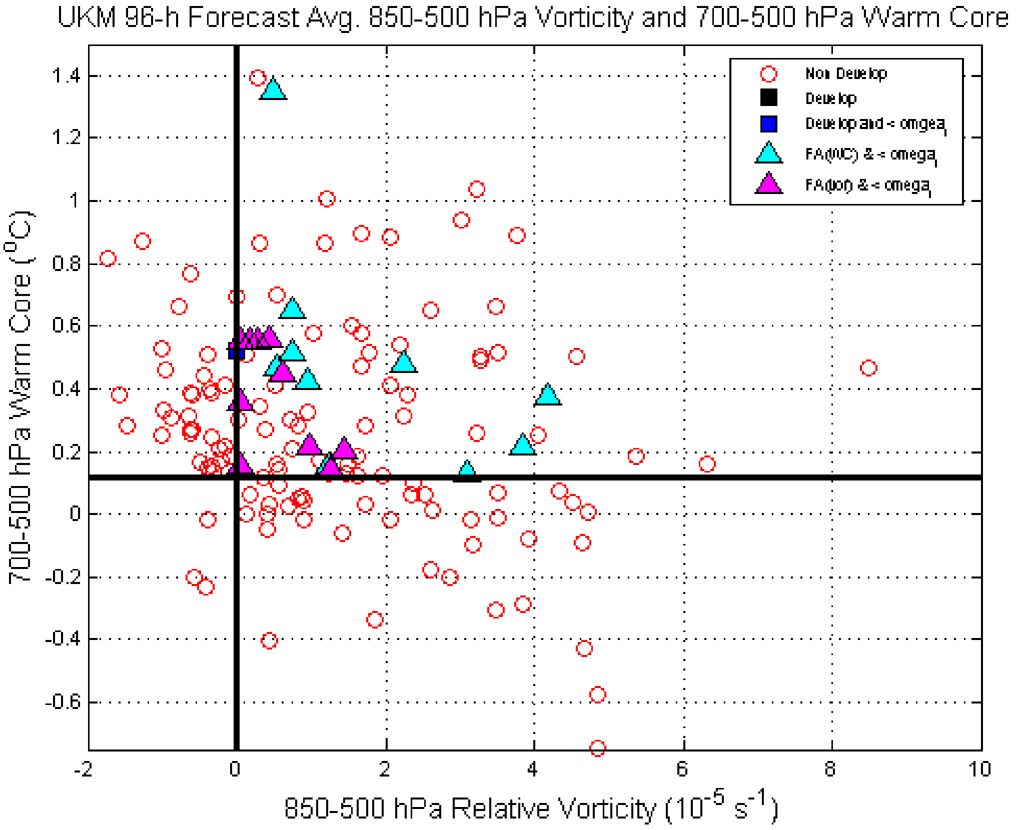
UKM 96-h Forecast Avg. 850-500 hPa Vorticity and 700-500 hPa Warm Core
700-500 hPa Warm Core (°C)
850-500 hPa Relative Vorticity (10^{-5} s^{-1})
1.4
1.2
1
0.8
0.6
0.4
0.2
0
-0.2
-0.4
-0.6
-2
0
2
4
6
8
10
Non Develop
Develop
Develop and < omega_t
FA(WC) & < omega_t
FA(Vor) & < omega_t

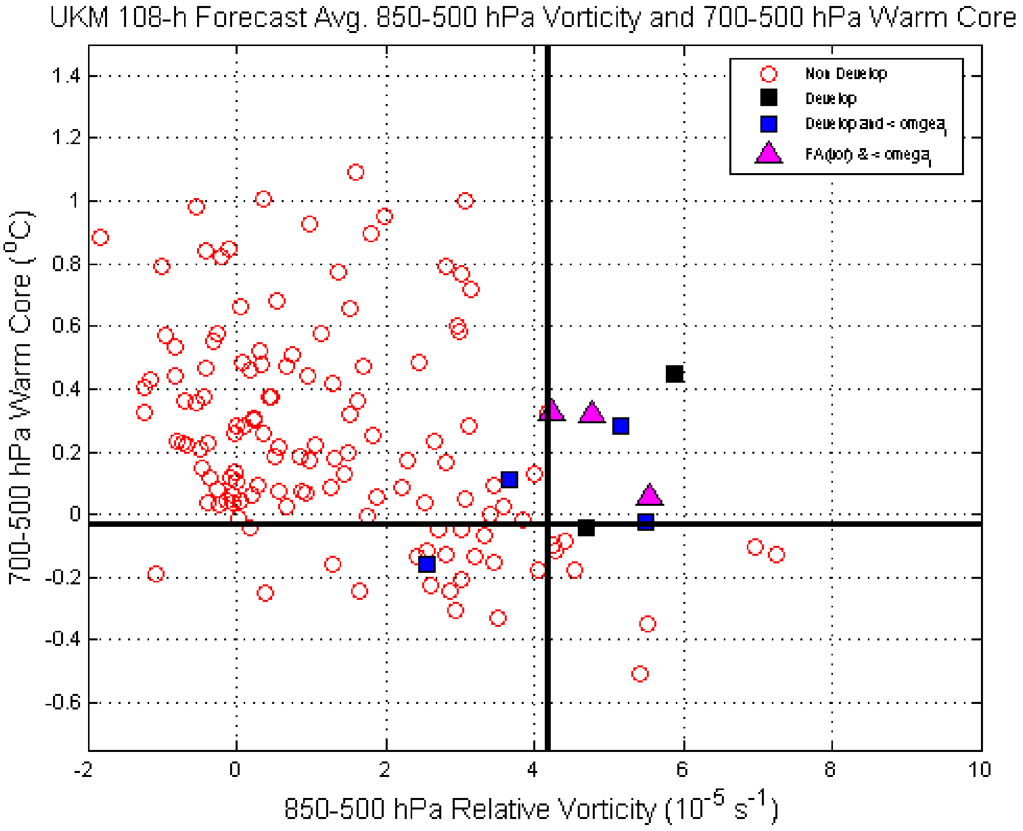
UKM 108-h Forecast Avg. 850-500 hPa Vorticity and 700-500 hPa Warm Core
700-500 hPa Warm Core (°C)
850-500 hPa Relative Vorticity (10^{-5} s^{-1})
1.4
1.2
1
0.8
0.6
0.4
0.2
0
-0.2
-0.4
-0.6
-2
0
2
4
6
8
10
Non Develop
Develop
Develop and < omega_t
FA(Vor) & < omega_t

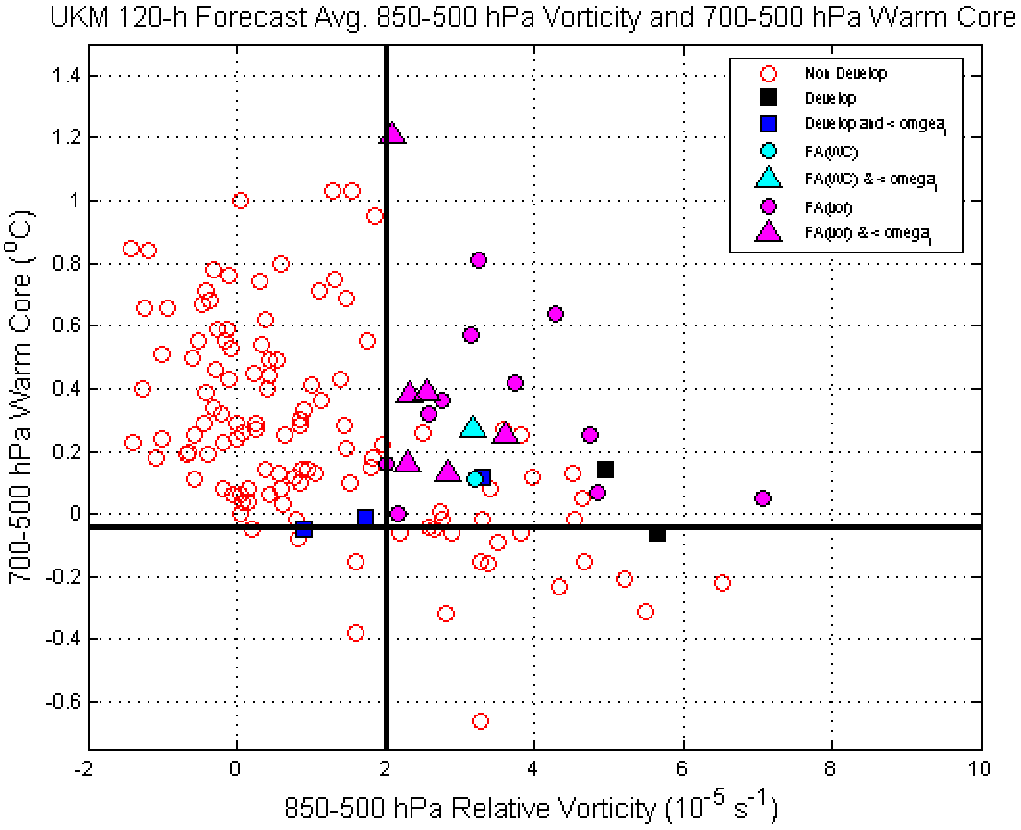
UKM 120-h Forecast Avg. 850-500 hPa Vorticity and 700-500 hPa Warm Core
700-500 hPa Warm Core (^oC)
850-500 hPa Relative Vorticity (10^{-5} s^{-1})
1.4
1.2
1
0.8
0.6
0.4
0.2
0
-0.2
-0.4
-0.6
-2
0
2
4
6
8
10
Non Develop
Develop
Develop and < omgea
FA(WC)
FA(WC) & < omega
FA(vor)
FA(vor) & < omega

APPENDIX C. PROBABILITY DISTRIBUTION FUNCTIONS

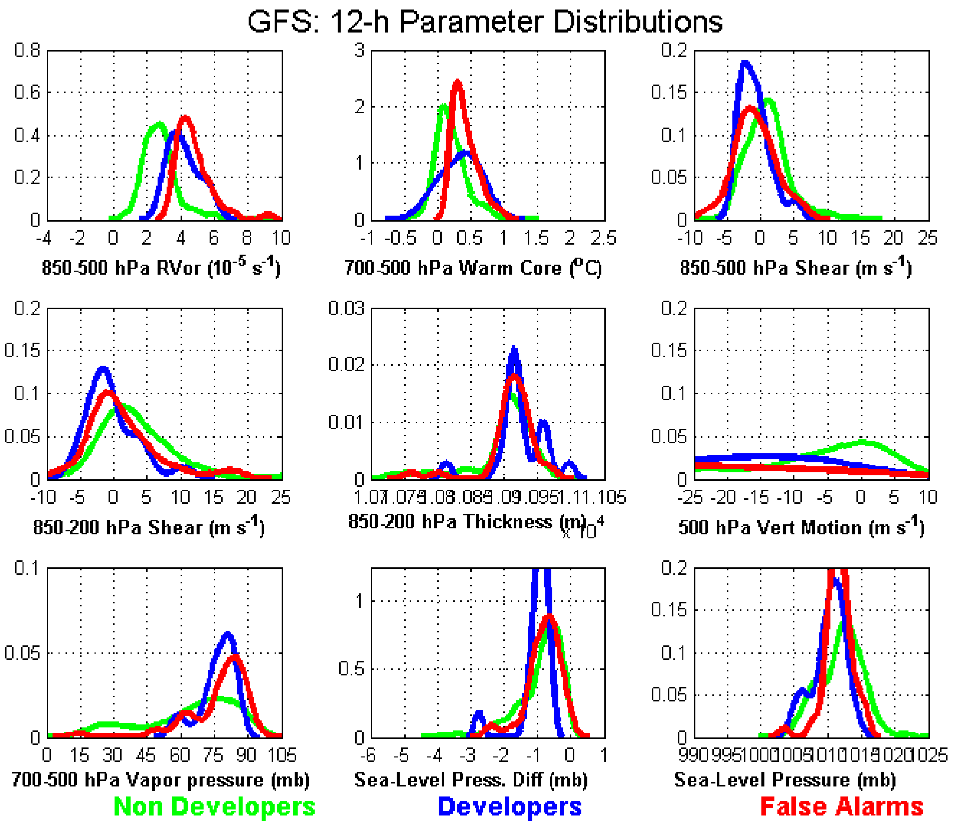

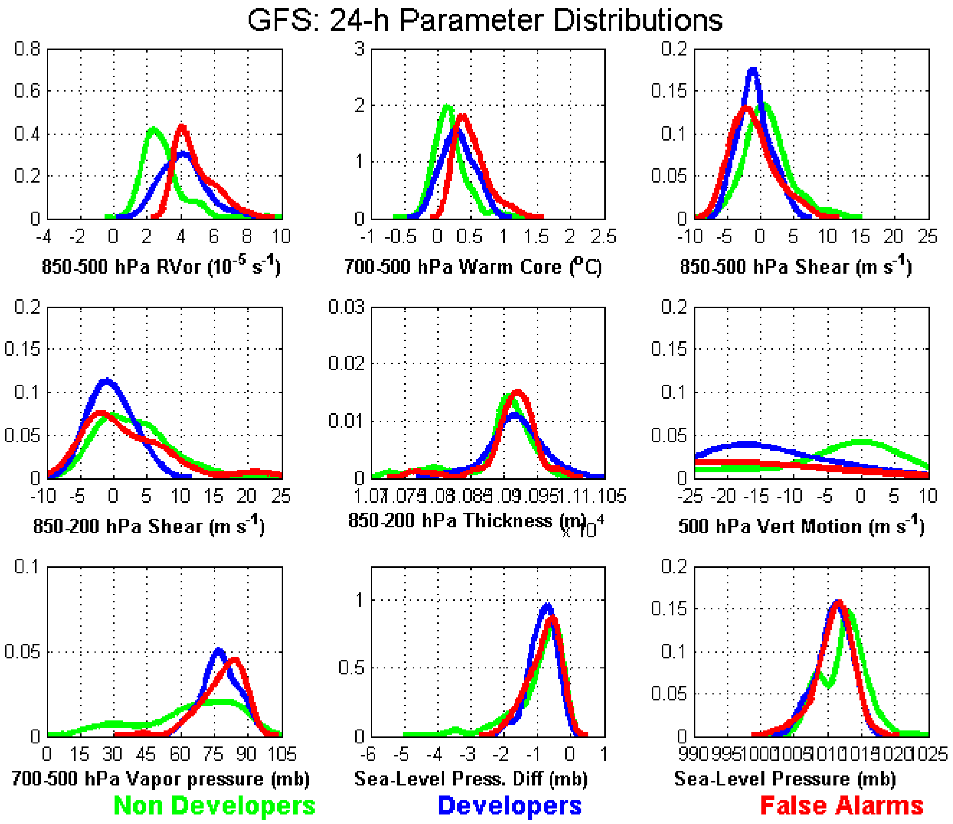
GFS: 24-h Parameter Distributions
850-500 hPa RVor (10^{-5} s^{-1})
700-500 hPa Warm Core (°C)
850-500 hPa Shear (m s^{-1})
850-200 hPa Shear (m s^{-1})
850-200 hPa Thickness (m) x 10^4
500 hPa Vert Motion (m s^{-1})
700-500 hPa Vapor pressure (mb)
Sea-Level Press. Diff (mb)
Sea-Level Pressure (mb)
Non Developers
Developers
False Alarms

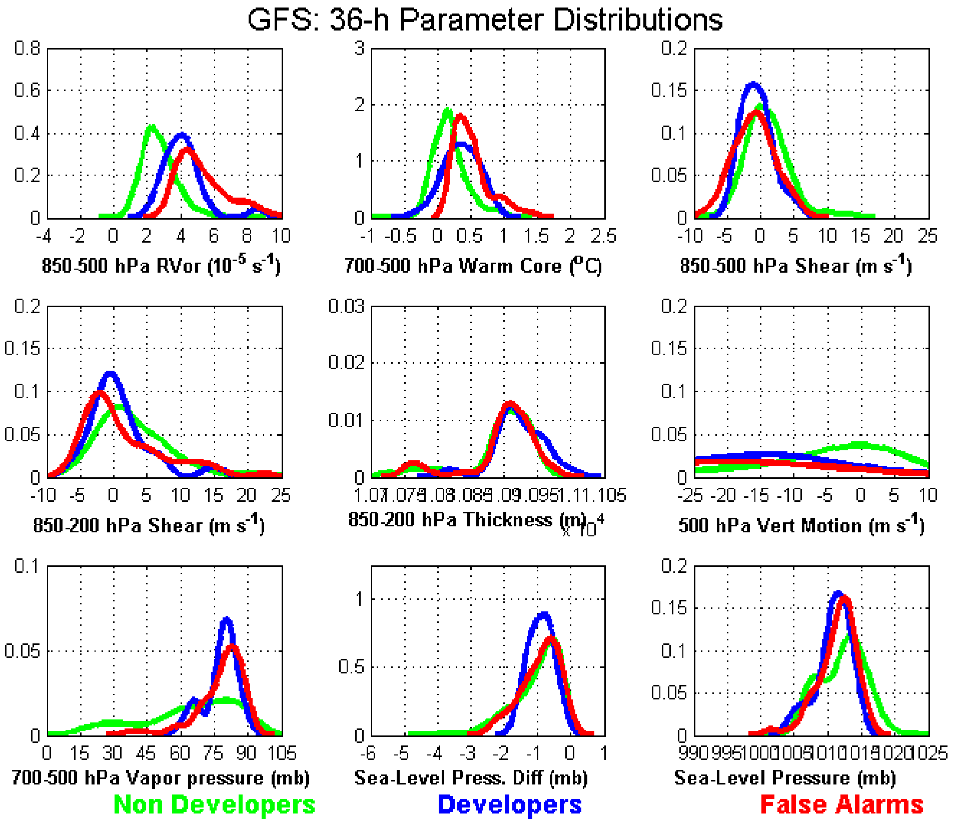
GFS: 36-h Parameter Distributions
850-500 hPa RVor (10^{-5} s^{-1})
700-500 hPa Warm Core (°C)
850-500 hPa Shear (m s^{-1})
850-200 hPa Shear (m s^{-1})
850-200 hPa Thickness (m) x 10^4
500 hPa Vert Motion (m s^{-1})
700-500 hPa Vapor pressure (mb)
Sea-Level Press. Diff (mb)
Sea-Level Pressure (mb)
Non Developers
Developers
False Alarms

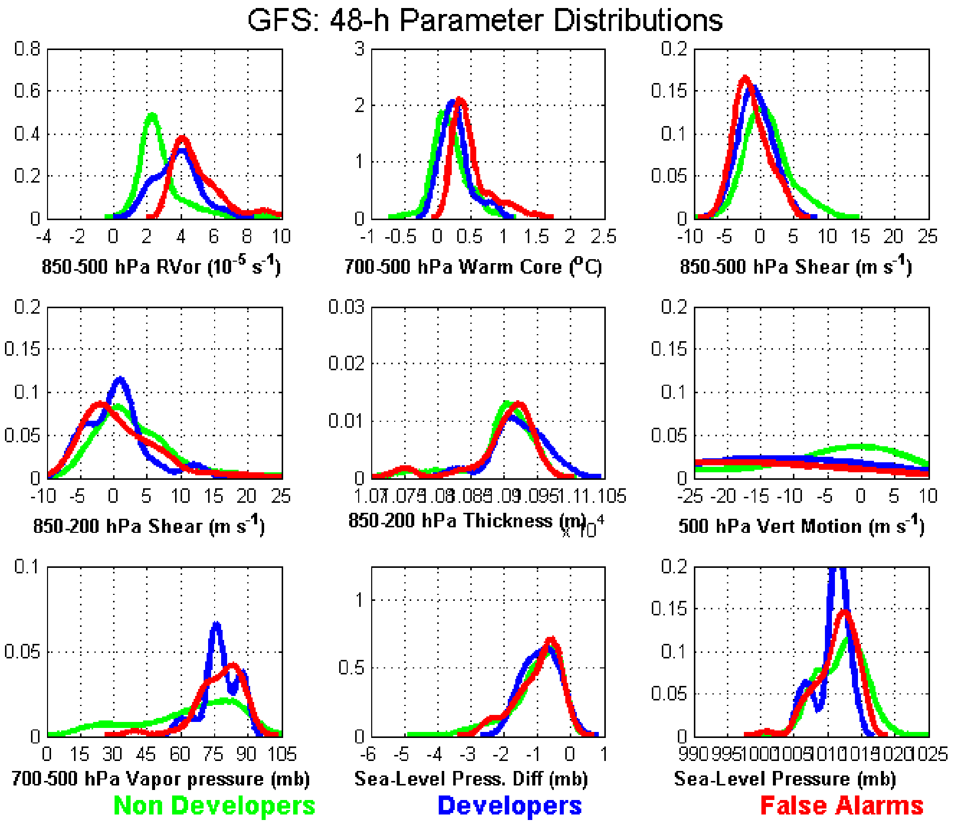
GFS: 48-h Parameter Distributions
850-500 hPa RVor (10^{-5} s^{-1})
700-500 hPa Warm Core (^oC)
850-500 hPa Shear (m s^{-1})
850-200 hPa Shear (m s^{-1})
850-200 hPa Thickness (m)
x 10^4
500 hPa Vert Motion (m s^{-1})
700-500 hPa Vapor pressure (mb)
Sea-Level Press. Diff (mb)
Sea-Level Pressure (mb)
Non Developers
Developers
False Alarms

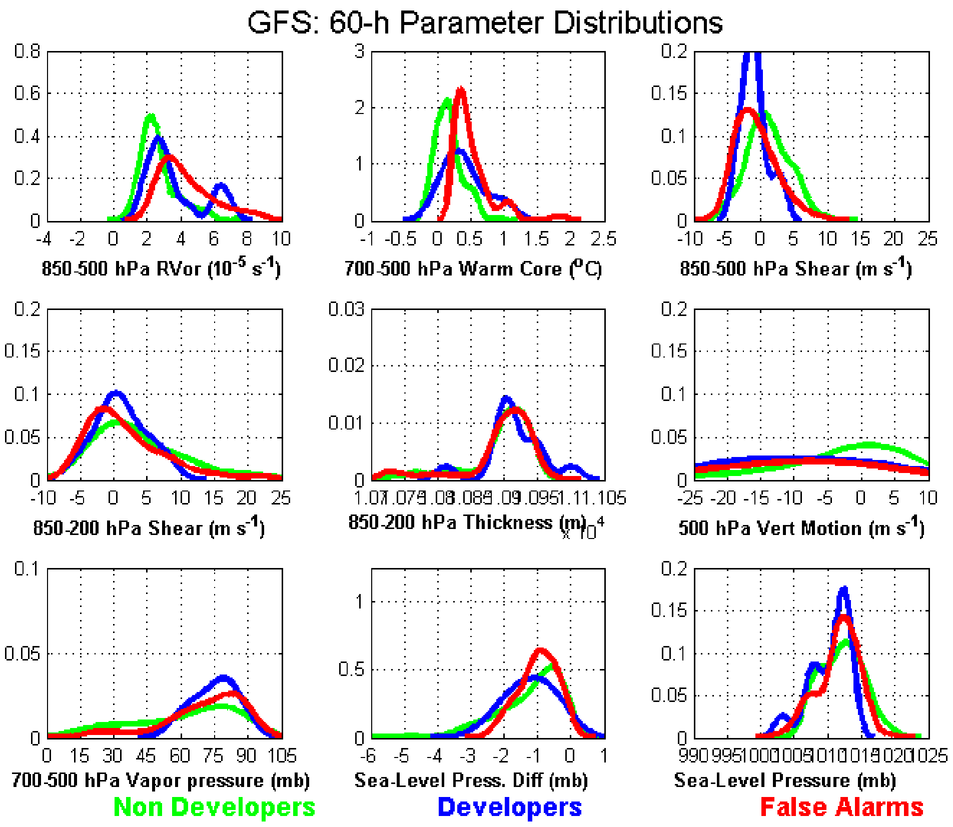
GFS: 60-h Parameter Distributions
850-500 hPa RVor (10^{-5} s^{-1})
700-500 hPa Warm Core (^oC)
850-500 hPa Shear (m s^{-1})
850-200 hPa Shear (m s^{-1})
850-200 hPa Thickness (m)
x 10^4
500 hPa Vert Motion (m s^{-1})
700-500 hPa Vapor pressure (mb)
Sea-Level Press. Diff (mb)
Sea-Level Pressure (mb)
Non Developers
Developers
False Alarms

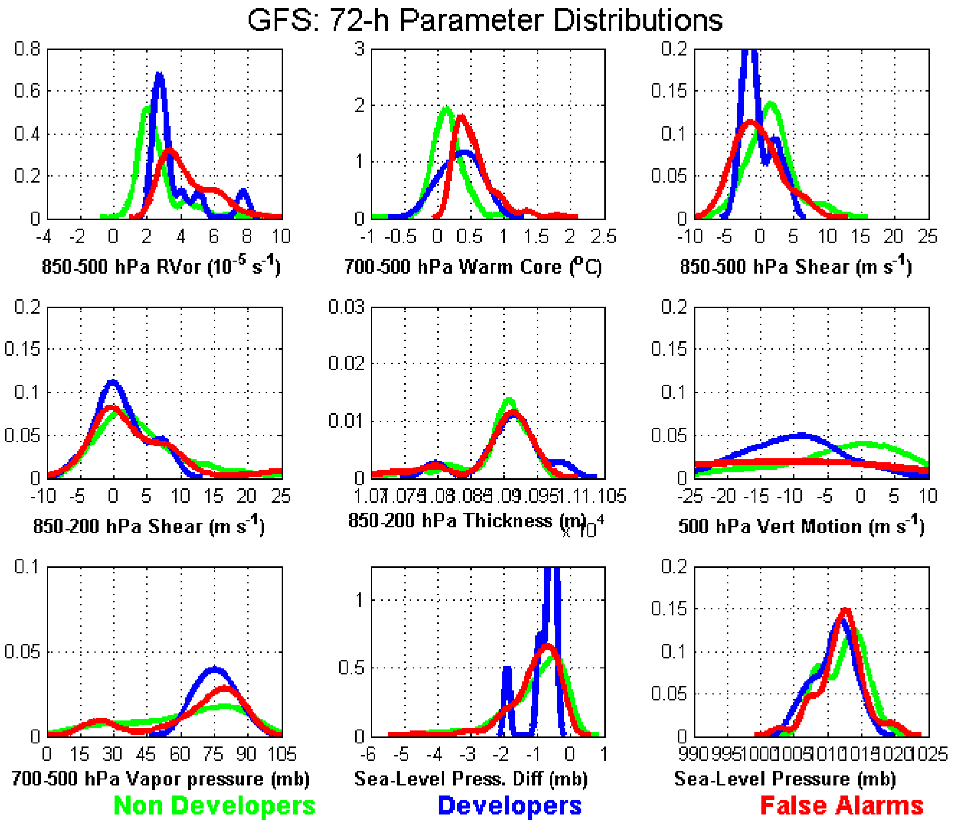
GFS: 72-h Parameter Distributions
850-500 hPa RVor (10^-5 s^-1)
700-500 hPa Warm Core (°C)
850-500 hPa Shear (m s^-1)
850-200 hPa Shear (m s^-1)
850-200 hPa Thickness (m) x 10^4
500 hPa Vert Motion (m s^-1)
700-500 hPa Vapor pressure (mb)
Sea-Level Press. Diff (mb)
Sea-Level Pressure (mb)
Non Developers
Developers
False Alarms

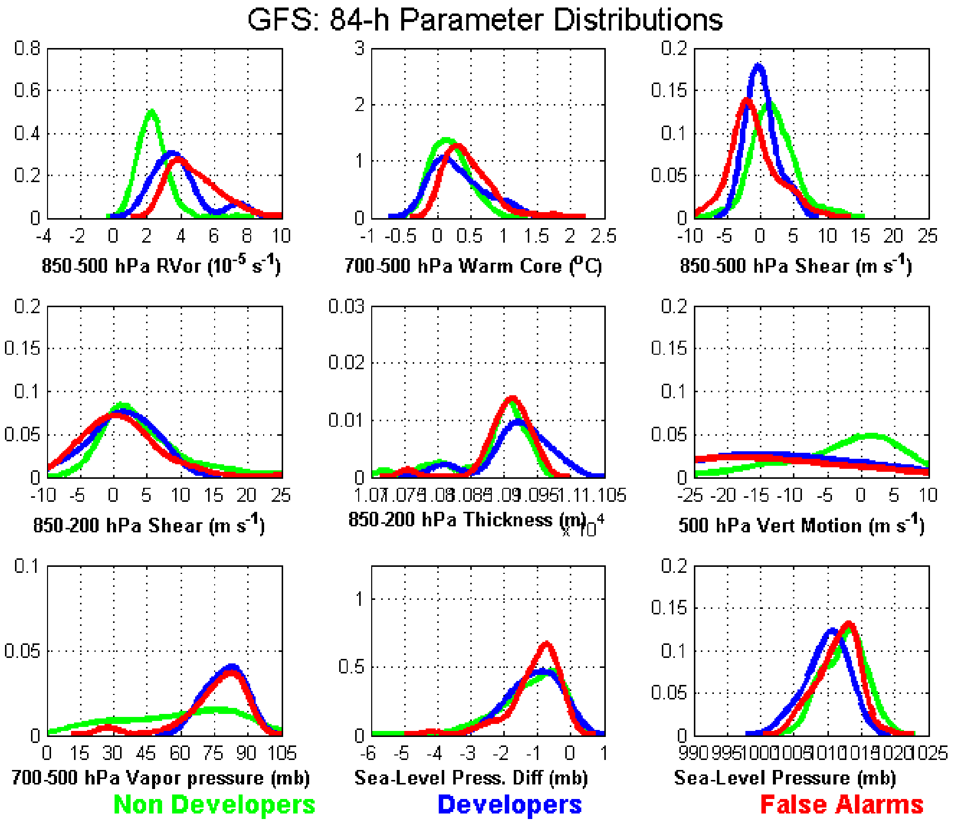
GFS: 84-h Parameter Distributions
850-500 hPa RVor (10^-5 s^-1)
700-500 hPa Warm Core (°C)
850-500 hPa Shear (m s^-1)
850-200 hPa Shear (m s^-1)
850-200 hPa Thickness (m) x 10^4
500 hPa Vert Motion (m s^-1)
700-500 hPa Vapor pressure (mb)
Sea-Level Press. Diff (mb)
Sea-Level Pressure (mb)
Non Developers
Developers
False Alarms

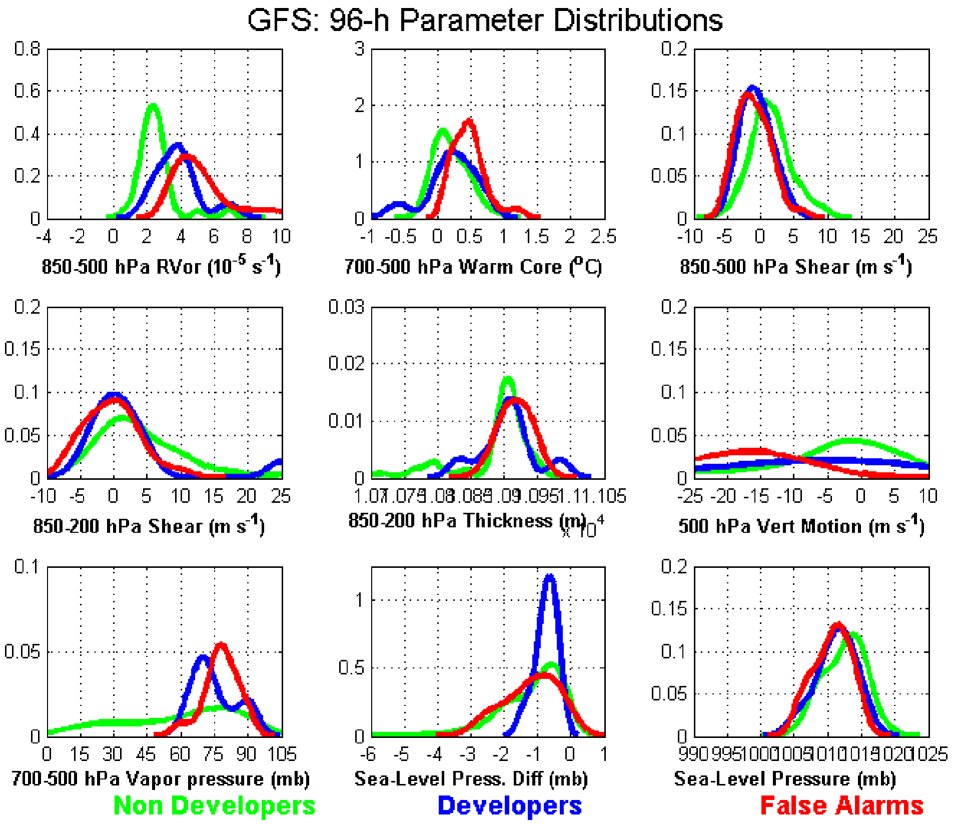

GFS: 96-h Parameter Distributions

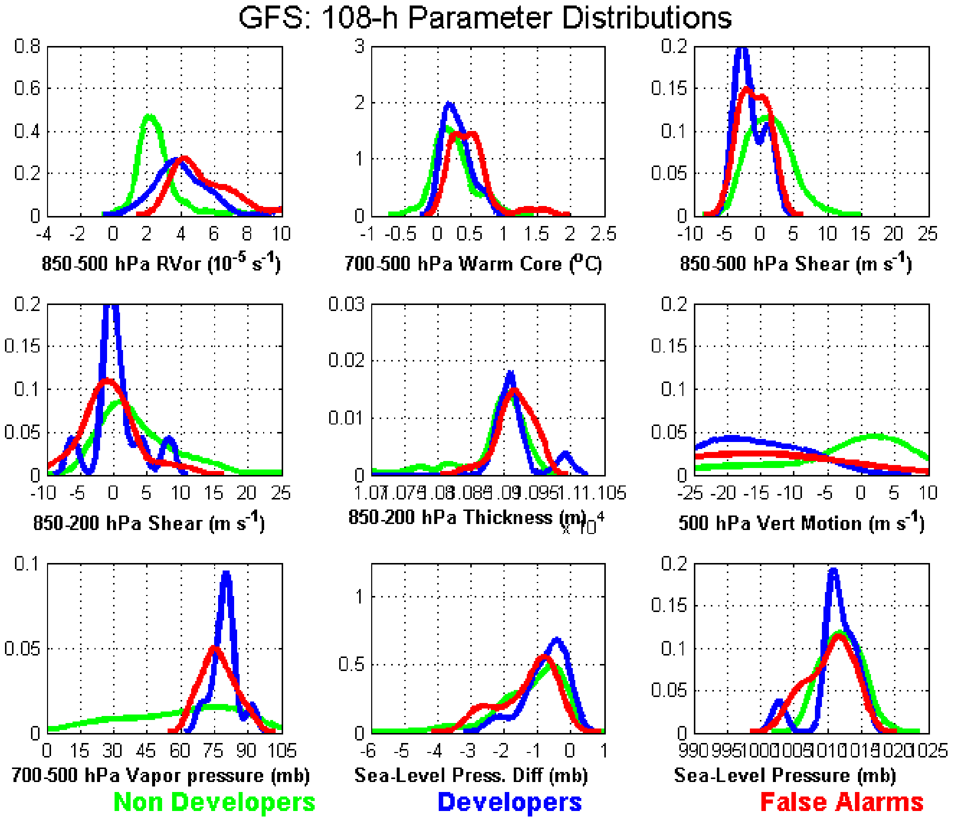

GFS: 108-h Parameter Distributions

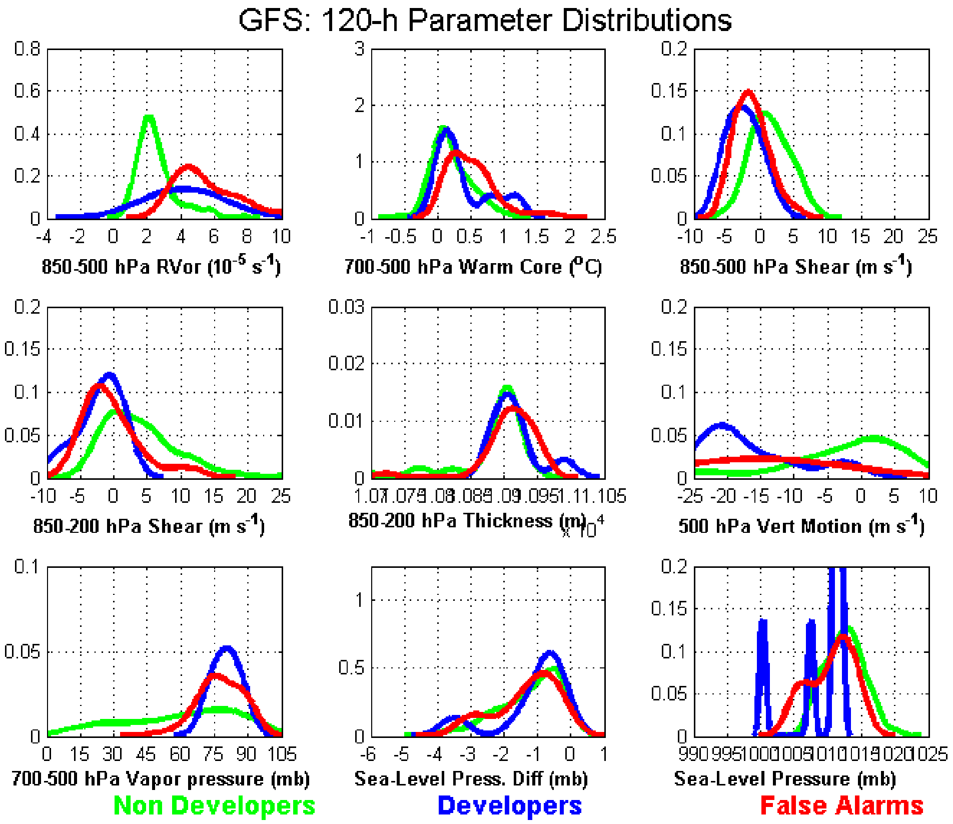
GFS: 120-h Parameter Distributions

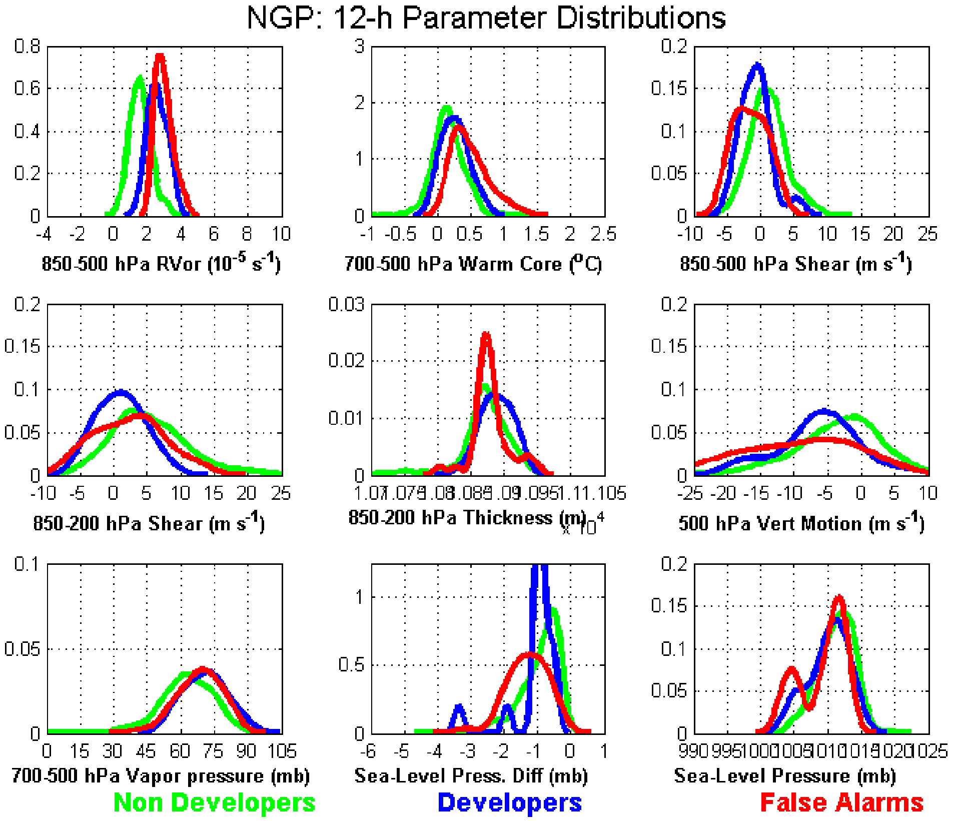
NGP: 12-h Parameter Distributions

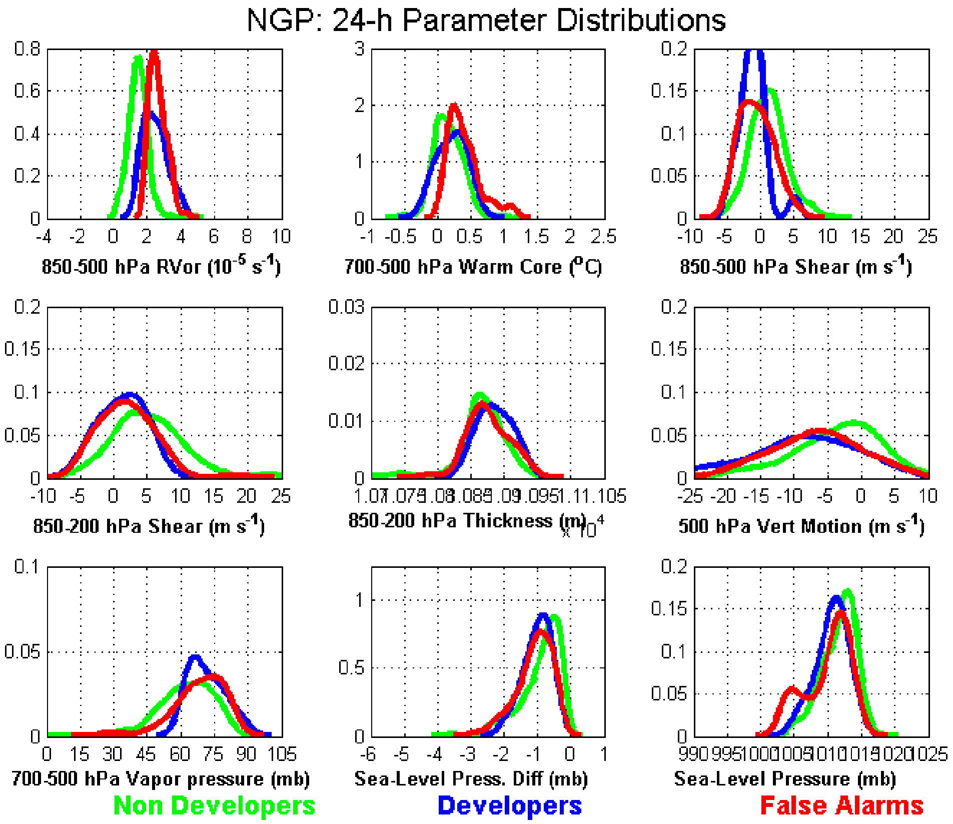
NGP: 24-h Parameter Distributions
850-500 hPa RVor (10-5 s-1)
700-500 hPa Warm Core (oC)
850-500 hPa Shear (m s-1)
850-200 hPa Shear (m s-1)
850-200 hPa Thickness (m)
x 10^4
500 hPa Vert Motion (m s-1)
700-500 hPa Vapor pressure (mb)
Sea-Level Press. Diff (mb)
Sea-Level Pressure (mb)
Non Developers
Developers
False Alarms

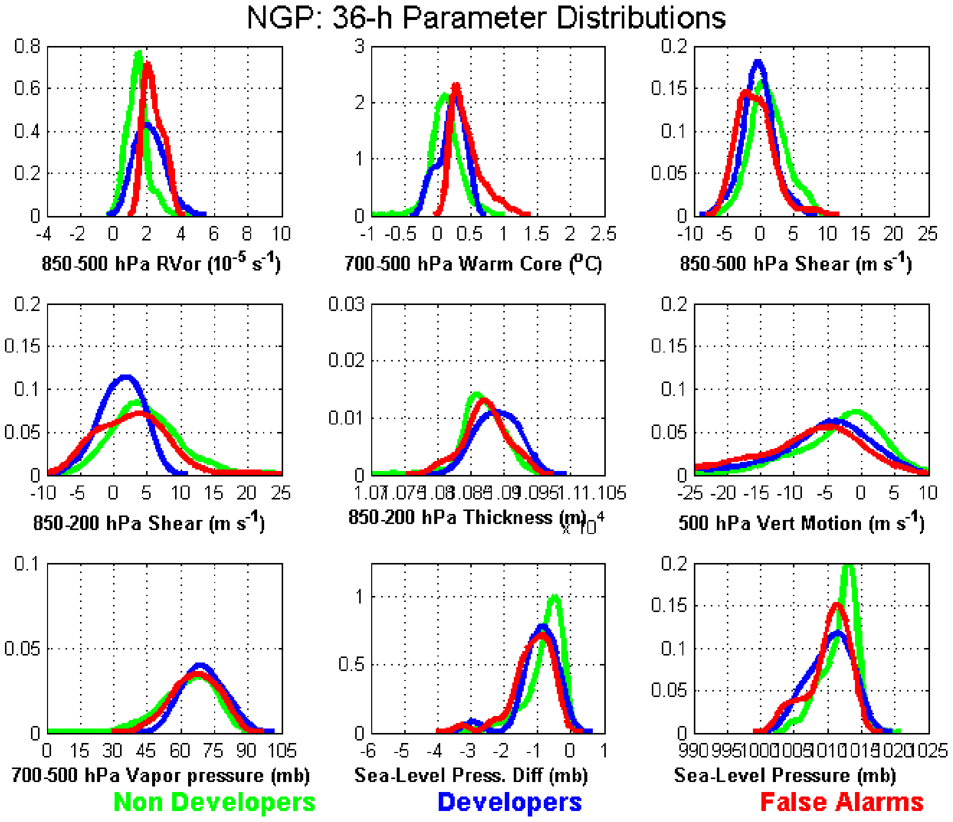
NGP: 36-h Parameter Distributions
850-500 hPa RVor (10-5 s-1)
700-500 hPa Warm Core (oC)
850-500 hPa Shear (m s-1)
850-200 hPa Shear (m s-1)
850-200 hPa Thickness (m)
x 10^4
500 hPa Vert Motion (m s-1)
700-500 hPa Vapor pressure (mb)
Sea-Level Press. Diff (mb)
Sea-Level Pressure (mb)
Non Developers
Developers
False Alarms

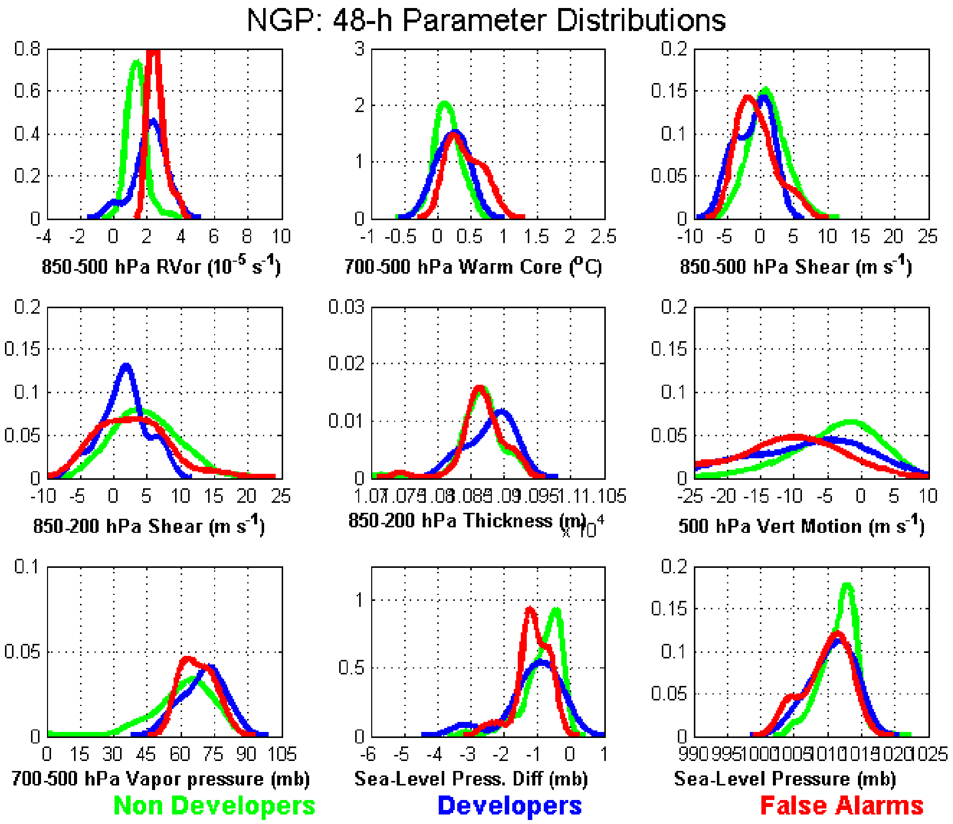
NGP: 48-h Parameter Distributions

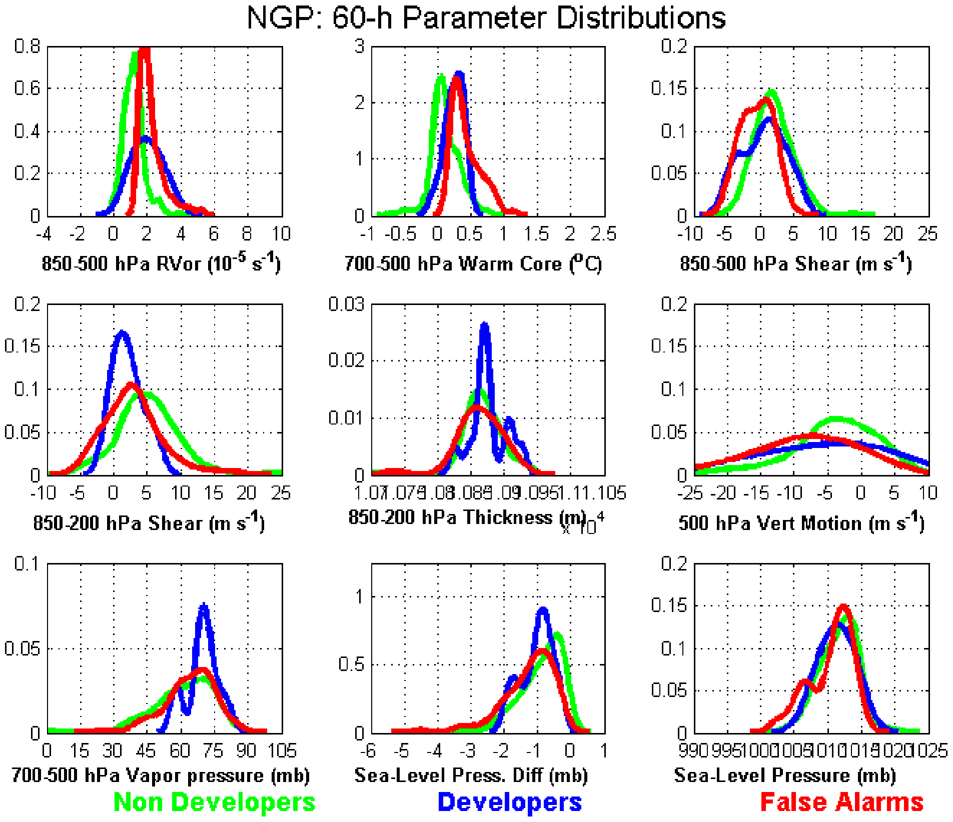
NGP: 60-h Parameter Distributions

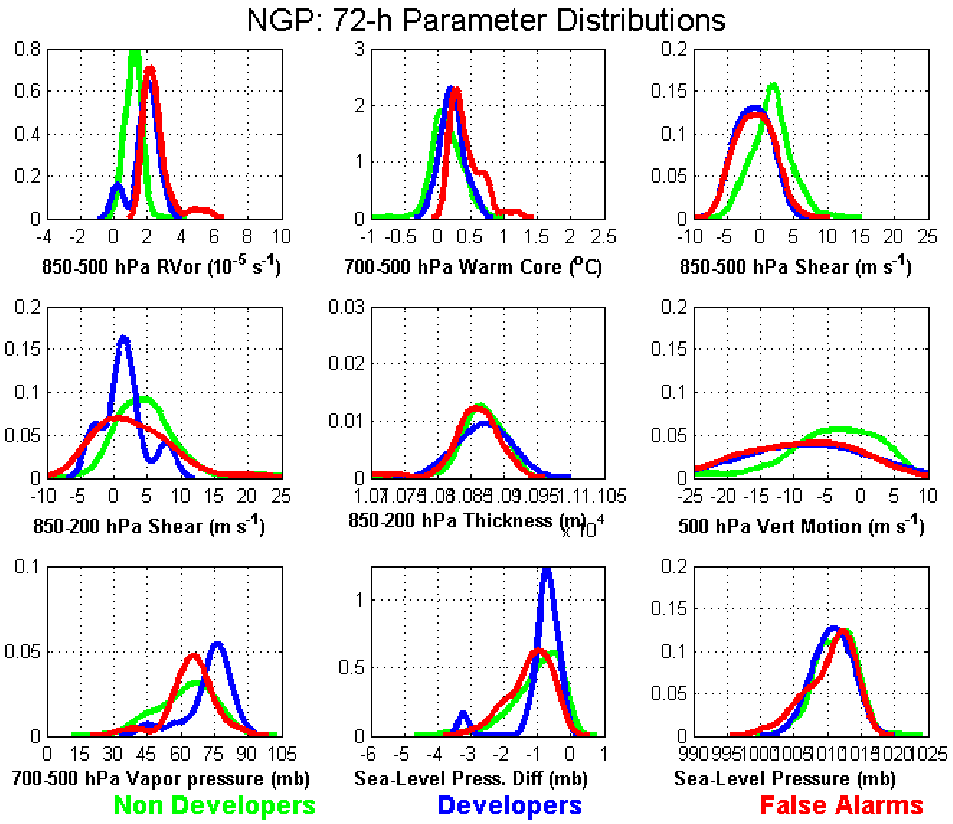
NGP: 72-h Parameter Distributions
850-500 hPa RVor (10^-5 s^-1)
700-500 hPa Warm Core (°C)
850-500 hPa Shear (m s^-1)
850-200 hPa Shear (m s^-1)
850-200 hPa Thickness (m) x 10^4
500 hPa Vert Motion (m s^-1)
700-500 hPa Vapor pressure (mb)
Sea-Level Press. Diff (mb)
Sea-Level Pressure (mb)
Non Developers
Developers
False Alarms

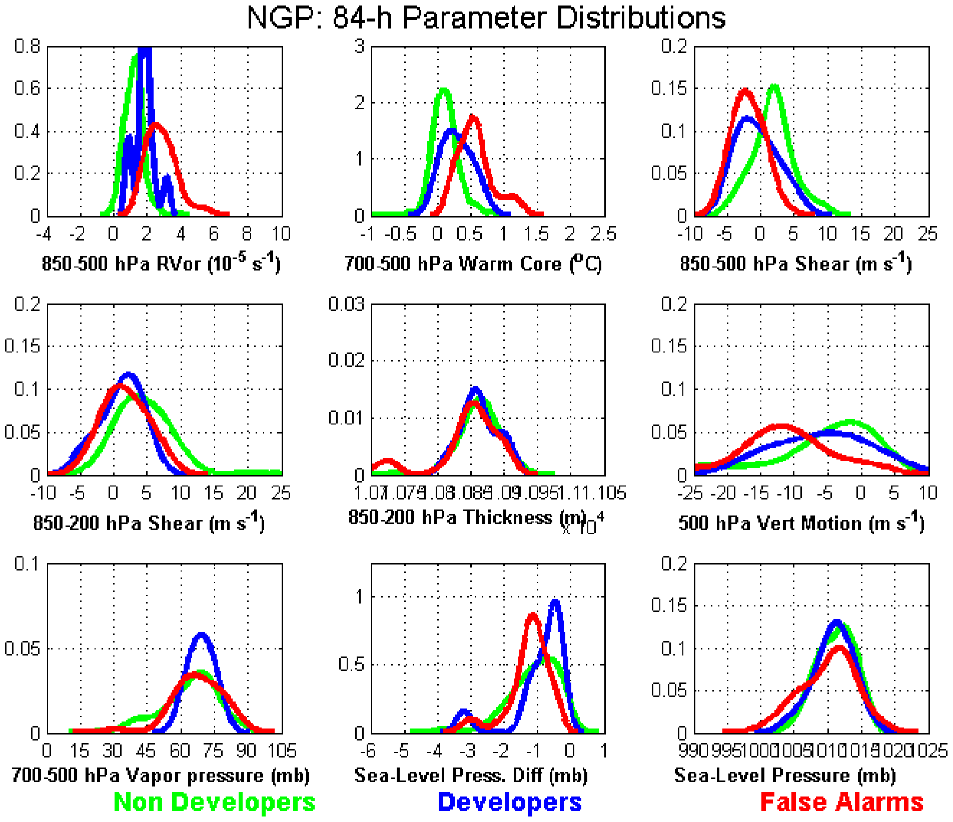
NGP: 84-h Parameter Distributions
850-500 hPa RVor (10^-5 s^-1)
700-500 hPa Warm Core (°C)
850-500 hPa Shear (m s^-1)
850-200 hPa Shear (m s^-1)
850-200 hPa Thickness (m) x 10^4
500 hPa Vert Motion (m s^-1)
700-500 hPa Vapor pressure (mb)
Sea-Level Press. Diff (mb)
Sea-Level Pressure (mb)
Non Developers
Developers
False Alarms

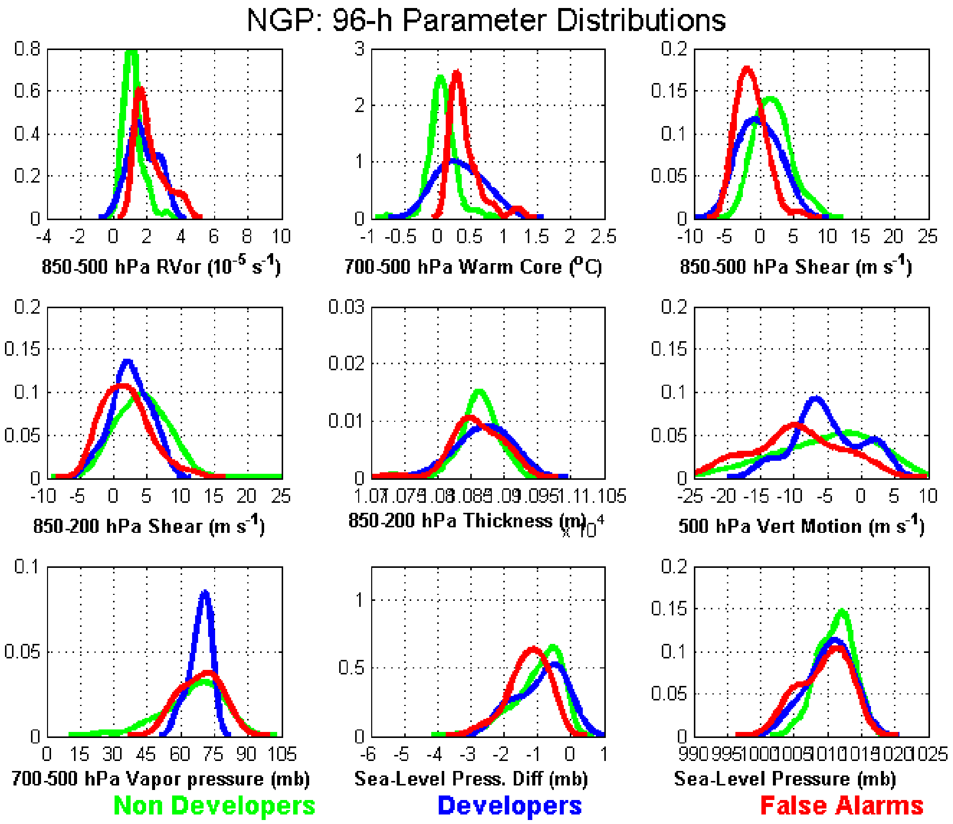
NGP: 96-h Parameter Distributions
850-500 hPa RVor (10^{-5} s^{-1})
700-500 hPa Warm Core (^{o}C)
850-500 hPa Shear (m s^{-1})
850-200 hPa Shear (m s^{-1})
850-200 hPa Thickness (m)
x 10^4
500 hPa Vert Motion (m s^{-1})
700-500 hPa Vapor pressure (mb)
Sea-Level Press. Diff (mb)
Sea-Level Pressure (mb)
Non Developers
Developers
False Alarms

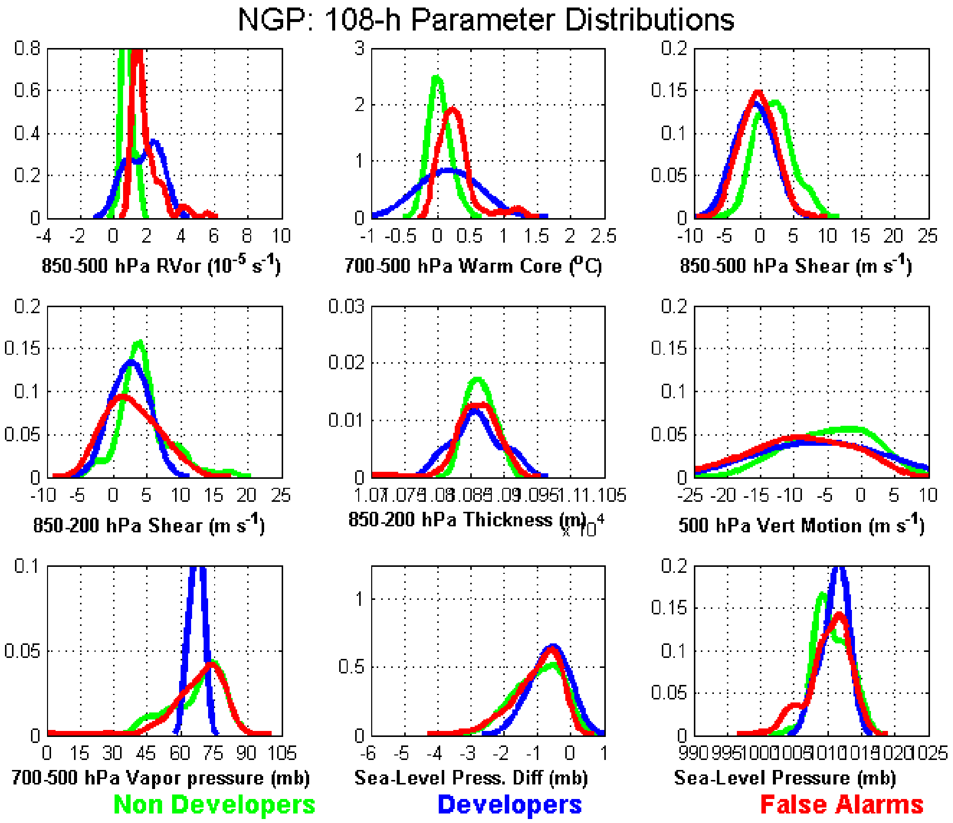
NGP: 108-h Parameter Distributions
850-500 hPa RVor (10^{-5} s^{-1})
700-500 hPa Warm Core (^{o}C)
850-500 hPa Shear (m s^{-1})
850-200 hPa Shear (m s^{-1})
850-200 hPa Thickness (m)
x 10^4
500 hPa Vert Motion (m s^{-1})
700-500 hPa Vapor pressure (mb)
Sea-Level Press. Diff (mb)
Sea-Level Pressure (mb)
Non Developers
Developers
False Alarms

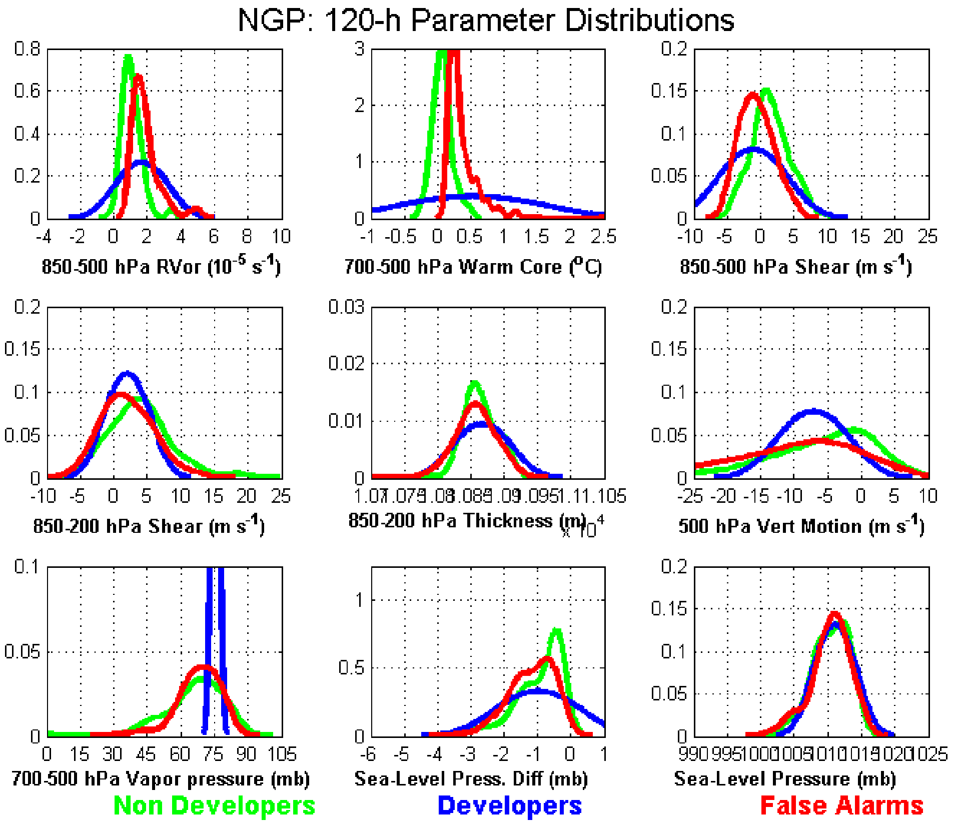
NGP: 120-h Parameter Distributions

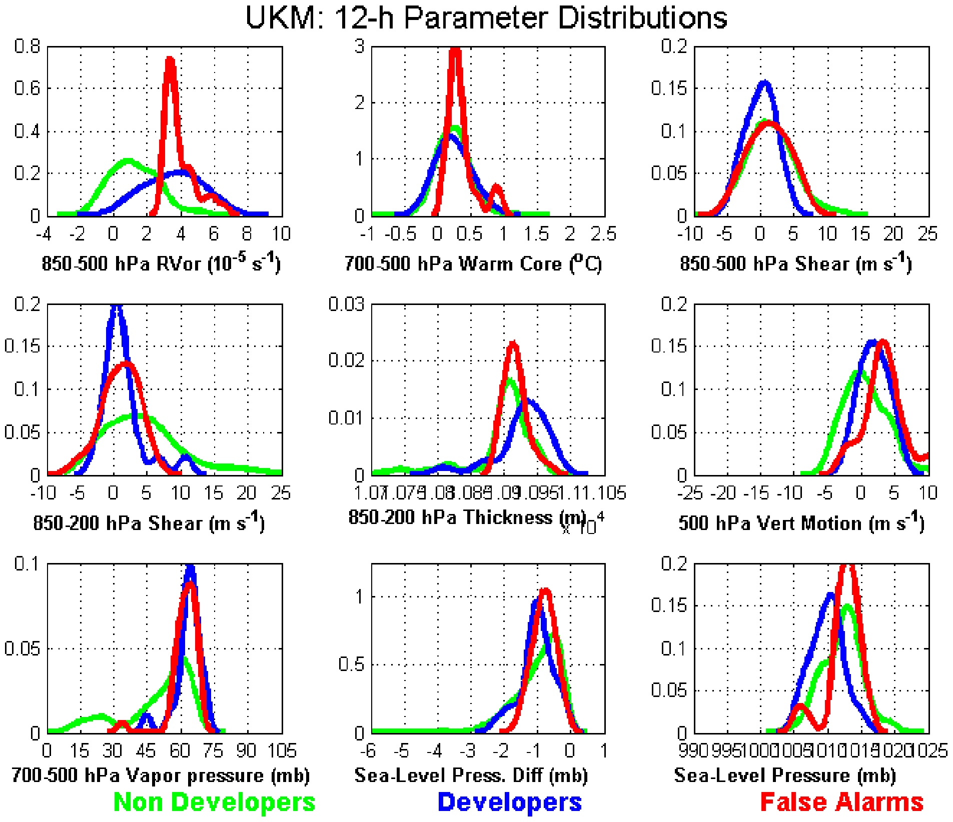
UKM: 12-h Parameter Distributions

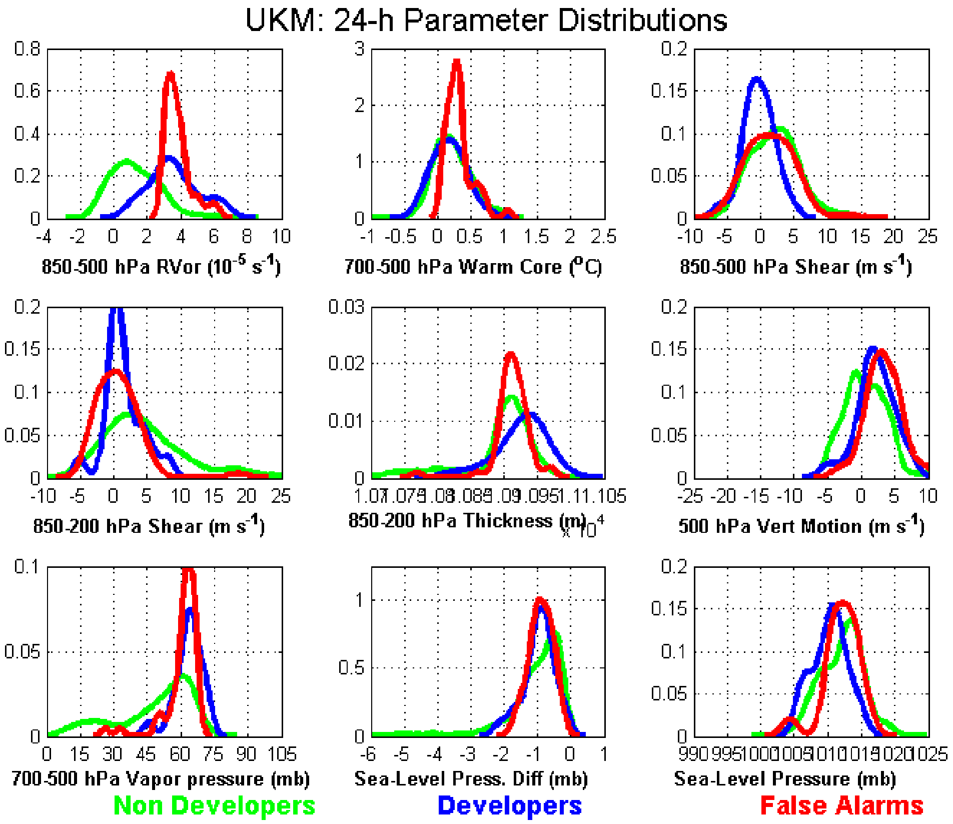
UKM: 24-h Parameter Distributions
0.8
0.6
0.4
0.2
0
-4 -2 0 2 4 6 8 10
850-500 hPa RVor (10^{-5} s^{-1})
3
2
1
0
-1 -0.5 0 0.5 1 1.5 2 2.5
700-500 hPa Warm Core (^oC)
0.2
0.15
0.1
0.05
0
-10 -5 0 5 10 15 20 25
850-500 hPa Shear (m s^{-1})
0.2
0.15
0.1
0.05
0
-10 -5 0 5 10 15 20 25
850-200 hPa Shear (m s^{-1})
0.03
0.02
0.01
0
1.07 1.075 1.08 1.085 1.09 1.095 1.1 1.105
850-200 hPa Thickness (m)
x 10^4
0.2
0.15
0.1
0.05
0
-25 -20 -15 -10 -5 0 5 10
500 hPa Vert Motion (m s^{-1})
0.1
0.05
0
0 15 30 45 60 75 90 105
700-500 hPa Vapor pressure (mb)
1
0.5
0
-6 -5 -4 -3 -2 -1 0 1
Sea-Level Press. Diff (mb)
0.2
0.15
0.1
0.05
0
990 995 1000 1005 1010 1015 1020 1025
Sea-Level Pressure (mb)
Non Developers
Developers
False Alarms

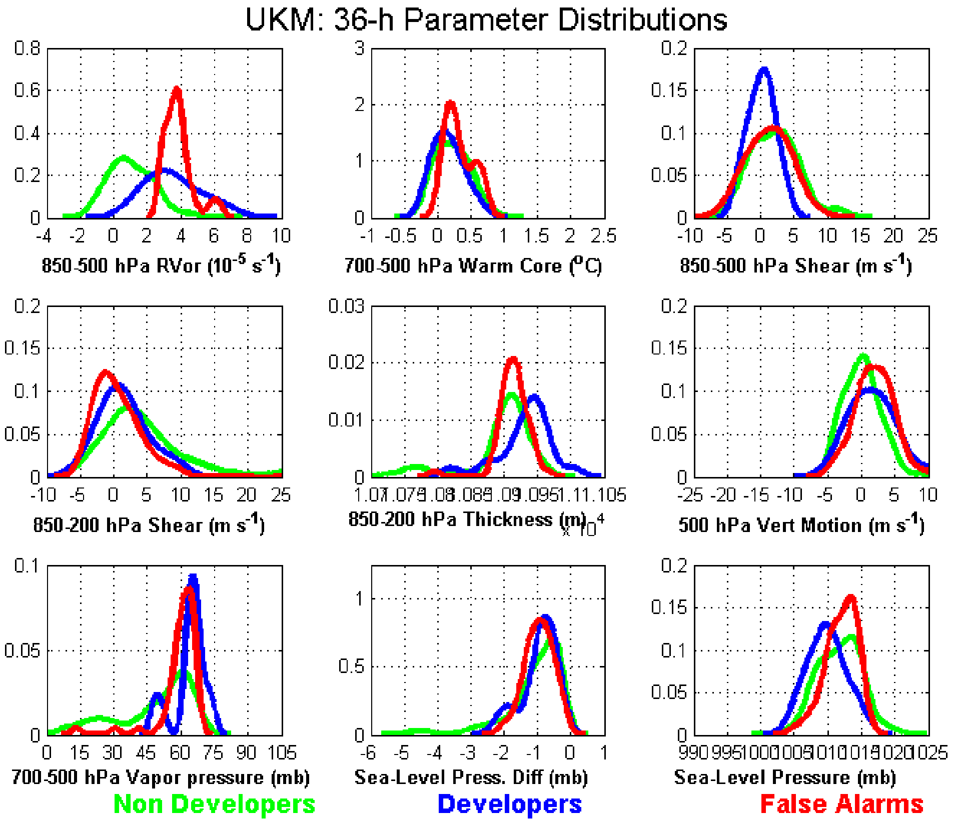
UKM: 36-h Parameter Distributions
0.8
0.6
0.4
0.2
0
-4 -2 0 2 4 6 8 10
850-500 hPa RVor (10^{-5} s^{-1})
3
2
1
0
-1 -0.5 0 0.5 1 1.5 2 2.5
700-500 hPa Warm Core (^oC)
0.2
0.15
0.1
0.05
0
-10 -5 0 5 10 15 20 25
850-500 hPa Shear (m s^{-1})
0.2
0.15
0.1
0.05
0
-10 -5 0 5 10 15 20 25
850-200 hPa Shear (m s^{-1})
0.03
0.02
0.01
0
1.07 1.075 1.08 1.085 1.09 1.095 1.1 1.105
850-200 hPa Thickness (m)
x 10^4
0.2
0.15
0.1
0.05
0
-25 -20 -15 -10 -5 0 5 10
500 hPa Vert Motion (m s^{-1})
0.1
0.05
0
0 15 30 45 60 75 90 105
700-500 hPa Vapor pressure (mb)
1
0.5
0
-6 -5 -4 -3 -2 -1 0 1
Sea-Level Press. Diff (mb)
0.2
0.15
0.1
0.05
0
990 995 1000 1005 1010 1015 1020 1025
Sea-Level Pressure (mb)
Non Developers
Developers
False Alarms

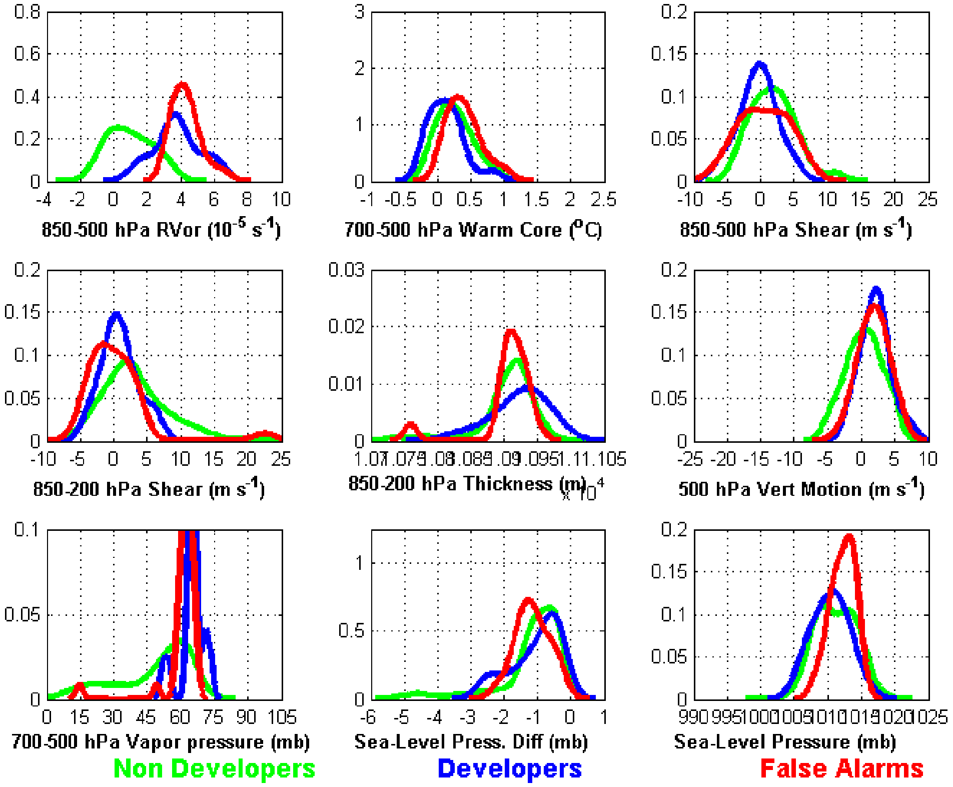

UKM: 48-h Parameter Distributions

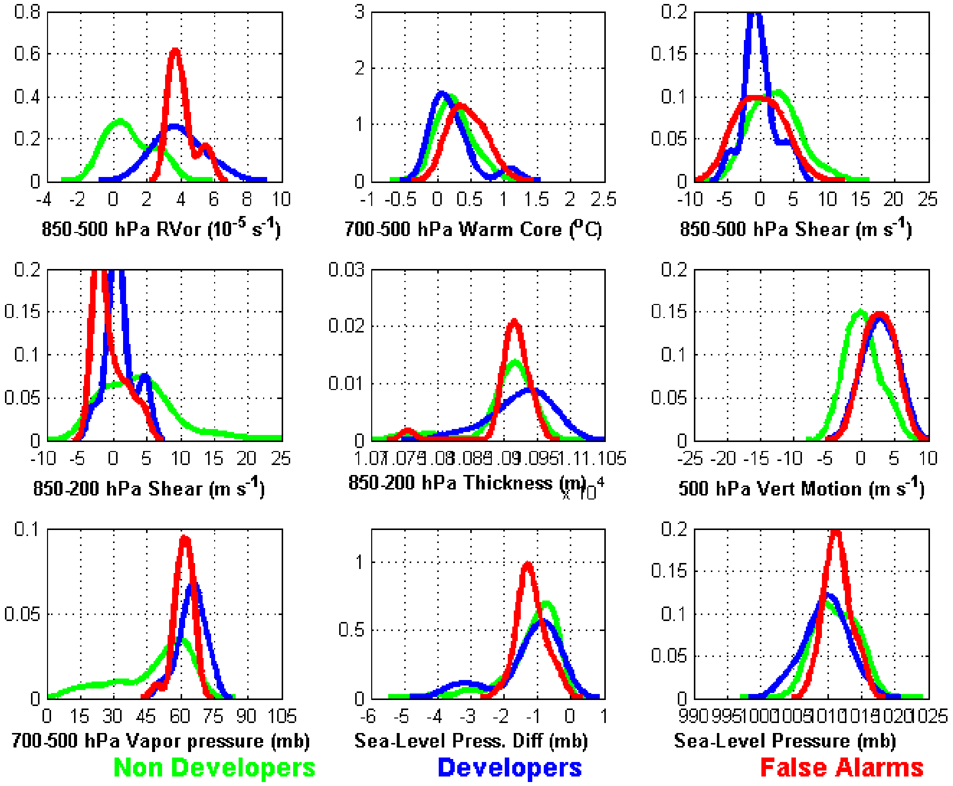

UKM: 60-h Parameter Distributions

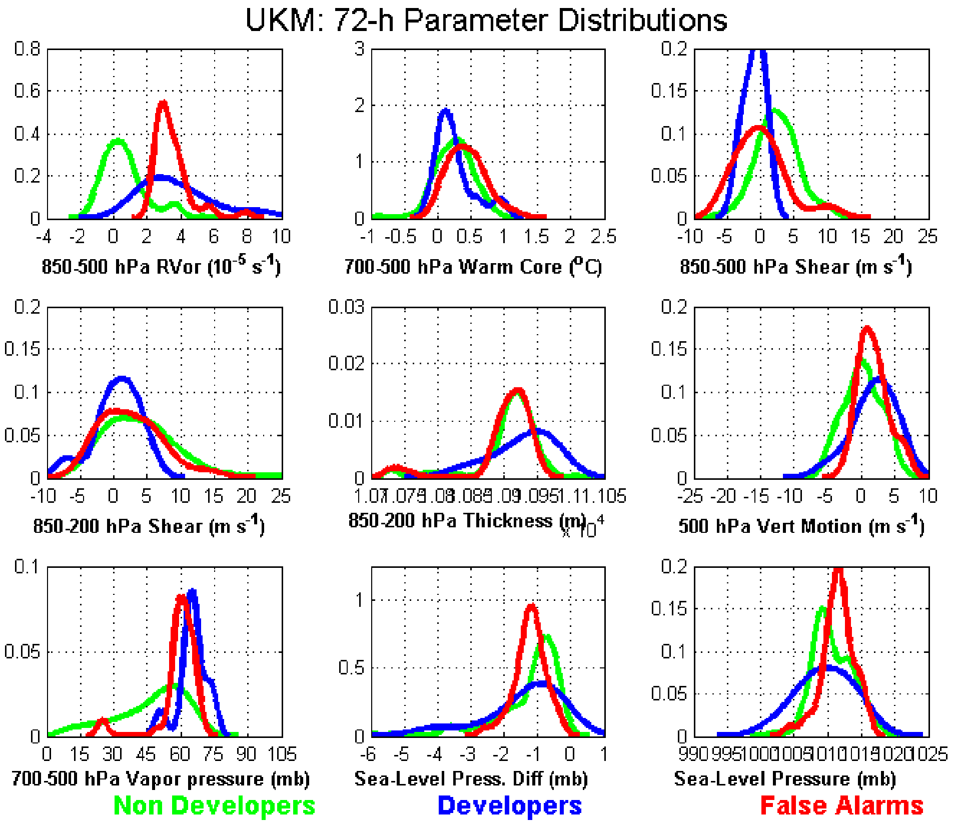
UKM: 72-h Parameter Distributions

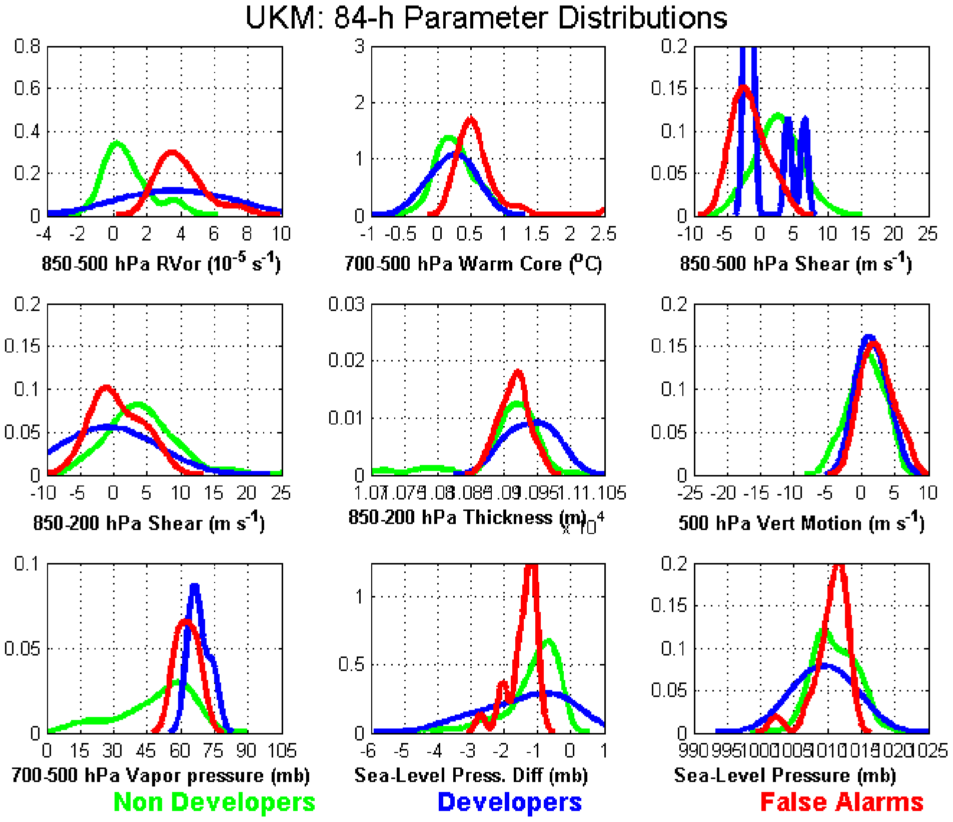
UKM: 84-h Parameter Distributions

UKM: 96-h Parameter Distributions

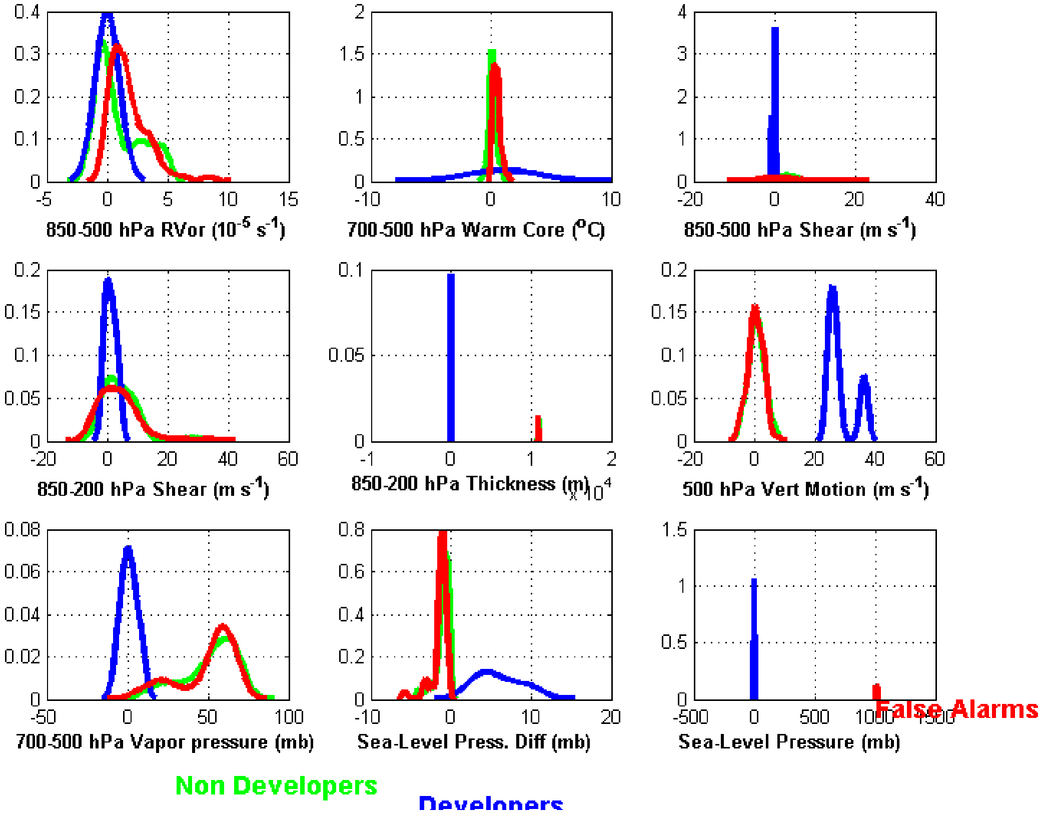

UKM: 108h Parameter Distributions

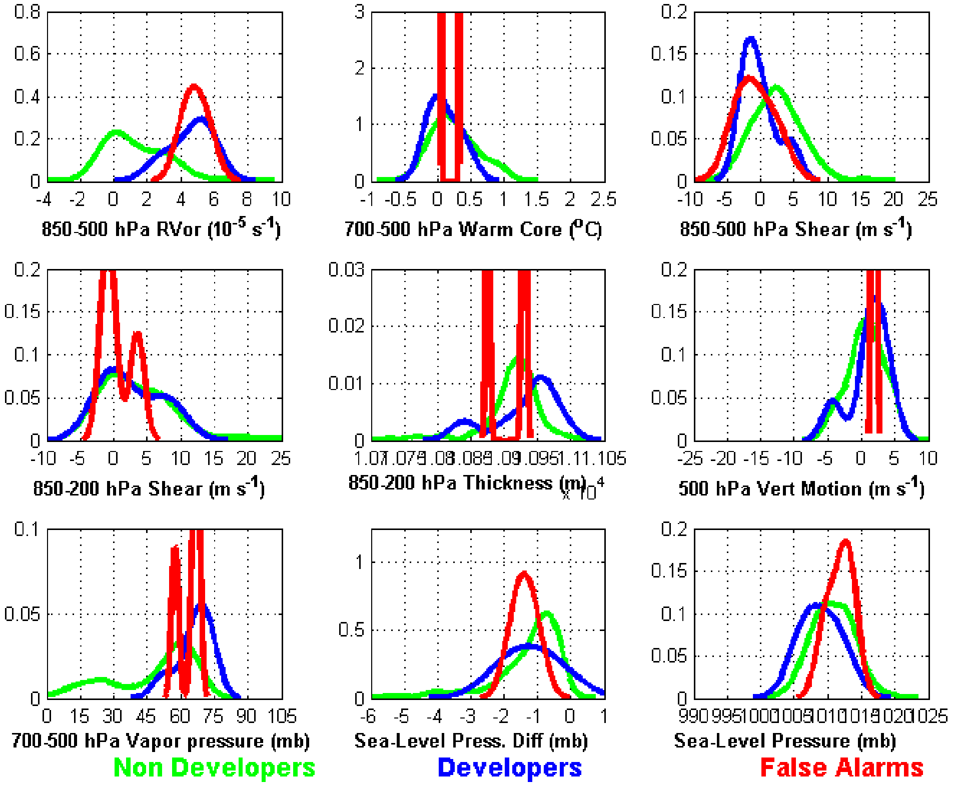

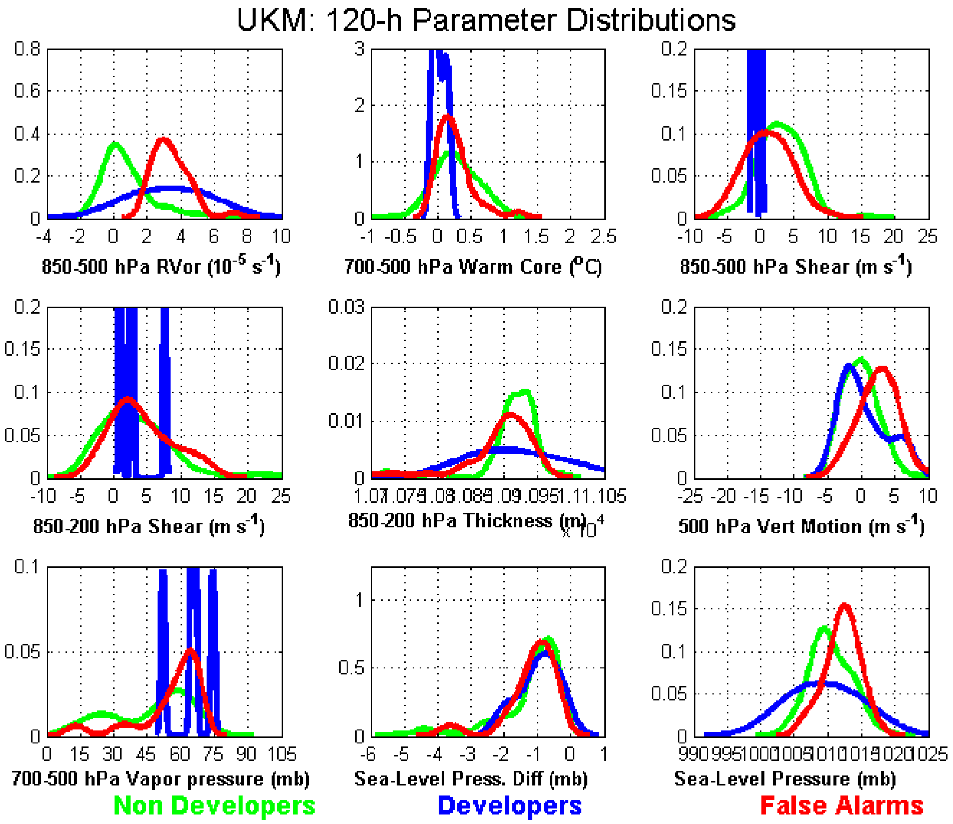
UKM: 120-h Parameter Distributions
0.8
0.6
0.4
0.2
0
-4 -2 0 2 4 6 8 10
850-500 hPa RVor (10^{-5} s^{-1})
3
2
1
0
-1 -0.5 0 0.5 1 1.5 2 2.5
700-500 hPa Warm Core (^{o}C)
0.2
0.15
0.1
0.05
0
-10 -5 0 5 10 15 20 25
850-500 hPa Shear (m s^{-1})
0.2
0.15
0.1
0.05
0
-10 -5 0 5 10 15 20 25
850-200 hPa Shear (m s^{-1})
0.03
0.02
0.01
0
1.07 1.075 1.08 1.085 1.09 1.095 1.1 1.105
850-200 hPa Thickness (m)
x 10^{4}
0.2
0.15
0.1
0.05
0
-25 -20 -15 -10 -5 0 5 10
500 hPa Vert Motion (m s^{-1})
0.1
0.05
0
0 15 30 45 60 75 90 105
700-500 hPa Vapor pressure (mb)
1
0.5
0
-6 -5 -4 -3 -2 -1 0 1
Sea-Level Press. Diff (mb)
0.2
0.15
0.1
0.05
0
990 995 1000 1005 1010 1015 1020 1025
Sea-Level Pressure (mb)
Non Developers
Developers
False Alarms

LIST OF REFERENCES

Avila, L. A., and R. J. Pasch, 1995: Atlantic tropical systems of 1993. *Monthly Weather Review*, **123**, 887-896.

Beven, J. L., 1999: The boguscane- a serious problem with the NCEP medium range forecast model in the tropics. Preprints, 23rd Conf. on Hurricanes and Tropical Meteorology, Dallas, TX, American Meteorology Society, 845-848.

Davis, C. A., and L. F. Bosart, 2001: Numerical simulations of the genesis of Hurricane Diana (1984). Part I: Control simulation. *Monthly Weather Review*, **129**, 1859-1881.

Davis, C. A., and L. F. Bosart, 2003: Baroclinically induced tropical cyclogenesis. *Monthly Weather Review*, **131**, 2730-2747.

Demaria, M., J. A. Knaff, and B. H. Connell, 2001: A tropical cyclone genesis parameter for the tropical Atlantic. *Weather and Forecasting*, **16**, 219-233.

Elsberry, R. L., 2003: Tropical cyclone formation. Tropical meteorology (MR3252) course notes, Chapter 2. Naval Postgraduate School, Monterey, CA, 93 pp.

Gray, W. M., 1975: Tropical cyclone genesis. Department of Atmospheric Sciences Paper 234. Colorado State University, Ft. Collins, CO, 121 pp.

Harr, P. A., 2006: Objective and automated assessment of operational global forecast model predictions of tropical cyclone formation and life cycle. Final Report, Joint Hurricane Testbed Project. [Available at http:// www.nhc.noaa.gov/jht/03-05_proj.shtml]

Hennon, C. C., and J.S. Hobgood, 2003: Forecasting tropical cyclogenesis over the Atlantic basin using large-scale data. *Monthly Weather Review*, **131**, 2927-2940.

Molinari, J., D. Vollaro, S. Skubis, and M. Dickson, 2000: Origins and mechanisms of eastern Pacific tropical cyclogenesis: A case study. *Monthly Weather Review*, **128**, 125-139.

Wilks, D. S., 2005: *Statistical Methods in the Atmospheric Sciences*. 2nd ed. Academic Press, 627 pp.

INITIAL DISTRIBUTION LIST

1. Defense Technical Information Center
   Ft. Belvoir, Virginia

2. Dudley Knox Library
   Naval Postgraduate School
   Monterey, California

3. LCDR Christy Cowan
   Naval Postgraduate School
   Monterey, California

4. Patrick Harr
   Naval Postgraduate School
   Monterey, California

5. Russell Elsberry
   Naval Postgraduate School
   Monterey, California

6. Director
   Joint Typhoon Warning Center
   Pearl Harbor, Hawaii

7. Richard Pasch
   National Hurricane Center
   Miami, Florida

8. Steve Tracton
   Office of Naval Research
   Arlington, Virginia

9. Grant Elliot
   Bureau of Meteorology
   Perth, Australia